Cells Have Feelings Too:

How Cells Generate and Respond to Mechanical Cues in Tissues

by

Torey Ray Arnold

A dissertation submitted in partial fulfillment
of the requirements for the degree of
Doctor of Philosophy
(Molecular, Cellular, and Developmental Biology)
In The University of Michigan
2018

Doctoral Committee:

Associate Professor Ann L. Miller, Chair
Professor Matthew Chapman
Associate Professor Erik Nielsen
Professor Kristen Verhey

Torey R. Arnold

toreya@umich.edu

ORCID ID: 0000-0002-1663-1953

Acknowledgements

First, I would like to thank my mothers. Thank you moms for raising me with an open mind about the world around me, which helped steer me towards science. Specifically, I would like to thank my biological mother. While not a trained scientist herself, she is genuinely fascinated by the natural world. Thank you for all the trips to the library and fossil hunts at the beach. To both of my mothers, thank you for supporting me even when I was a jerk. You two never gave up on me and stuck with me until I was able to change and better myself. It has been a long journey to this point, and I literally would not have made it if it wasn't for the two of you. I love you so dang much!

Being a graduate student at the University of Michigan has changed my life. The amount of personal and professional growth I have gone through astounds me, and I would not have had that opportunity without being accepted into the PiBS program. I would like to give a huge thanks to those on the admission committee, whoever you may be, for seeing potential in me. I would also like to thank those involved in organizing the Summer Institute Program for all of their hard work. That program gave me a jump start in graduate school and allowed me to connect with a close group of graduate students that I still appreciate to this day.

I would like to thank Matthew Chapman and the members of his lab for taking me under their wings during my first rotation. I was super nervous about starting grad school because the environment of my undergraduate research was productive but also very laidback and fun. The

Chapman lab showed me that this can still be the case in grad school! I also learned super important skills like molecular cloning during this rotation; thank you Margery Evans for being such a supportive and patient rotation mentor. I want to give a big thanks to Matt for teaching me that no matter how badly you are losing, you can always trash talk harder. As a committee member, Matt gave me one of the most useful pieces of advice in grad school which was “Don’t get caught up in what *you* think is going on. Be changeable and listen to the data”. Thanks Matt.

I want to thank Kristen Verhey for allowing me to rotate in her lab of tall people. It was the first time in my life I ever felt short, so that was a nice new perspective for me. All the members of Kristen’s lab continued to prove that grad school can be fun while doing super cool research. I would like to give an extra thanks to Kristen for turning her head when we were doing ridiculous food eating challenges in the lab. Stephen Norris was my rotation mentor in Kristen’s lab and he was incredible. His detail in explaining protocols and concepts was superb, and I remember having a moment where I said to myself “I want to be like Stephen when I mentor rotations students.” I’m not sure if I ever achieved this, but I did always try to be as pleasant and informative as him. Thanks Stephen. Also, thanks Kirsten for singing Poker Face with me and Ann. Just because we are scientists doesn’t mean we don’t have pipes of pure gold! As a committee member, I loved your attitude of, yeah you could poke at this forever or you could publish it and these are the critical experiments to get there. This way of thinking helped me and Ann see that I couldn’t to all these dang experiments I was proposing. You definitely helped me graduate on time! A big ole thanks for that!

Erik, while I never rotated in your lab I have always appreciated your feedback. Ever since my prelim, you have challenged me to think about my project differently. On that prelim

day, as nervous as could I be, you kept challenging me and asking me clarifying questions. After I passed, I knew I wanted you on my committee because you would help keep my mind open to the possibilities of what the data was actually telling us. Since day one you always challenged the idea of tension on junctions, and as it turns out you were right! Anillin wasn't pulling in line with the junctions! You kept my mind open to new ideas, and this openness is what ultimately drove my project. Thank you so much for this.

Rachel Stephenson, I'm sorry for the first time we met during our PiBS interview and I was super hungover and blew you off. Thanks for looking past this rudeness and becoming my best friend. Grad school would not have been the same without you. I would have never challenged myself to drink a 40 in 4 minutes and 1 second had you not made me watch the Bachelor. You've always been there for me and have literally made me a better person. You may not realize it but you were like a second mentor to me that helped develop me into the scientist I am today. I always enjoyed talking science with you even when it is about whatever new thing you just read about on Wikipedia. Thanks for being my videogame and improv bud. For helping convince me to write my first rap. For teaching me how to cook. For doing your best at making me a better writer. For "singing" "Hello" by Adele to me in the microinjector room. I cannot thank you enough for your support when I was going through my divorce, you made that difficult time enjoyable and were a mirror that was always willing to reflect my good qualities back on me. The question is still unanswered though, WTF is Wee-Bey up to? Love you.

Kayla, thanks for being an amazing undergraduate. Your intelligence and ability to get stuff done impressed me and drove me to work harder. You had the output of a graduate

student, and I thank you for your hard work making all them dang clones and for the fun times we had together. Thanks for being the chillest tubing bud and sharing cute animal pics with me to stave off the grad school woes. You were always willing to be weird and silly in your own special Kayla way. Thanks for giving plenty of head nods and taking care of mine and Rachel's birds.

Farah, thanks for bringing your quirky self to the Miller lab. I don't even know where to start. You are a conundrum of a human being and I have always loved how unique you are. You bring an energy to a space that is unmatched. You have worked so hard and produced such amazing data for the SGEF project. I also do not have enough nice things to say about your curiosity when it comes to science. You want to solve all the scientific questions and come with intelligent new experiments to answer them. This is an amazing quality that I never would have expected to see from an undergraduate. I certainly didn't have this aptitude. Remember plates are good vessels for food too.

Tomo, you are my science idol. You were like a second mentor to all of us and I seriously have no idea how we would have made it without you. Thank you so much for letting me add to your story about epithelial cell division. This process really helped prepare me for my own publications and was such a great opportunity to have early in my graduate career. The expertise you brought to the lab and your calm nature made the lab a more informed and welcoming space. Your sense of humor brought me joy, and I still treasure all the little surprises you left me. You gave me support, challenged me at just the right times, and talked videogames when I needed to decompress. I miss having you in the lab every day, but thank you for talking cats, Pokeman, factories, and science when we still had ya. Thank you for being a role model for

me. Showing me that a scientist can be calm, cool, smart, funny, fashionable, and talented in more than just science. Muah!

Sara, thanks for putting up with me and always being so great to talk to. You impress me with how much you get done. I love your personality and want to be your best friend. Thanks for talking science with me and always being super supportive with feedback and encouragement. Thanks for falling asleep on the bus that one time, that was super funny, and thanks most of all for allowing me to be fake mean to you. It's really fun and I enjoy it. It means the world to me.

Nisha, thanks for keeping me entertained and sane with clementime. Brandon, thanks for never sharing your pizza meals with me. I bet they're gross. Lauren, thanks for being fun but simultaneously more of an adult than I am. How is this possible? Shahana, thanks for doing whatever I tell you to do without even thinking about the consequences. It's fun and gets us into trouble. Jen, thanks for being the spark to get lab improv going, it is my favorite part of lab meeting. I also admire your level of organization and ability to orally present ideas, especially in the chalk talk style. It's impressive. Lotte, thanks for being a great rotation mentee, my first of four to join! I'm not a failure! Your baked goods are on point too. Yum. Thanks to Megan, Ciara, and Elaina for being there in the formative years of the Miller lab. I have lots of great memories with all of you and thanks for all of you help training me and answering my questions.

I would also like the thank Lance Davison, Deepthi Vijayraghavan, and Joseph Shawky for showing me the ropes on making *Xenopus* tissue explants and an extra big thanks to Joe for performing the tissue stiffness experiments in Chapter 3. Lance you have always been such a

great source of information and inspiration, thanks for always having awesome discussions with me at my posters. One last shout out to Deepthi and Joe for making sure I survived our epic bike ride around Pittsburgh. What an awesome ride. Thanks!

Finally I guess I will thank my graduate school mentor, Ann Miller. Seriously, Ann, where I would I be without you? You changed my friggen life. I joined your lab because I thought to myself “If I can be half of the mentor Ann is, I will be a great mentor.” You have never once made me feel like I can’t be a great scientist, but you have always driven me to be one. You accomplish this not with draconian BS, but by leading by example. I always wanted to strive to do my best because I saw you doing yours. Granted your best is like some super human level of getting stuff done that I know I can never achieve, but I had to at least try. You have a special ability to never become frustrated with your trainees, or at least not show it to them, and when drama is going on you always work to resolve it in a professional, fair manner. I’ve been through some dramatic life stuff in graduate school, and you always had my back, making it clear that I needed to take care of myself first. You treated me as a human being that you wanted to help succeed first instead of as a cog in your lab machine. You pushed me to pursue my teaching interests, got me direct funding to help build them, and then spent time working with me to improve them. You sent me all over the planet to represent the lab at conferences. You didn’t get super mad at me when I kept forgetting about our weekly meetings. Sorry about that. You are a true mentor: you help your trainees reach their potential in the lab and out. For this I cannot thank you enough. You don’t just lead by example when it comes to science, but also fun. I have never met another PI who commits as hard as you do, to any task. For example you still commit to keeping peoples birthday celebrations a secret even though everyone knows

exactly what's up. Your commitment to being silly in lab improv, laser tag, and quiz games is astounding and sometimes dangerous. Ann you are the bee's knees, its legs, and its wings. You're the whole dang bee! The only way you have ever truly failed me as mentor is by making finding a good postdoc so dang hard. No other PI will ever come close to you. From the apex of my ventricles, thank you Ann.

Table of Contents

List of Figures

Abstract

Cells are mechanical units, and their ability to orchestrate forces across a tissue allows them to shape organisms. In adults, cellular forces drive a flux of cell generation and extrusion to replenish tissues. In diseases, such as cancer, the mechanical properties of the tumor drive disease progression. These facets make understanding how cells generate and respond to mechanical signals an important area of study.

Epithelial tissues act as barriers that protect organisms from dehydration, infection, and chemical damage. An unanswered question in epithelial biology is how or if epithelial tissues maintain their barrier as distortions in cell shape occur during cell division. To determine if cells maintain the epithelial barrier during cell division, we used a dye penetration assay in *Xenopus laevis* embryos and found that the epithelial barrier remains intact during cytokinesis. Using confocal microscopy, we determined that the contractile ring that drives cell division is coupled to the structures that adhere cells together, cell-cell junctions. Investigating the molecular dynamics of junctions, I found that adherens junction, but not tight junction, proteins are stabilized at the cleavage furrow. Using inhibitors, I demonstrated that forces from the contractile ring are coupled to adherens junctions, but not tight junctions. Finally, we found forces from the contractile ring recruit Vinculin to adherens junctions to reinforce the junctions during cell division. These results position adherens junctions as the load bearing junctions

during cell division, which may be important for maintaining the barrier function in proliferative tissues.

Understanding which proteins cells use to produce force and change their mechanical properties is critical for our understanding of development, tissue homeostasis, and disease progression. Previous work from our lab showed that Anillin, which is known to regulate cytokinesis, is also an important regulator of cell-cell junctions. Based on this work, we proposed that Anillin promotes tensile forces on junctions. Here, I tested this hypothesis by using two complementary methods to assess junctional tension in *Xenopus laevis* embryos. I found that increased Anillin expression correlated with increased Vinculin recruitment to junctions, indicating increased junctional tension; however, increased Anillin expression inversely correlated with junction recoil after laser ablation, consistent with reduced junctional tension. These seemingly contradictory results led us to hypothesize that Anillin transitions the load-bearing actomyosin structures from the junction-associated actomyosin to medial-apical actomyosin.

Using immunostaining and live imaging, I showed that Anillin organizes the contractile medial-apical actomyosin network across the apical surface of the cells. We hypothesized that Anillin functions to integrate force transmission throughout a tissue and embryo as a whole by organizing medial-apical actomyosin. Indeed, I found that when Anillin was depleted, tissues lost force transmission capabilities, and this loss of tissue-scale force coordination disrupted embryo-level coordination. Building on this, we measured the stiffness of explanted *Xenopus* tissue and found that tissue stiffness was reduced when Anillin was depleted. These results are of interest because changes in tissue stiffness are required for developmental morphogenesis

and significantly impact cancer prognosis. Our results highlight a new role for Anillin in regulating epithelial mechanics at both the cellular and tissue levels.

Together, our findings demonstrate that epithelia are not static structures, but heterogeneous mechanical environments that are continually changing. These findings have laid the groundwork for studies on how junctions mechanically respond to cell division and how Anillin-orchestrated force production impacts development, tissue homeostasis, and disease.

Chapter 1
Introduction

Building cell and tissue complexity from simple structures

The complexity of a cell is mind-boggling! A cell contains 42 *million* proteins whirling around inside (Ho 2018) - building, holding, activating, and digesting each other - and proteins are only one type of macromolecule that makes up a cell. Now, imagine 37 *trillion* cells all stuck together, organized into tissues and organs, and cooperating to perform specialized tasks, and the complexity of a human being becomes apparent (Bianconi et al. 2013). Remarkably, this complexity of multicellular organisms originates from a single cell, which divides *trillions* of times, and different daughter cells differentiate to carry out specialized functions. How can such complexity originate from a single cell? There are many steps involved: cells must divide, adhere to one another, migrate, and produce mechanical forces to bend and fold tissues in order to make the organs, which must work together to maintain the life of the organism. If every animal starts as a single cell, then the first cell must contain all of the information needed to build an organism. How can something so tiny contain so much information? The simple yet complex, unique yet consistent six-pointed geometry of a snowflake provides an analogy.

The six-pointed geometry of snowflakes emerges from the physical and chemical properties of water molecules. **(Fig. 1.1 A)**. When frozen, the bent geometry and polar nature of water molecules forms a hexagonal crystal lattice resulting in the six-pointed structure of

Portions of this chapter were published in a review entitled "Rho GTPases and actomyosin: partners in regulating epithelial cell-cell junction structure and function." (Arnold et al. 2017). Figure 1.2, 1.3, 1.4, and 1.6 are modified from (Arnold et al. 2017) Figure 1.5 is a modified version from (Higashi et al. 2016)

snowflakes **(Fig. 1.1 A)**. Atmospheric forces propel each snowflake through a unique path through a temperature gradient, causing melting and freezing to occur at different rates and giving each snowflake its unique shape. A tiny water molecule, just a mere 2.5 Angstroms, contains all the information necessary to provide the six-pointed ruleset for a snowflake, and because of forces acting on the snowflake, an infinite number of unique yet consistently six-pointed snowflakes can be born **(Fig. 1.1 A)**. Knowing this, it becomes, somewhat easier to comprehend how a cell, which is made up of *trillions* of molecules, with infinite possible arrangements and force production capabilities can provide the framework for something as simultaneously simple, complex, and unique as a human being.

The process of building a cell follows a similar template as building a snowflake; the physical and chemical properties of small building blocks direct the structure of larger macromolecules **(Fig 1.1 B)**. Hydrogen-bonded nucleotides make up DNA, 20 different types of amino acids make up proteins, fatty acids, glycerol, and phosphate combine to make up lipids, and sugars link together to make up polysaccharides **(Fig 1.1 B)**. The physical and chemical properties and the specific arrangement of these building blocks result in the elegant double helix of DNA, the diverse 3 dimensional shapes of proteins, the water loving and water hating structure of lipids, and the beautiful chain or branched array of polysaccharides **(Fig 1.1 B)**. These macromolecules dictate the ruleset of cells, where a lipid membrane encases the other macromolecules to establish an internal environment for the cell that is different from the external environment. Additionally, specific arrangements and interactions between polymer-forming proteins of the cytoskeleton help shape cells, and these polymeric proteins can dynamically rearrange to drive cell shape change **(Fig 1.1 B)**. Just as snowflakes rely on external

forces to gain their unique shape, the mechanical outputs from cells pushing and pulling on one another coordinated across many cells give tissues and organs their shape.

The mechanical forces generated by proteins that shape cells and tissues is the focus of my dissertation: specifically, how cells respond to mechanical inputs and adjust their mechanical properties to make an effective tissue. I will examine how the structures that adhere cells together, cell-cell junctions, respond to the mechanical force generated by dividing cells and how the actin scaffolding protein Anillin regulates cell and tissue mechanics by organizing actomyosin contractility across the apical surface of epithelial cells.

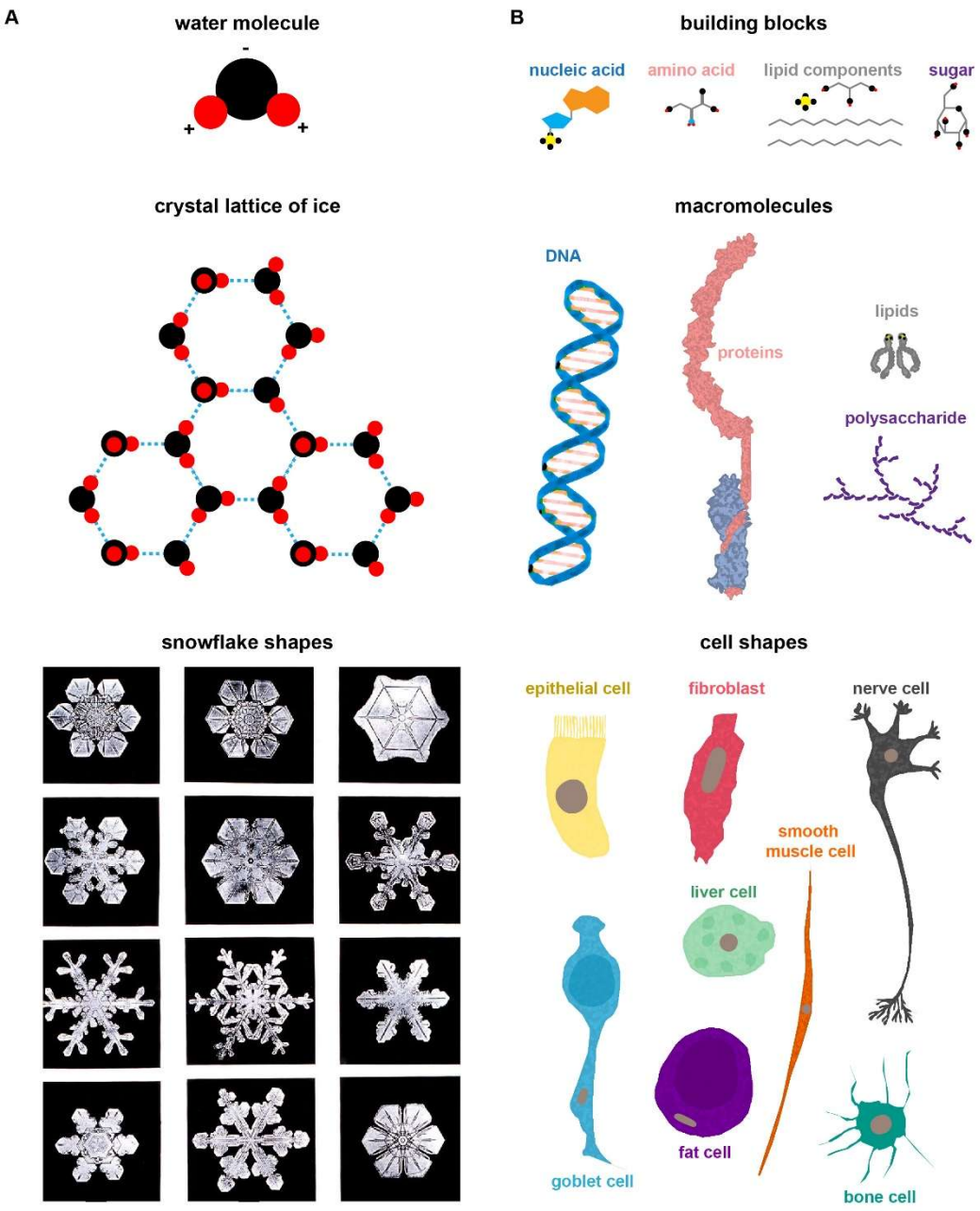

Figure 1.1: From simple physical and chemical properties comes complexity
A) (Top) Diagram of the geometry and charge of a water molecule. (Middle) Diagram of the crystal lattice water forms when frozen in ice. (Bottom) Pictures of snowflakes from “Annual Summary of the "Monthly Weather Review”" for 1902, Wilson Bently. **B)** (Top) The building blocks of macromolecules where nucleic acids build DNA, amino acids build proteins, fatty acids, glycerol, and phosphates build lipids, and sugars build polysaccharides. (Middle) Diagram of the cellular components, DNA from James Hedberg jameshedberd.com (CC), proteins, lipids, and sugar chains that store short term structural and charge information for the cell. Images inspired by artwork by David Goodsell. (Bottom) Diagrams of various cell types and shapes.

Mechanical forces drive cytokinesis

For a multicellular organism, the first cell division is a mechanical change that spans their entire being. Cytokinesis is the physical process of splitting a cell in two. This mechanical process has fascinated scientists for over a century, and we have unraveled many secrets of cytokinesis (Pollard 2010) **(Fig. 1.2)**. In many eukaryotes - from amoebas to yeasts to frogs to humans - cytokinesis is driven by piconewton-scale forces generated by the motor protein Myosin II sliding actin filaments (F-actin), to pinch the cell in two. However, other organisms have found different methods to accomplish this task. For example, plants rely on membrane-vesicle fusion and the addition of cell wall material to divide cells (Assaad 2001), while slime mold can use traction forces to drive cytokinesis (Reichl et al. 2008; Neujahr, Heizer, and Gerisch 1997). Other data indicate that filament sliding is not even required in all actomyosin-based cytokinesis; yeast can divide with severely disabled myosin motors (Lord and Pollard 2004), and cytokinesis can occur in vertebrates with Myosin II mutants that cannot slide actin filaments (Ma et al. 2012). While actomyosin contraction is often thought as the main driver of cytokinesis cells have found many different molecular solutions to pinch themselves in two.

Besides F-actin and Myosin II, there are many additional proteins involved in cytokinesis. The most robustly, quantitatively characterized eukaryotic cytokinesis is that of the fission yeast, in which over 150 different proteins are involved (Pollard and Wu 2010). Why does a seemingly simple process involve so many different proteins? A cell must overcome several obstacles in order to successfully divide. First, the cell must properly position the contractile ring. Second, the cell must assemble the actomyosin ring and connect it to the plasma membrane to generate the cleavage furrow. Third, contraction of the ring must be established,

tuned, and maintained even as the ring disassembles while contracting. Finally, the membrane must be fused to separate the daughter cells.

Figure 1.2: A contractile ring of actomyosin drives cytokinesis

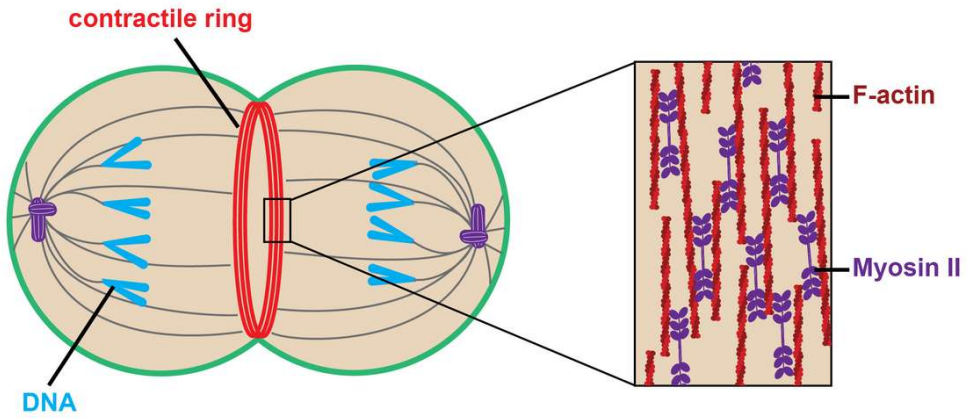

Figure 1.2: A contractile ring of actomyosin drives cytokinesis
Diagram of an isolated cell dividing. Zoom in (right) shows that the major components of the contractile ring are filaments of actin (F-actin) and the motor protein Myosin II. Contraction is generated through the sliding of actin filaments via the motor function of Myosin II. When connected to the plasma membrane, actomyosin contraction drives membrane furrowing during division.

RhoA signals to build a contractile ring

The master regulator of contractile forces in cells is the small GTPase RhoA (Arnold, Stephenson, and Miller 2017). It is not simply the expression of RhoA that matters, but the precise, localized activation of RhoA that ensures successful cytokinesis. RhoA cycles between and active form facilitated by guanine nucleotide exchange factors (GEFs) and an inactive form facilitated by GTPase activating proteins (GAPs) (Arnold, Stephenson, and Miller 2017). When in the active GTP-bound conformation, RhoA associates with the plasma membrane and activates specific effector proteins, resulting in localized effects on the cytoskeleton. For example, active RhoA promotes formation of actomyosin contractile arrays via its key effector proteins:

formins, which nucleate unbranched actin filament polymerization, and Rho-associated coiled-coil kinase (ROCK), which phosphorylates the regulatory light chain of Myosin II to activate Myosin II **(Fig. 1.3)**. RhoA activity is properly positioned during cytokinesis through the delivery of GEFs and GAPs along microtubules to the division site. In brief, MLKP1, a motor protein, transports MgcRacGAP, which can bind and concentrate the Rho GEF Ect2 (Zhao 2005). The co-accumulation and MgcRacGAP and Ect2 results in flux of RhoA between the active and inactive states at the division site, thus maintaining properly focused zone of RhoA activation (Miller and Bement 2009). This is a prime example of how gene expression is not the critical factor that drives the complex process of cytokinesis, but rather it is the tightly localized RhoA activity zone that initiates a cell-scale contractile array resulting in a major cell shape change.

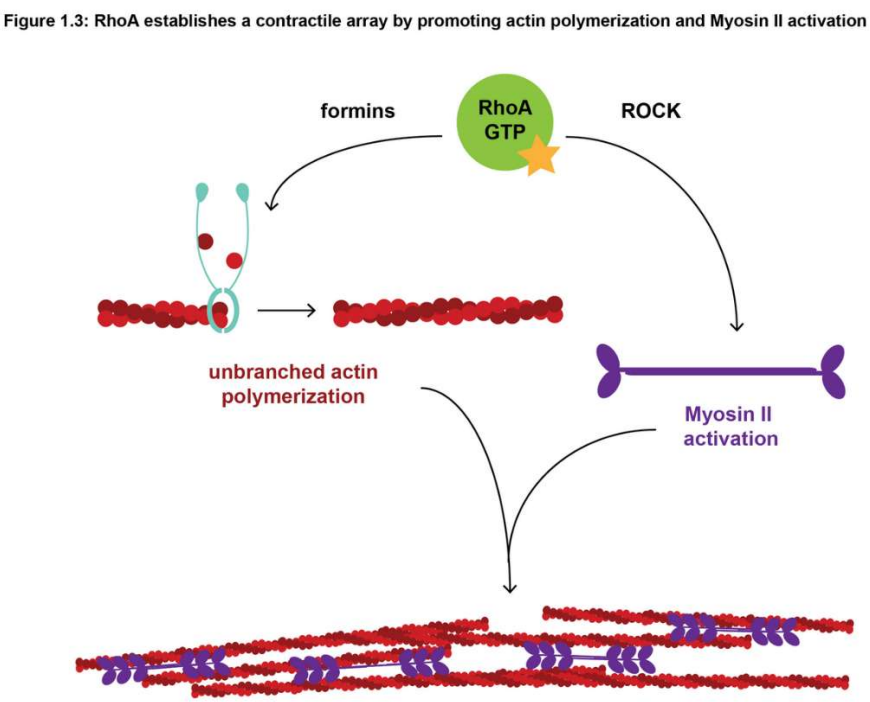

Figure 1.3: RhoA establishes a contractile array by promoting actin polymerization and Myosin II activation
Diagram of how the small GTPase RhoA signals for actomyosin contractility. Active RhoA binds to and activates formins, which drive the polymerization of unbranded actin filaments. RhoA also binds to and activates Rho-associated coiled-coil kinase (ROCK), which phosphorylates Myosin II to activate it. F-actin and Myosin II then form contractile bundles

Anillin fine-tunes and mechanically links forces from the contractile ring to the plasma membrane

Without a properly organized actomyosin ring that is connected to the plasma membrane and anchored in place, forces from cytokinesis would not appropriately pinch the cell in two, as the ring would aberrantly slide to one of the cellular poles (Straight 2005). Anillin is a scaffolding protein that plays a well-characterized role in cytokinesis (Piekny and Maddox 2010). In **Chapter 3** of this dissertation, I demonstrate a new role for Anillin in promoting cell and tissue stiffness by organizing contractile actomyosin across the apical surface of cells. During cell division, Anillin ensures successful cytokinesis by bundling F-actin, linking F-actin and Myosin II to the membrane, and fine-tuning RhoA activation at the contractile ring (Piekny and Maddox 2010) **(Fig. 1.4)**. The N-terminal domains of Anillin participate in actomyosin binding/assembly, while the C-terminal domains include PH and C2 domains, which anchor Anillin to the membrane, a RhoA binding domain, which allows it to interact with active RhoA, and the C-terminus also contains binding sites for interacting with the GEF Ect2 and the GAPs MgcRacGAP and p190RhoGAP-A (Piekny and Maddox 2010; Frenette et al. 2012; Manukyan et al. 2014; Sun et al. 2015) **(Fig. 1.4)**. Through direct binding to active RhoA, Anillin helps reset the clock on RhoA activation, acting as a buffer to extend the lifespan of active RhoA before passing it off to downstream RhoA effectors (Budnar et al. 2018). Early in cytokinesis, Anillin participates in a positive feedback loop, in which its accumulation at the contractile ring is both dependent on and enhances Rho activation (Piekny and Glotzer 2008). Later in cytokinesis, it interacts with p190RhoGAP-A in a tension-sensitive manner, inactivating RhoA in response to excessive force (Manukyan et al. 2014) **(Fig. 1.4)**. Finally, Anillin's bundling of F-actin also affects contractility in the ring, where moderate levels of Anillin promote efficient contraction

of actomyosin (Descovich et al. 2017). Thus, Anillin helps to promote efficient contraction by fine-tuning RhoA signaling, bundling F-actin, and linking the contractile ring to the plasma membrane **(Fig. 1.4)**.

Figure 1.4: Anillin fine-tunes RhoA signaling, bundles F-actin, and links the contractile ring to the membrane

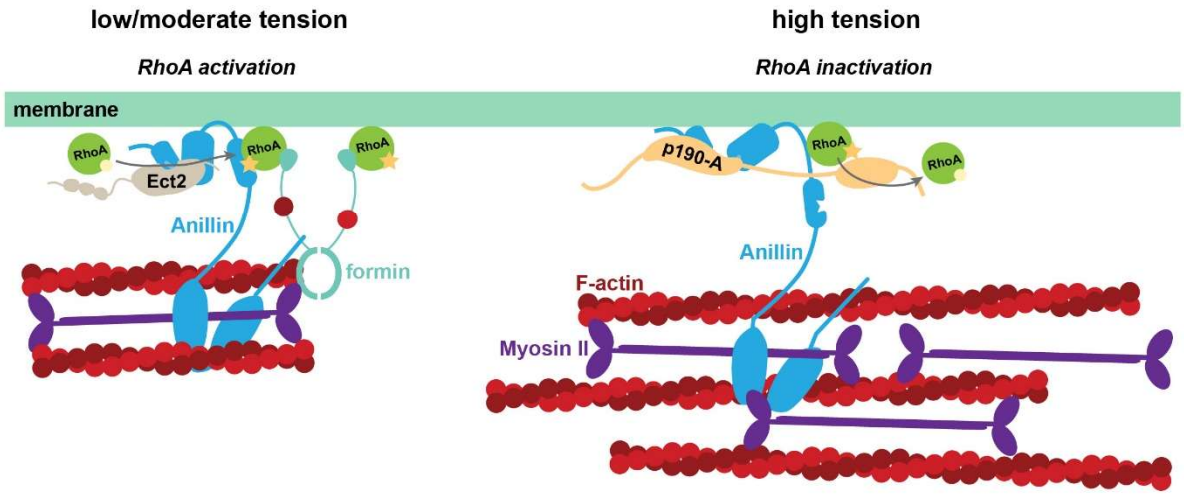

Figure 1.4: Anillin fine-tunes RhoA signaling, bundles F-actin, and links the contractile ring to the plasma membrane
Diagram of how in the contractile ring Anillin bundles F-actin and binds the plasma membrane, Myosin II, formins, active RhoA, and regulators of RhoA: Ect2 and p190RhoGAP-A. Anillin also functions to regulate the contractility of the ring. When tension is too high in the ring, Anillin binds to the negative regulator of RhoA, p190RhoGAP-A, to turn RhoA off.

How do cells divide in an epithelial tissue?

Most of the research in the cytokinesis field has focused on the first division of multicellular organisms, division in single-celled organisms, or division of isolated cultured mammalian cells (Pollard 2010; Rappaport 1996; Green, Paluch, and Oegema 2012). From these studies, we have learned a great deal about the mechanisms of contractile ring constriction, but cells in multicellular organisms do not divide in isolation. Cells in tissues are connected to one another via cell-cell junctions, which mechanically link the cells together and can transmit force

between cells. In addition to the challenge of generating the force to cleave the cell in two, cells dividing in an epithelial tissue, which act as barriers to protect multicellular organisms from pathogens and other environmental insults and create specialized compartments within the body, must overcome additional challenges created by their neighbors, which raise interesting questions about epithelial cytokinesis **(Fig. 1.5)**. Do dividing cells in a tissue communicate with their neighbors? Do neighboring cells actively participate in cell division? How does the dividing cell overcome the resistive force of neighboring cells? Do cells in a tissue need to produce more force than isolated cells to successfully divide, or do neighboring cells become more compliant? Is the barrier of an epithelium maintained during cell division and if so, how?

Early studies using electron microscopy and immunostaining showed that epithelial cells remain in contact with one another during cell division (Jinguji and Ishikawa 1992; Baker and Garrod 1993). This means that both the dividing cell and the neighboring cell undergo large shape changes during cell division **(Fig. 1.5)**. How does each cell respond to these mechanical inputs? Three very exciting papers showed that in dividing cells in *Drosophila* epithelial tissues, the membrane at the cleavage furrow is decoupled from cell-cell junctions as it ingresses during cell division (Guillot and Lecuit 2013; Founounou, Loyer, and Le 2013; Herszterg et al. 2013). One of these papers even found that there was a loss of adhesion between the dividing cell and its neighbor (Guillot and Lecuit 2013). This raises several interesting questions: do the forces from cytokinesis disrupt cell adhesion? Or is cell adhesion regulated by a force-independent mechanism? Additionally, why does junction disengagement happen in some tissues (Guillot and Lecuit 2013), but not others (Jinguji and Ishikawa 1992; Baker and Garrod 1993; Founounou, Loyer, and Le 2013; Herszterg et al. 2013)? Is the barrier function of epithelial

tissues disrupted by forces from cytokinesis? If so, what impact does this have on the organism? For example, the cells lining the small intestine are dividing so rapidly that the epithelial lining turns over every 2-4 days. If the epithelial barrier is being breached during each cell division this could compromise the intestinal barrier, allowing toxins and pathogens to gain entry into the body. **Chapter 2** of my dissertation addresses whether the epithelial barrier is maintained during cytokinesis in vertebrate frog embryos and how cell-cell junctions respond to the mechanical cues from cytokinesis.

Figure 1.5: Division in an epithelial tissue requires large shape changes of both the dividing cell and its neighbors

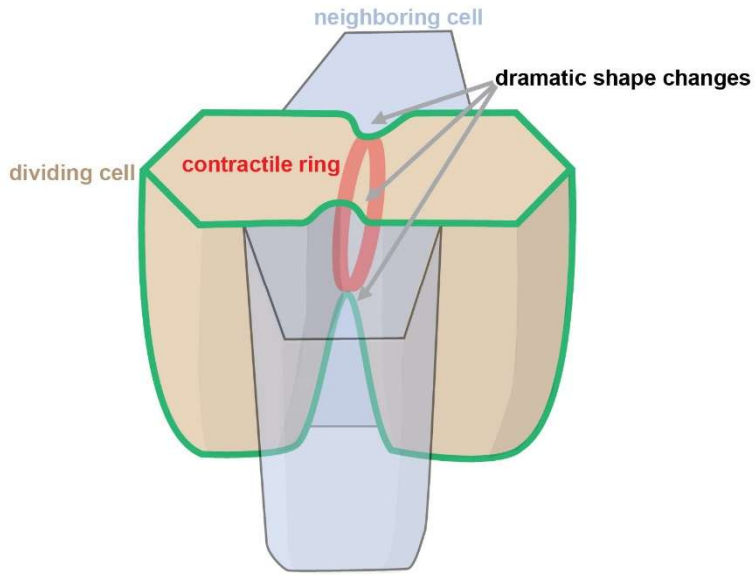

Figure 1.5: Division in an epithelial tissue requires large shape changes of both the dividing cell and its neighbors
Diagram of a dividing epithelial cell. Dividing epithelial cells and neighboring cells undergo large shape changes at both their apical and basal surface and they are attached to each other via cell-cell junctions. Little is known about how cells overcome this challenges and whether or not the epithelial barrier function is maintained during cell division.

Cell-cell junctions create barriers and mechanically link cells in a tissue

Without the ability of cells to adhere to one another, all life on this planet would be destined to be unicellular. To achieve multicellularity, life evolved the ability to mechanically

connect the two daughter cells generated by cytokinesis. Interestingly, many of the proteins that are found in the contractile ring during cytokinesis are also found at cell-cell junctions, such as RhoA, F-actin, Myosin II, Anillin, MgcRacGAP, Ect2, and p190RhoGAP-A (Arnold, Stephenson, and Miller 2017; Zaidel-Bar, Zhenhuan, and Luxenburg 2015). However, the functions of these cellular structures are very different; the contractile ring functions to cleave a cell in two, while cell-cell junctions function to mechanically link cells together and allow tissues to form barriers. Interestingly, some organisms, such as Choanoflagellates, the closest living relatives of animals, can live as a unicellular or multicellular organisms. They achieve multicellularity not with specialized cell-cell junctions, but by skipping the last step of cytokinesis, thus remaining connected via an intracellular bridge and sharing cytoplasm (Dayel et al. 2011), again highlighting the link between cell division and cell adhesion. To achieve multicellularity on a larger scale, cells had to evolve specialized adhesion structures which couple to the cytoskeleton so that epithelia could be robust enough to maintain tissue and barrier integrity, while being dynamic enough to maintain tissue homeostasis through the flux of cell proliferation and cell death.

Cell-cell junctions may have emerged around 600 million years ago (Chen et al. 2014), but the ultrastructure of vertebrate cell-cell junctions was first identified only a few decades ago in a seminal electron microscopy study by Farquhar and Palade (Farquhar and Palade 1963). The authors described the apical junctional complex in vertebrates being composed of tight junctions (or *zonula occludens*), where the space between epithelial cells is almost completely obliterated, adherens junctions (or *zonula adherens*), located just basal to the tight junction, where the cell membranes are brought in close proximity (~20 nm apart), and

"conspicuous bands of dense material located in the subjacent cytoplasmic matrix", which we now know to be junctional actomyosin (Farquhar and Palade 1963) **(Fig. 1.6 A,B)**. The apical junctional complex in vertebrates plays the critical role of sealing the paracellular space and adhering epithelial cells to one another (Hartsock and Nelson 2008; Van Itallie and Anderson 2014) **(Fig. 1.6 A,B)**.

Figure 1.6: Cell-cell junctions establish the epithelial barrier, cell adhesion, and integrity of epithelial tissues.

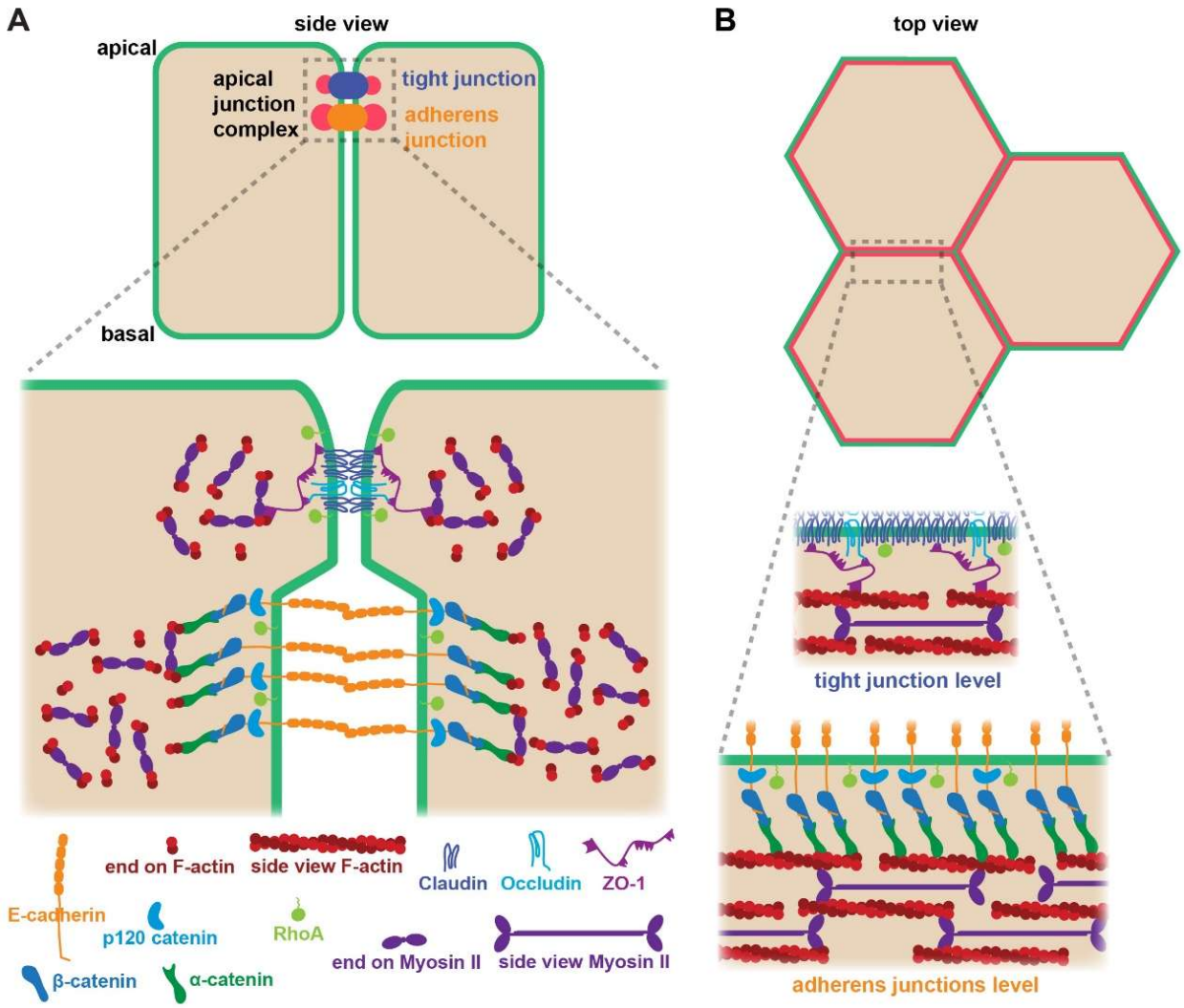

Figure 1.6: Cell-cell junctions establish the epithelial barrier, cell adhesion, and integrity of epithelial tissues. **A)** A side view schematic of epithelial cells showing the two types of cell-cell junctions connected to the actin cytoskeleton, the tight junction, which establishes the barrier function, and the adherens junction, which regulates cell-cell adhesion. In the enlarged view below, the architecture of core tight junction and adherens proteins is shown (see legend identifying key proteins). Transmembrane proteins facilitate interaction between cells, and scaffolding proteins connect the transmembrane proteins to bundles of contractile F-actin and Myosin II. Note that in this view, the bundles of actomyosin are oriented perpendicular to the plane of the cross-section. **B)** A top view schematic of epithelial cells. In the enlarged views below, one model for the organization of actomyosin is depicted with bundled antiparallel F-actin and decorated with Myosin II motors.

Tight junctions seal the space between cells and regulate and respond to mechanical cues

Tight junctions are well known to be important determinant of epithelial barrier function (Zihni 2016); however, recent studies have also revealed that they can sense and regulate apical forces (Spadaro et al. 2017, Fanning, Van, and Anderson 2012; Choi et al. 2016, Hatte, Prigent, and Tassan 2018). Classically, tight junctions seal the intercellular spaces between adjacent epithelial cells and form regulated, selective (size- and charge-selective) barriers. Barrier function can be acutely regulated in epithelial tissues by signaling mechanisms – notably by changes in actomyosin contractility (Shen et al. 2011). To achieve these functions, the tight junction transmembrane proteins (Claudins, Occludin, immunoglobulin-like Junction Adhesion Molecules) form tight junction strands, which are linked to the underlying actomyosin cytoskeleton via cytoplasmic plaque proteins (Zonula Occludens (ZO) proteins, Cingulin, Afadin, etc.) (Van Itallie and Anderson 2014) **(Fig. 1.6 A, B)**. ZO proteins are proposed to initiate the polymerization of Claudins into TJ strands (Umeda et al. 2006), and ZO-1 has the ability to stabilize Claudin strands (Van Itallie, Tietgens, and Anderson 2017).

In addition to their role in regulating the barrier of epithelial sheets, it is becoming clear that tight junctions are also important regulators of epithelial mechanics **(Fig. 1.7)**. For example,

when ZO-1 and ZO-2 are depleted, F-actin and Myosin II dramatically increase at adherens junctions and generate high tension in line with the junction (Fanning, Van, and Anderson 2012; Choi et al. 2016, Hatte, Prigent, and Tassan 2018), indicating that tight junctions negatively regulate tension on adherens junctions. Additional work has shown that ZO-1 itself is mechanosensitive (Spadaro et al. 2017). Tensile force on ZO-1 opens it to reveal a binding site for the transcription factor DbpA, thus sequestering it at tight junctions to inhibit cell proliferation, with additional possible effects on barrier function and epithelial morphogenesis (Spadaro et al. 2017) **(Fig. 1.7)**. These studies position tight junctions as emerging mechanical signaling centers in addition to their classic role in regulating epithelial barrier function.

Figure 1.7: Mechanical signaling through ZO-1 regulates gene expression

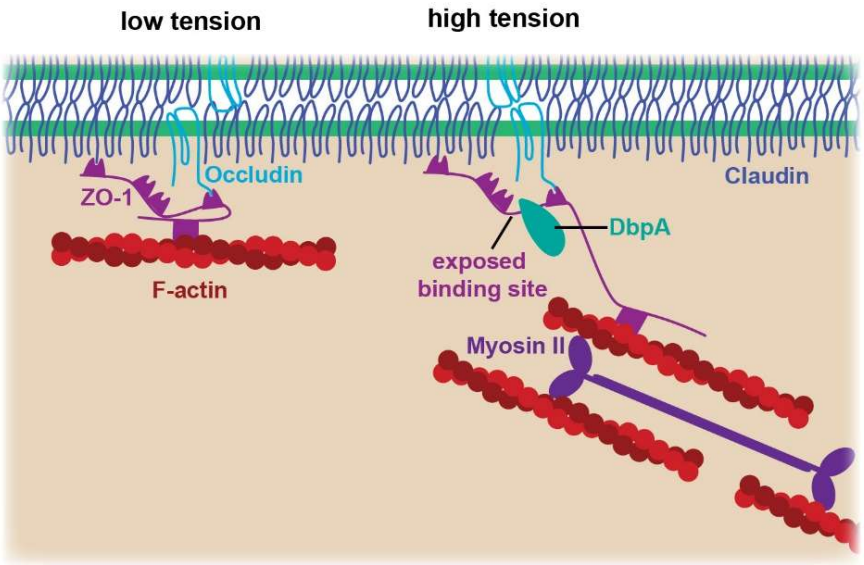

Figure 1.7: Mechanical signaling through ZO-1 regulates gene expression
A top down view of one side of a tight junction. When under low tension ZO-1 is in a folded conformation which masks the binding site for the transcription factor DbpA. When actomyosin tension is applied across ZO-1, the binding site for DbpA is exposed, sequestering DbpA at the tight junction, thus inhibiting cell proliferation.

Adherens junctions mechanically integrate epithelial cells

Adherens junctions, located just basal to the tight junction, mediate cell-cell adhesion and transmit mechanical forces across epithelial cells **(Fig. 1.6 A, B)**. Adherens junctions are functionally important for epithelial homeostasis and morphogenesis. For example, contraction of actomyosin coupled to adherens junctions can promote apical constriction of individual cells, which collectively leads to tissue folding (Coravos and Martin 2016; Takeichi 2014), or intercalation, during which cells remodel their cell-cell contacts through neighbor exchange (Lecuit and Yap 2015), leading to tissue elongation. Each of these functional roles of adherens junctions is dependent on regulated linkage of the core molecular components of adherens junctions to the actomyosin cytoskeleton.

The core AJ components include the transmembrane proteins (E-cadherin and Nectins) and cytoplasmic plaque proteins (β-catenin, α-catenin, p120-catenin, Vinculin, Afadin, etc.) (Quiros and Nusrat 2014; Ratheesh and Yap 2012) **(Fig. 1.6 A, B)**. E-cadherin forms both small spot-like clusters along the lateral membrane as well as an apical belt-like structure (the *zonula adherens*), which is located just basal to the tight junction. F-actin plays an important role in corralling the small E-cadherin clusters (Wu, Kanchanawong, and Zaidel-Bar 2015), and actomyosin drives their coalescence and stabilization at the apical *zonula adherens* (Ratheesh and Yap 2012). The linkage of E-cadherin to F-actin is achieved via catenin proteins. β-catenin binds to the cytoplasmic tail of E-cadherin, and α-catenin binds to β-catenin. α-catenin can bind F-actin, but only under actomyosin-generated force (Buckley et al. 2014; Nelson and Weis 2016). Furthermore, actomyosin-mediated tension promotes a conformational change in α-catenin, which reveals a binding site for Vinculin (Yonemura et al. 2010) **(Fig. 1.8)**. Vinculin is

only recruited to cell-cell junctions under mechanical tension to function in reinforcing cell adhesion and the linkage to F-actin in the face of mechanical force (le Duc et al. 2010; Yonemura et al. 2010) **(Fig. 1.8)**.

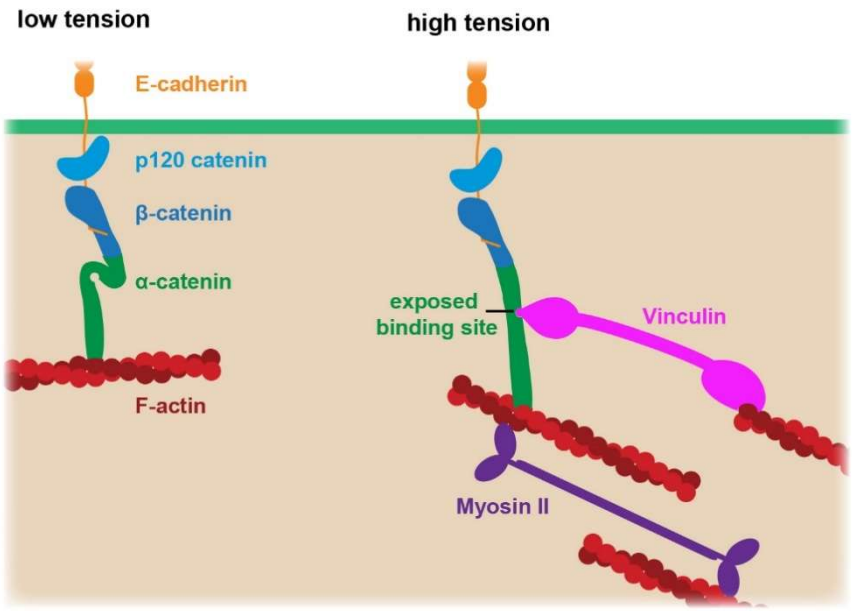

Figure 1.8: Mechanical signaling through α-catenin reinforces junctions
A top down view of one side of an adherens junction. When under low tension, α-catenin is in a folded conformation, which masks the binding site for Vinculin. When actomyosin-mediated tension is applied across ZO-1, the binding site for Vinculin is exposed. Vinculin reinforces the connection between the junction and the cytoskeleton.

How are forces generated at the epithelial surface?

Without the ability to actively orient mechanical forces and adjust the mechanical properties, any attempt to achieve multicellularity would be destined to remain as one-dimensional chain, a two-dimensional sheet, or a three-dimensional sphere of cells, depending on the orientation of cell divisions. The production of forces from individual cells coordinated across a tissue drives tissue bending and elongation events to sculpt organisms. These mechanical events, in conjunction with cell division and controlled cell death, allow organisms to take the variety of shapes we see in multicellular organisms.

In addition to shaping organisms epithelial cell mechanics directly impact disease. For example, 80-90% of cancers are epithelial in origin and changes in the mechanical properties of epithelial tumors directly affect the prognosis of certain diseases, where tumor stiffness correlates with poor prognosis for the patient (Kumar and Weaver 2009). Cells within a tumor can deposit extracellular matrix components to influence tumor stiffness (Kumar and Weaver 2009) and internal cellular mechanics also directly impacts tumor metastasis (Swaminathan et al. 2011; Guo et al. 2014). To fully understand the amazing process of development and how to treat and prevent diseases such as cancer, we need a comprehensive understanding of how epithelial sheets regulate their mechanical properties.

Circumferential actomyosin is a contractile network attached to cell-cell junctions

A key mechanical change in epithelial cells during development is the constriction of the apical surface of cells. This constriction shrinks the apical surface, which causes the tissue to bend in on itself. This tissue shape changes is key step for gastrulation in order to form the primary tissue layers of the organism and for neurulation in order to form the spinal cord. Early electron microscopy studies in frog, salamander, and chick provided evidence that circumferential actin filaments directly associated with adherens junctions were likely driving apical constriction during neurulation (Baker and Schroeder 1967; Burnside 1971; Karfunkel 1972) **(Fig. 1.9 A)**. Later immunostaining work in brush border epithelial cells of the small intestine induced to apically constrict highlighted that Myosin associated strongly with cell edges before and after apical constriction (Hirokawa et al. 1983). Using quick-freeze deep-etch electron microscopy, Hirokawa and colleagues convincingly showed that brush border cells apically constrict by squeezing in at the adherens junctions (*zonula adherens*), leaving their

apical surfaces bulging out (Hirokawa et al. 1983) **(Fig. 1.9 B)**. The contractile nature of the circumferential actomyosin network was demonstrated directly by isolating the actomyosin apparatus from chicken pigmented retinal epithelial cells (Owaribe and Masuda 1982). Upon addition of ATP to the purified actomyosin apparatuses, the rings of actomyosin constricted (Owaribe and Masuda 1982) **(Fig. 1.9)**. Additional work on embryonic tissue wounds demonstrated the importance of supracellular junctional cables that from to close the wound via a purse string constriction method (Martin and Lewis 1992; Nodder and Martin 1997). With this evidence it is not surprising that circumferential actomyosin alone was thought to drive apical epithelial mechanics for over 50 years.

Figure 1.9: Seminal evidence that demonstrated circumferential actomyosin was a contractile apparatus in epithelial cells

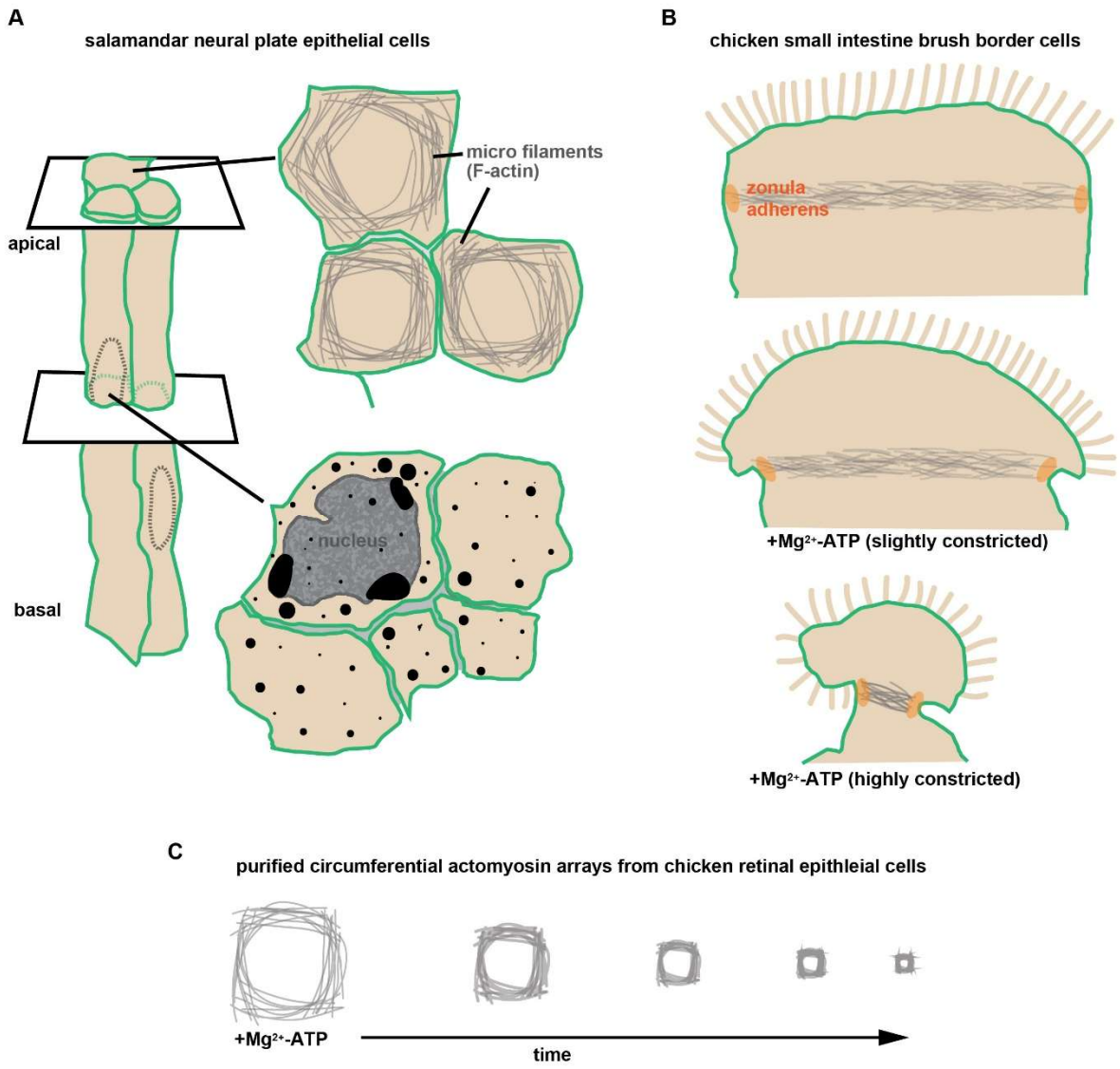

Figure 1.9: Seminal evidence that demonstrated circumferential actomyosin forms a contractile apparatus in epithelial cells

A) Transmission electron microscopy in salamander epithelial cells revealed a dense meshwork of filaments found only at the apical circumference of cells, which we now know is actomyosin. Artistic rendering of (Burnside 1971). **B)** Use of quick-freeze deep-etch electron microscopy revealed that chicken brush border epithelial cells induced to apically constrict via addition of ATP constricted at their *zonula adherens* (adherens junctions). Artistic rendering of (Hirokawa et al. 1983). **C)** Circumferential actomyosin arrays were shown to be contractile units when purified from chick epithelial cells; after addition of ATP, they constricted into small rings. Artistic rendering of (Owaribe and Masuda 1982)

Medial-apical actomyosin is a contractile network that drives apical constriction

In addition to the band of circumferential actomyosin associated with junctions, there is another actomyosin network that produces mechanical forces in epithelial tissues. Probably because it is less conspicuous than circumferential actomyosin, it took much longer for researchers to appreciate the importance of the medial-apical actomyosin network **(Fig. 1.10 A)**. In fact, even when medial-apical actomyosin was directly observed, the more prominent purse string model was generally favored as the method epithelial cells used to constrict their apical surface. For example, the protein Shroom3 was shown to induce apical constriction for neural tube closure in both mice and frog (Haigo et al. 2003; Hildebrand and Soriano 1999; Nishimura and Takeichi 2008). Interestingly, the proposed mechanism for Shroom3-induced apical constriction was the accumulations of actomyosin around the circumference of cells, even though both junctional and medial-apical actomyosin increased (Haigo et al. 2003; Nishimura and Takeichi 2008).

Medial-apical actomyosin was first appreciated for its role in apical constriction when live imaging was performed on gastrulating *Drosophila* embryos (Martin, Kaschube, and Wieschaus 2009*)* **(Fig. 1.10 B)**. This work found that a temporal bursts of Myosin II accumulated medial-apically to induce apical constriction (Martin, Kaschube, and Wieschaus 2009) **(Fig. 1.10 B)**. Outside of morphogenic events such as apical constriction, medial-apical actomyosin has been shown to be a load-bearing structure in stable epithelia (Ma et al. 2009) **(Fig. 1.10 C)**. Laser ablation of both junctional and medial-apical F-actin revealed that epithelia act more as a continuous mechanical sheet rather than an array of contractile vertices (Ma et al. 2009) **(Fig.**

1.10 C). Even with these findings, epithelial tissues are still often thought of and modeled as an array of contractile vertices (Alt, Ganguly, and Salbreux 2017), and conclusions are made assuming the mechanical strain is stored only in circumferential actomyosin (Farhadifar et al. 2007; Fernandez-Gonzalez et al. 2009; Ratheesh et al. 2012; Leerberg et al. 2014; Van Itallie et al. 2015; Rauzi and Lenne 2015: Choi et al. 2016; Priya et al. 2016; Bertocchi et al. 2017). Medial-apical and circumferential actomyosin have distinct localization and organization, but also very similar components and contractile funcitons, and there are still many unanswered questions about the functions and interplay between the two. How are the medial-apical and circumferential actomyosin populations regulated and differentiated from one another, do they make the same molecular connects to junctions, do they promote the same mechanical signaling pathways, does one feed into the other?

Figure 1.10: Medial-apical actomyosin regulates apical forces in developing and steady state tissues

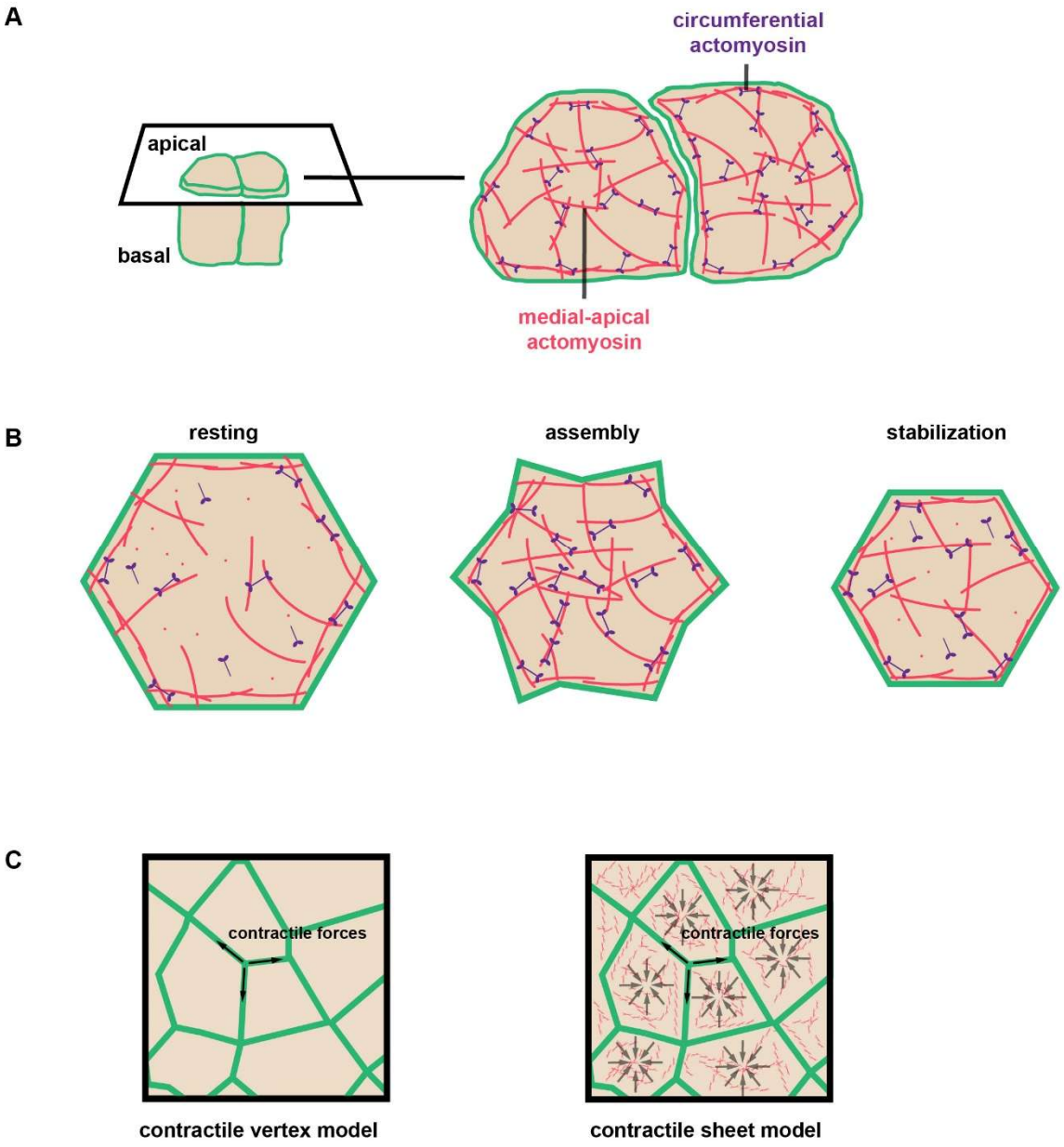

Figure 1.10: Medial-apical actomyosin regulates apical forces in developing and steady state tissues
A) A medial-apical actomyosin array is found across the apical surface of epithelial cells in addition to circumferential actomyosin. **B)** Pulses of increased medial-apical actomyosin assembly drive apical constriction during *Drosophila* gastrulation. **C)** At steady state, tissues are often thought of as a network that is only contractile at cell edges; however, the medial-apical actomyosin array is also a contractile load-bearing structure even in non-developing tissues.

Dissertation overview

In this dissertation, I investigate how epithelial cells respond to mechanical cues and regulate their cellular mechanics. In **Chapter 2**, I describe how vertebrate epithelial cells maintain the adhesion and barrier function of the tissue during cytokinesis by reinforcing their cell-cell junctions in response to forces generated by the contractile ring. In **Chapter 3**, I explore how the scaffolding protein Anillin contributes to epithelial cell and tissue mechanics. Preliminary experiments hinted that Anillin functions in generating tension in line with cell-cell junctions via the circumferential actomyosin belt; however, upon deeper investigation, I found a new role for Anillin in organizing medial-apical actomyosin, which has mechanical effects at the cell, tissue, and embryo level. In **Chapter 4**, I discuss the implications of my findings in the context of the field and propose future experiments that follow from my discoveries.

References

Alt, S, P Ganguly, G Salbreux. 2017. “Vertex Models: from Cell Mechanics to Tissue Morphogenesis”. *Philosophical Transactions of the Royal Society B: Biological Sciences* 372 (1720). The Royal Society: 20150520. doi:10.1098/rstb.2015.0520.

Arnold TR, RE Stephenson, AL Miller. 2017 “Rho GTPases and actomyosin: Partners in regulating epithelial cell-cell junction structure and function”. *Exp Cell Res* **358**, 20-30. doi: 10.1016/j.yexcr.2017.03.053.

Assaad, FF. 2001. “Plant Cytokinesis. Exploring the Links”. *PLANT PHYSIOLOGY* 126 (2). American Society of Plant Biologists (ASPB): 509–16. doi:10.1104/pp.126.2.509.

Baker, J, and D Garrod. 1993. “Epithelial Cells Retain Junctions during Mitosis”. *J Cell Sci* 104 (Pt 2): 415–25.

Baker, PC, and TE Schroeder. 1967. “Cytoplasmic Filaments and Morphogenetic Movement in the Amphibian Neural Tube”. *Developmental Biology* 15 (5). Elsevier BV: 432–50. doi:10.1016/0012-1606(67)90036-x.

Bertocchi, C, Y Wang, A Ravasio, Y Hara, Y Wu, T Sailov, MA Baird, et al. 2017. “Nanoscale Architecture of Cadherin-Based Cell Adhesions”. *Nat Cell Biol* 19: 28–37.

Bianconi, E, A Piovesan, F Facchin, A Beraudi, R Casadei, F Frabetti, L Vitale, MC Pelleri, S Tassani, F Pica, S Perez-Amodio, P Strippoli, S Canaider. 2013. “An Estimation of the Number of Cells in the Human Body”. *Ann Hum Biol* 40: 463–71. doi:10.3109/03014460.2013.807878.

Buckley, CD, J Tan, KL Anderson, D Hanein, N Volkmann, WI Weis, WJ Nelson, and AR Dunn. 2014. “Cell Adhesion. The Minimal Cadherin-Catenin Complex Binds to Actin Filaments under Force”. *Science* 346: 1254211. doi: 10.1126/science.1254211

Budnar, S, KB Husain, GA Gomez, M Naghibosidat, S Verma, NA Hamilton, RG Morris, and AS Yap. 2018. “Scaffolding of RhoA Contractile Signaling by Anillin: a Regulatory Analogue of Kinetic Proofreading”, March. Cold Spring Harbor Laboratory. doi:10.1101/282756.

Burnside, B. 1971. “Microtubules and Microfilaments in Newt Neuralation”. *Dev Biol* 26: 416–41.

Chen, L, S Xiao, K Pang, C Zhou, and X Yuan. 2014. “Cell Differentiation and Germ-Soma Separation in Ediacaran Animal Embryo-like Fossils”. *Nature* 516: 238–41.

Choi, W, BR Acharya, G Peyret, MA Fardin, RM Mège, B Ladoux, AS Yap, AS Fanning, and M Peifer. 2016. “Remodeling the Zonula Adherens in Response to Tension and the Role of Afadin in This Response”. *J Cell Biol* 213: 243–60.

Coravos, JS, and AC Martin. 2016. “Apical Sarcomere-like Actomyosin Contracts Nonmuscle Drosophila Epithelial Cells”. *Dev Cell* 39: 346–58.

Dayel, MJ, RA Alegado, SR Fairclough, TC Levin, SA Nichols, K McDonald, and N King. 2011. “Cell Differentiation and Morphogenesis in the Colony-Forming Choanoflagellate Salpingoeca Rosetta”. *Dev Biol* 357: 73–82.

Descovich, CP, DB Cortes, S Ryan, J Nash, L Zhang, PS Maddox, F Nedelec, and AS Maddox. 2017. “Crosslinkers Both Drive and Brake Cytoskeletal Remodeling and Furrowing in Cytokinesis”, June. Cold Spring Harbor Laboratory. doi:10.1101/150813.

Fanning, AS, BJ Jameson, LA Jesaitis, and JM Anderson. 1998. “The Tight Junction Protein ZO-1 Establishes a Link between the Transmembrane Protein Occludin and the Actin Cytoskeleton”. *J Biol Chem* 273: 29745–53.

Fanning, AS, CM Van Itallie, and JM Anderson. 2012. “Zonula Occludens-1 and -2 Regulate Apical Cell Structure and the Zonula Adherens Cytoskeleton in Polarized Epithelia”. *Mol Biol Cell* 23: 577–90.

Farhadifar, R, JC Röper, B Aigouy, S Eaton, and F Jülicher. 2007. “The Influence of Cell Mechanics Cell-Cell Interactions, and Proliferation on Epithelial Packing”. *Current Biology* 17 (24). Elsevier BV: 2095–2104. doi:10.1016/j.cub.2007.11.049.

Farquhar, MG, and GE Palade. 1963. “Junctional Complexes in Various Epithelia”. *J Cell Biol* 17: 375–412.

Fernandez-Gonzalez, R, SSM Simoes, JC Röper, S Eaton, and JA Zallen. 2009. “Myosin II Dynamics Are Regulated by Tension in Intercalating Cells”. *Developmental Cell* 17 (5). Elsevier BV: 736–43. doi:10.1016/j.devcel.2009.09.003.

Founounou, N, N Loyer, and R Le Borgne . 2013. “Septins Regulate the Contractility of the Actomyosin Ring to Enable Adherens Junction Remodeling during Cytokinesis of Epithelial Cells”. *Dev Cell* 24: 242–55. doi: 10.1016/j.devcel.2013.01.008.

Frenette, P, E Haines, M Loloyan, M Kinal, P Pakarian, and A Piekny. 2012. “An Anillin-Ect2 Complex Stabilizes Central Spindle Microtubules at the Cortex during Cytokinesis”. Edited by Claude Prigent. *PLoS ONE* 7 (4). Public Library of Science (PLoS): e34888. doi:10.1371/journal.pone.0034888.

Green, RA., E Paluch, and K Oegema. 2012. “Cytokinesis in Animal Cells”. *Annual Review of Cell and Developmental Biology* 28 (1). Annual Reviews: 29–58. doi:10.1146/annurev-cellbio-101011-155718.

Guillot, C, and T Lecuit. 2013. “Adhesion Disengagement Uncouples Intrinsic and Extrinsic Forces to Drive Cytokinesis in Epithelial Tissues”. *Dev Cell* 24: 227–41. doi: 10.1016/j.devcel.2013.01.010.

Guo, X, K Bonin, K Scarpinato, and M Guthold. 2014. “The Effect of Neighboring Cells on the Stiffness of Cancerous and Non-Cancerous Human Mammary Epithelial Cells”. *New Journal of Physics* 16 (10). IOP Publishing: 105002. doi:10.1088/1367-2630/16/10/105002.

Haigo, SL, JD Hildebrand, RM Harland, and JB Wallingford. 2003. “Shroom Induces Apical Constriction and Is Required for Hingepoint Formation during Neural Tube Closure”. *Curr Biol* 13: 2125–37.

Hartsock, A, and WJ Nelson. 2008. “Adherens and Tight Junctions: Structure Function and Connections to the Actin Cytoskeleton”. *Biochimica Et Biophysica Acta (BBA) - Biomembranes* 1778 (3). Elsevier BV: 660–69. doi:10.1016/j.bbamem.2007.07.012.

Hatte, G, C Prigent, and JP Tassan. 2018. “Tight Junctions Negatively Regulate Mechanical Forces Applied to Adherens Junctions in Vertebrate Epithelial Tissue”. *J Cell Sci* 131.

Herszterg, S, A Leibfried, F Bosveld, C Martin, and Y Bellaiche. 2013. “Interplay between the Dividing Cell and Its Neighbors Regulates Adherens Junction Formation during Cytokinesis in Epithelial Tissue”. *Dev Cell* 24: 256–70. doi: 10.1016/j.devcel.2012.11.019.

Hildebrand, JD, and P Soriano. 1999. “Shroom, a PDZ Domain-Containing Actin-Binding Protein, Is Required for Neural Tube Morphogenesis in Mice”. *Cell* 99: 485–97.

Hirokawa, N, TC Keller 3rd, R Chasan, and MS Mooseker. 1983. “Mechanism of Brush Border Contractility Studied by the Quick-Freeze, Deep-Etch Method”. *J Cell Biol* 96: 1325–36.

Ho B, A Baryshnikova, GW Brown. 2018 Unification of Protein Abundance Datasets Yields a Quantitative Saccharomyces cerevisiae Proteome”. *Cell Syst* **6**, 192-205.e3.

Itoh, M, M Furuse, K Morita, K Kubota, M Saitou, and S Tsukita. 1999. “Direct Binding of Three Tight Junction-Associated MAGUKs, ZO-1, ZO-2, and ZO-3, with the COOH Termini of Claudins”. *J Cell Biol* 147: 1351–63.

Jinguji, Y, and H Ishikawa. 1992. “Electron Microscopic Observations on the Maintenance of the Tight Junction during Cell Division in the Epithelium of the Mouse Small Intestine”. *Cell Structure and Function* 17 (1). Japan Society for Cell Biology: 27–37. doi:10.1247/csf.17.27.

Karfunkel, P. 1972. “The Activity of Microtubules and Microfilaments in Neurulation in the Chick”. *J Exp Zool* 181: 289–301.

Kumar, S, and VM Weaver. 2009. “Mechanics, Malignancy, and Metastasis: the Force Journey of a Tumor Cell”. *Cancer Metastasis Rev* 28: 113–27.

le Duc, Q, Q Shi, I Blonk, A Sonnenberg, N Wang, D Leckband, and J de Rooij. 2010. “Vinculin Potentiates E-Cadherin Mechanosensing and Is Recruited to Actin-Anchored Sites within Adherens Junctions in a Myosin II-Dependent Manner”. *J Cell Biol* 189: 1107–15. doi: 10.1083/jcb.201001149.

Lecuit, T, and AS Yap. 2015. “E-Cadherin Junctions as Active Mechanical Integrators in Tissue Dynamics”. *Nat Cell Biol* 17: 533–39. doi: 10.1038/ncb3136.

Leerberg, JM, GA Gomez, S Verma, EJ Moussa, SK Wu, R Priya, BD Hoffman, C Grashoff, MA Schwartz, and AS Yap. 2014. “Tension-Sensitive Actin Assembly Supports Contractility at the Epithelial Zonula Adherens”. *Curr Biol* 24: 1689–99.

Li, Y, AS Fanning, JM Anderson, and A Lavie. 2005. “Structure of the Conserved Cytoplasmic C-Terminal Domain of Occludin: Identification of the ZO-1 Binding Surface”. *J Mol Biol* 352: 151–64.

Lord, M, and TD Pollard. 2004. “UCS Protein Rng3p Activates Actin Filament Gliding by Fission Yeast Myosin-II”. *J Cell Biol* 167: 315–25.

Ma, X, HE Lynch, PC Scully, and MS Hutson. 2009. “Probing Embryonic Tissue Mechanics with Laser Hole Drilling”. *Physical Biology* 6 (3). IOP Publishing: 036004. doi:10.1088/1478-3975/6/3/036004.

Ma, X., M Kovacs, MA Conti, A Wang, Y Zhang, JR Sellers, and RS Adelstein. 2012. “Nonmuscle Myosin II Exerts Tension but Does Not Translocate Actin in Vertebrate Cytokinesis”. *Proceedings of the National Academy of Sciences* 109 (12). Proceedings of the National Academy of Sciences: 4509–14. doi:10.1073/pnas.1116268109.

Manukyan, A, K Ludwig, S Sanchez-Manchinelly, SJ Parsons, and PT Stukenberg. 2014. “A Complex of p190RhoGAP-A and Anillin Modulates RhoA-GTP and the Cytokinetic Furrow in Human Cells”. *Journal of Cell Science* 128 (1). The Company of Biologists: 50–60. doi:10.1242/jcs.151647.

Martin, AC, M Kaschube, and EF Wieschaus. 2009. “Pulsed Contractions of an Actin-Myosin Network Drive Apical Constriction”. *Nature* 457: 495–99.

Martin, P, and J Lewis. 1992. “Actin Cables and Epidermal Movement in Embryonic Wound Healing”. *Nature* 360: 179–83.

Miller, AL, and WM Bement. 2008. “Regulation of Cytokinesis by Rho GTPase Flux”. *Nature Cell Biology* 11 (1). Springer Nature: 71–77. doi:10.1038/ncb1814.

Nelson, WJ, and WI Weis. 2016. “25 Years of Tension over Actin Binding to the Cadherin Cell Adhesion Complex: The Devil Is in the Details”. *Trends Cell Biol* 26: 471–73.

Neujahr, R, C Heizer, and G Gerisch. 1997. “Myosin II-Independent Processes in Mitotic Cells of Dictyostelium Discoideum: Redistribution of the Nuclei, Re-Arrangement of the Actin System and Formation of the Cleavage Furrow”. *J Cell Sci* 110 (Pt 2): 123–37.

Nishimura, T, and M Takeichi. 2008. “Shroom3-Mediated Recruitment of Rho Kinases to the Apical Cell Junctions Regulates Epithelial and Neuroepithelial Planar Remodeling”. *Development* 135: 1493–1502.

Nodder, S, and P Martin. 1997. “Wound Healing in Embryos: a Review”. *Anat Embryol (Berl)* 195: 215–28.

Owaribe, K, and H Masuda. 1982. “Isolation and Characterization of Circumferential Microfilament Bundles from Retinal Pigmented Epithelial Cells”. *J Cell Biol* 95: 310–15.

Piekny, AJ, and AS Maddox. 2010. “The Myriad Roles of Anillin during Cytokinesis”. *Seminars in Cell & Developmental Biology* 21 (9). Elsevier BV: 881–91. doi:10.1016/j.semcdb.2010.08.002.

Piekny, AJ, and M Glotzer. 2008. “Anillin Is a Scaffold Protein That Links RhoA Actin and Myosin during Cytokinesis”. *Current Biology* 18 (1). Elsevier BV: 30–36. doi:10.1016/j.cub.2007.11.068.

Pollard, TD, and JQ Wu. 2010. “Understanding Cytokinesis: Lessons from Fission Yeast”. *Nature Reviews Molecular Cell Biology* 11 (2). Springer Nature: 149–55. doi:10.1038/nrm2834.

Pollard, TD. 2010. “Mechanics of Cytokinesis in Eukaryotes”. *Current Opinion in Cell Biology* 22 (1). Elsevier BV: 50–56. doi:10.1016/j.ceb.2009.11.010.

Priya, R, X Liang, JL Teo, K Duszyc, AS Yap, and GA Gomez. 2016. “ROCK1 but Not ROCK2 Contributes to RhoA Signaling and NMIIA-Mediated Contractility at the Epithelial Zonula Adherens”. Edited by Jeffrey D. Hardin. *Molecular Biology of the Cell* 28 (1). American Society for Cell Biology (ASCB): 12–20. doi:10.1091/mbc.e16-04-0262.

Quiros, M, and A Nusrat. 2014. “RhoGTPases Actomyosin Signaling and Regulation of the Epithelial Apical Junctional Complex”. *Seminars in Cell & Developmental Biology* 36 (December). Elsevier BV: 194–203. doi:10.1016/j.semcdb.2014.09.003.

Rappaport, R. 1996. *Cytokinesis in Animal Cells*. Cambridge University Press. doi:10.1017/cbo9780511529764.

Ratheesh, A, and AS Yap. 2012. “A Bigger Picture: Classical Cadherins and the Dynamic Actin Cytoskeleton”. *Nat Rev Mol Cell Biol* 13: 673–79.

Ratheesh, A, GA Gomez, R Priya, S Verma, EM Kovacs, K Jiang, NH Brown, A Akhmanova, SJ Stehbens, and AS Yap. 2012. “Centralspindlin and α-Catenin Regulate Rho Signalling at the Epithelial Zonula Adherens”. *Nat Cell Biol* 14: 818–28.

Rauzi M, PF Lenne. 2015 Probing cell mechanics with subcellular laser dissection of actomyosin networks in the early developing Drosophila embryo”. *Methods Mol Biol* **1189**, 209-18.

Reichl, EM, Y Ren, MK Morphew, M Delannoy, JC Effler, KD Girard, S Divi, PA Iglesias, SC Kuo, and DN Robinson. 2008. “Interactions between Myosin and Actin Crosslinkers Control Cytokinesis Contractility Dynamics and Mechanics”. *Curr Biol* 18: 471–80.

Shen, L, CR Weber, DR Raleigh, D Yu, and JR Turner. 2011. “Tight Junction Pore and Leak Pathways: a Dynamic Duo”. *Annu Rev Physiol* 73: 283–309.

Spadaro, D, S Le, T Laroche, I Mean, L Jond, J Yan, and S Citi. 2017. “Tension-Dependent Stretching Activates ZO-1 to Control the Junctional Localization of Its Interactors”. *Curr Biol* 27: 3783–95.e8.

Straight AF, CM Field, TJ Mitchison. 2005 Anillin binds nonmuscle myosin II and regulates the contractile ring”. *Mol Biol Cell* **16**, 193-201.

Sun, L, R Guan, IJ Lee, Y Liu, M Chen, J Wang, JQ Wu, and Z Chen. 2015. “Mechanistic Insights into the Anchorage of the Contractile Ring by Anillin and Mid1”. *Developmental Cell* 33 (4). Elsevier BV: 413–26. doi:10.1016/j.devcel.2015.03.003.

Swaminathan, V, K Mythreye, ET O’Brien, A Berchuck, GC Blobe, and R Superfine. 2011. “Mechanical Stiffness Grades Metastatic Potential in Patient Tumor Cells and in Cancer Cell Lines”. *Cancer Res* 71: 5075–80.

Takeichi, M. 2014. “Dynamic Contacts: Rearranging Adherens Junctions to Drive Epithelial Remodelling”. *Nat Rev Mol Cell Biol* 15: 397–410.

Umeda, K, J Ikenouchi, S Katahira-Tayama, K Furuse, H Sasaki, M Nakayama, T Matsui, S Tsukita, M Furuse, and S Tsukita. 2006. “ZO-1 and ZO-2 Independently Determine Where Claudins Are Polymerized in Tight-Junction Strand Formation”. *Cell* 126: 741–54.

Van Itallie, CM, AJ Tietgens, and JM Anderson. 2017. “Visualizing the Dynamic Coupling of Claudin Strands to the Actin Cytoskeleton through ZO-1”. *Mol Biol Cell* 28: 524–34.

Van Itallie, CM, AJ Tietgens, E Krystofiak, B Kachar, and JM Anderson. 2015. “A Complex of ZO-1 and the BAR-Domain Protein TOCA-1 Regulates Actin Assembly at the Tight Junction”. *Mol Biol Cell* 26: 2769–87.

Van Itallie, CM, and JM Anderson. 2014. “Architecture of Tight Junctions and Principles of Molecular Composition”. *Semin Cell Dev Biol* 36: 157–65.

Wittchen, ES, J Haskins, and BR Stevenson. 1999. “Protein Interactions at the Tight Junction. Actin Has Multiple Binding Partners, and ZO-1 Forms Independent Complexes with ZO-2 and ZO-3”. *J Biol Chem* 274: 35179–85.

Wu, Y, P Kanchanawong, and R Zaidel-Bar. 2015. “Actin-Delimited Adhesion-Independent Clustering of E-Cadherin Forms the Nanoscale Building Blocks of Adherens Junctions”. *Dev Cell* 32: 139–54.

Yonemura, S, Y Wada, T Watanabe, A Nagafuchi, and M Shibata. 2010. “Alpha-Catenin as a Tension Transducer That Induces Adherens Junction Development”. *Nat Cell Biol* 12: 533–42.

Zaidel-Bar, R, G Zhenhuan, and C Luxenburg. 2015. “The Contractome - a Systems View of Actomyosin Contractility in Non-Muscle Cells”. *Journal of Cell Science* 128 (12). The Company of Biologists: 2209–17. doi:10.1242/jcs.170068.

Zhao WM, G Fang. 2005. MgcRacGAP controls the assembly of the contractile ring and the initiation of cytokinesis”. *Proc Natl Acad Sci U S A* **102**, 13158-63.

Chapter 2

Maintenance of the epithelial barrier and mechanical reinforcement of adherens junctions during epithelial cytokinesis

Abstract

Epithelial integrity and barrier function must be maintained during the complex cell shape changes that occur during cytokinesis in vertebrate epithelial tissue. Here, we investigate how cell-cell junctions are maintained and remodeled during cell division in the *Xenopus laevis* embryo. We find that epithelial barrier function is not disrupted during cytokinesis and is mediated by sustained tight junctions. Using fluorescence recovery after photobleaching (FRAP), we demonstrate that adherens junction proteins are stabilized at the cleavage furrow by increased tension. We find that Vinculin, which is localized to adherens junctions under tension to reinforce their connection to the cytoskeleton, is recruited to the adherens junction at the cleavage furrow and that inhibiting recruitment of Vinculin by expressing a dominant negative mutant increases the rate of furrow ingression. Our data provide new insight into how epithelial integrity and barrier function are maintained throughout cytokinesis in vertebrate epithelial tissue.

This chapter is a modified version of the manuscript published in *Current Biology* "Maintenance of the Epithelial Barrier and Remodeling of Cell-Cell Junctions During Cytokinesis" (Higashi 2016). Tomohito Higashi performed experiments in 2.1, 2.2, 2.6, S2.2, & generated Figure 2.7. Kayla Dinshaw, an undergraduate who I mentored, assisted with experiments in Figure 2.6.

Introduction

Polarized cells make epithelial sheets and maintain tissue homeostasis by serving as barriers that separate distinct compartments in the body. Cells in epithelial sheets exhibit high rates of turnover, and the number of dying cells must be balanced by the number of dividing cells (Eisenhoffer and Rosenblatt 2013). Epithelial sheets are dynamic and undergo cell shape changes such as cell division, extrusion, or intercalation and it is unknown if barrier function is maintained during these dynamic processes (Guillot and Lecuit 2013). Cell-cell junctions are essential for maintaining epithelial integrity and barrier function of epithelial sheets during homeostasis and morphogenesis.

Vertebrate apical junctional complexs consists of tight junctions, adherens junctions, and desmosomes (Hartsock and Nelson 2008; Van Itallie and Anderson 2014; Green et al. 2009). Connections to the actomyosin cytoskeleton are important for the structural integrity and regulation of both tight junctions and adherens junctions (Rodgers and Fanning 2011). Tight junctions seal the intercellular spaces between adjacent cells and form a selective, regulated barrier. Tight junctions consist of Claudin-based strands (Furuse et al. 1998) and cytoplasmic plaque proteins, including ZO-1, which binds to the cytoplasmic tail of Claudins (Itoh, Morita, and Tsukita 1999) and links tight junctions to actin filaments. Adherens junctions mediate cell-cell adhesion and are important for epithelial tissue integrity, which is challenged when cells undergo shape changes (Lecuit and Yap 2015). Adherens junction structure is dependent upon E-cadherin; its extracellular domain mediates strong adhesion between adjacent cells, whereas its cytoplasmic tail is associated with the cytoplasmic plaque proteins β-catenin and α-catenin (Yonemura et al. 2010; Huveneers et al. 2012). Adherens

junctions can be linked to actin filaments via α-catenin (Buckley et al. 2015), as well other proteins, some of which help reinforce cell adhesion during mechanical stress (Leerberg et al. 2014; Nowotarski and Peifer 2014; Choi et al. 2016; Ratheesh and Yap 2012).

Until recently, cell-cell junctions were considered highly stable protein complexes (Sasaki et al. 2003). However, fluorescence recovery after photobleaching (FRAP) experiments in cultured epithelial cells demonstrated that, whereas overall junction structure is maintained at steady state, individual tight junction and adherens junction proteins are, in fact, highly dynamic (Shen, Weber, and Turner 2008; Huang et al. 2011; Yamada et al. 2005). Importantly, changes in the dynamics of individual junction proteins can regulate epithelial function (Yu et al. 2010). This plasticity of cell-cell junction structure is likely important for maintenance of barrier function when cells undergo shape changes during morphogenesis or cell division.

Cell division helps shape the organization of epithelial tissues by generating a new cell interface and two new cell vertices with each cell division (Guillot and Lecuit 2013; Gibson et al. 2006). During cytokinesis, an actomyosin-based contractile ring is formed at the cell equator and generates force to physically separate one cell into two daughter cells (Fededa and Gerlich 2012; Green, Paluch, and Oegema 2012). In epithelial cells, both the dividing cell and its neighboring cells undergo shape changes, and, accordingly, cell-cell junctions must be dynamically reorganized. Pioneering work using electron or immunofluorescence microscopy in fixed epithelial tissues or cultured epithelial cells reported that cell-cell junctions are maintained throughout cytokinesis (Jinguji and Ishikawa 1992; Baker and Garrod 1993). However, junction maintenance and remodeling during cytokinesis has not been investigated in live vertebrate epithelial tissues, and it remains unclear how epithelial cells maintain barrier

function and epithelial integrity while at the same time dynamically changing shape during cytokinesis.

In this study, we used live-cell imaging of fluorescently tagged junctional proteins in the epithelium of gastrula-stage *Xenopus laevis* embryos to investigate how cell-cell junctions, including tight junctions and adherens junctions, are maintained and remodeled during cytokinesis. Further, I examined how tension generated by the contractile ring affects the stability of tight and adherens junction proteins, and we identified a mechanism that strengthens the adherens junction at the cleavage furrow. Together, these results shed new light on how barrier properties are maintained in proliferating vertebrate epithelial tissues.

Results

Epithelial barrier function is maintained during vertebrate epithelial cytokinesis

Although data from electron micrographs and immunostaining of fixed samples suggested that epithelial barrier function is maintained throughout cytokinesis (Jinguji and Ishikawa 1992; Baker and Garrod 1993), there has been no direct evidence of barrier maintenance during cell division in live cells. In order to evaluate barrier function during cytokinesis in live cells, we imaged fluorescein (332 Da) applied to the apical side of the epithelium of gastrula-stage *Xenopus* embryos expressing mRFP-ZO-1 and mCherry-H2B as markers for tight junctions and chromosomes, respectively. Embryos were mounted in medium containing fluorescein and imaged using time-lapse confocal microscopy **(Fig. 2.1A)**. In dividing cells, fluorescein was restricted to the apical side of the tight junction **(Fig. 2.1B)**. When the barrier function was disrupted by injecting embryos with EGTA, which chelates Ca^{2+} and results in adherens junction disruption and tight junction dysfunction (Takeichi 1995; Liu and Cheney

2012), fluorescein breached the tight junction, spreading to the basolateral side **(Fig. 2.1C and D)**. These results indicate that epithelial barrier function is maintained throughout cytokinesis.

Figure 2.1: Barrier function is maintained during Xenopus epithelial cytokinesis

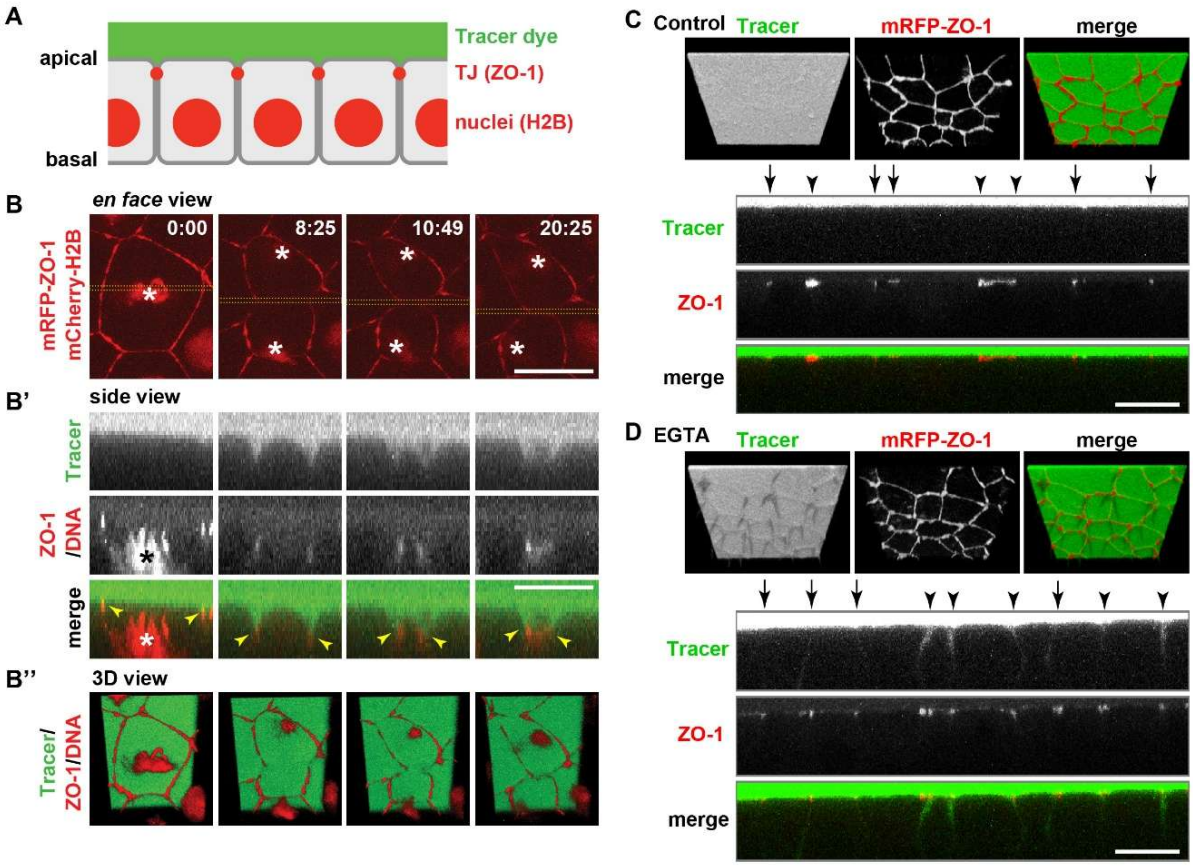

Figure 2.1: Barrier function is maintained during *Xenopus* epithelial cytokinesis
A) Experimental setup for fluorescent tracer penetration assay. Gastrula-stage embryos expressing mRFP-ZO-1 (tight junctions) and mCherry-H2B (chromosomes) were mounted in 0.1X MMR containing 10 mM fluorescein (tracer dye) and observed. **B)** Fluorescent tracer penetration assay of a representative dividing cell. Three views of the same region of interest are shown: *en face* view (B), side view of the region indicated with yellow rectangles in **(B)**, **(B')**, and 3D view **(B")**. Note that the tight junction labeled by mRFP-ZO-1 (red) is initially pulled basally, but fluorescein (green) at the apical side (top) does not breach through the tight junction (yellow arrowheads in B') to the basal side (bottom). Time, mins. Asterisks in **(B)** and at 0:00 in **(B')** indicate chromosomes (red), which are not visible at other time points in **(B')**. **C)** and **D)** Embryos expressing mRFP-ZO-1 (red) were injected with 5 nl of 0.1X MMR **(C)** or 100 mM EGTA **(D)** into the blastocoel, mounted in 10 mM fluorescein (green), and observed. Upper panels show 3D view; lower panels show side view. Note that fluorescein tracer breaches the tight junction in **(D)** (EGTA-treated), but not in **(C)** (control). Arrows and arrowheads indicate bicellular and tricellular junctions, respectively. Scale bars represent 20 µm.

Adherens junctions and tight junctions remain continuous and connected to the contractile ring during cytokinesis

To understand how epithelial cells maintain barrier function during cytokinesis, we investigated how tight junctions are reorganized during cytokinesis by confocal imaging of embryos expressing mRFP-ZO-1 and Lifeact-GFP. Lifeact-GFP binds to F-actin and labels both the actomyosin contractile ring and apical actomyosin at cell-cell junctions **(Fig. 2.2A)**. Before cytokinesis onset, ZO-1 and F-actin were present at cell-cell junctions surrounding the dividing cell, and cortical actin was visible at the apical surface **(Fig. 2.2A)**. The contractile ring formed at the cell equator orthogonal to the junctional plane **(Fig. 2.2A)**. Consistent with previous reports of polarized epithelial cell cleavage (Jinguji and Ishikawa 1992; Guillot and Lecuit 2013; Le et al. 2011; Reinsch and Karsenti 1994), the contractile ring ingressed anisotropically where the basal side of the ring contracts more rapidly than the apical side. Importantly, tight junctions remained continuous and appeared to be connected to the contractile ring throughout cytokinesis **(Fig. 2.2A)**. We then examined the behavior of adherens junctions during cytokinesis using E-cadherin-3xGFP (E-cad-3xGFP) as a probe. Notably, adherens junctions were also unbroken and maintained connection to the ingressing contractile ring throughout cytokinesis **(Fig. 2.2B)**. We conclude that, in the *Xenopus* gastrula epithelium, tight junctions and adherens junctions remain continuous and connected with the contractile ring during cytokinesis, which likely contributes to maintenance of the epithelial barrier function.

Figure 2.2: Tight and adherens junctions remain continuous and connected to the contractile ring during cytokinesis

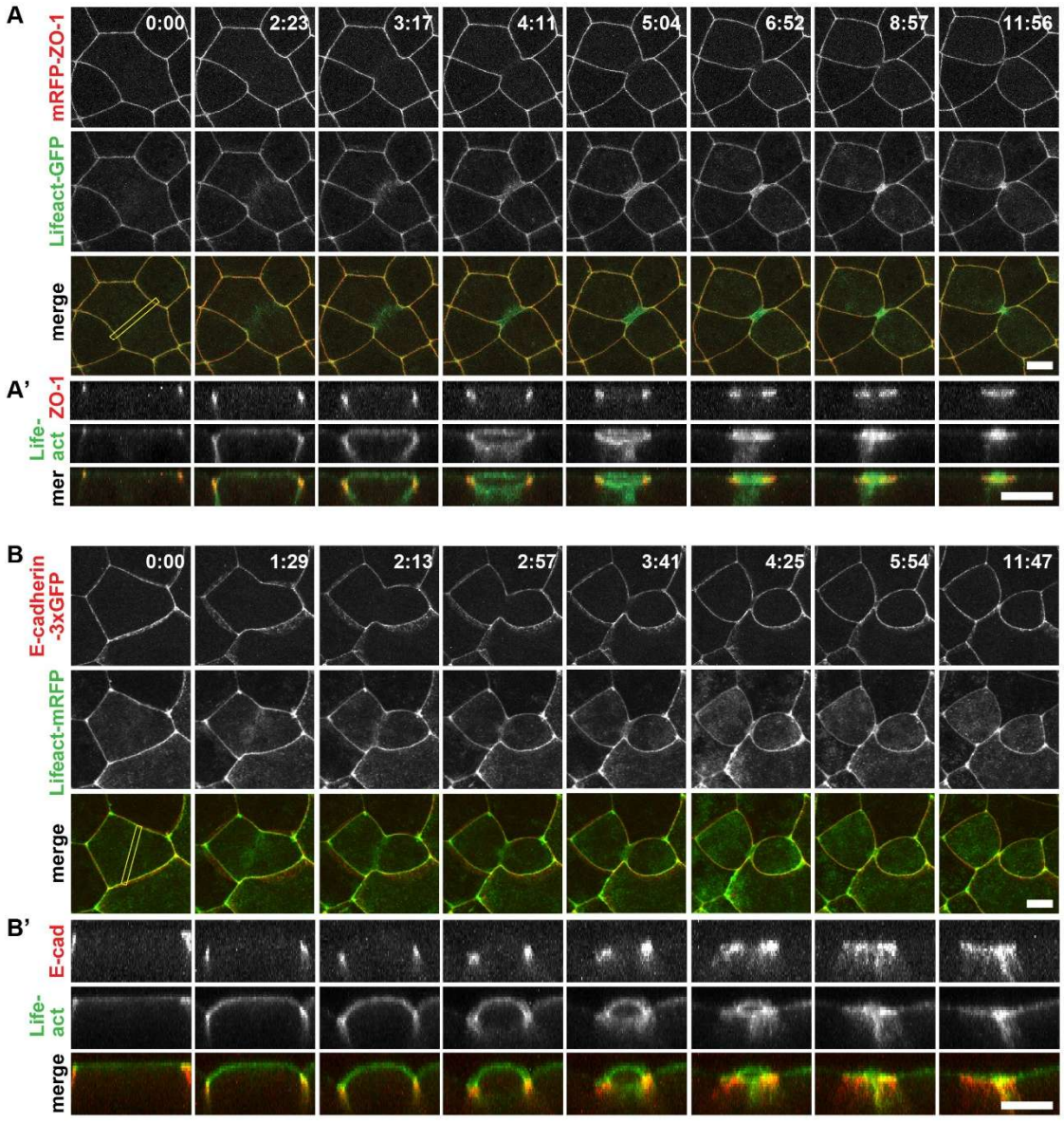

Figure 2.2: Adherens junctions and tight junctions remain continuous and connected to the contractile ring during cytokinesis

A) Live imaging of tight junctions and the cytokinetic contractile ring in embryos expressing mRFP-ZO-1 (red, tight junctions) and Lifeact-GFP (green, F-actin). Projected multi-plane *en face* images **(A)** and side views at the cleavage plane **(A')** (yellow rectangle in the *en face* view) are shown. Note that the cytokinetic ring remains connected to tight junctions throughout cytokinesis. **B)** Live imaging of adherens junctions and the cytokinetic contractile ring in embryos expressing E-cad-3xGFP (pseudocolored red, adherens junctions) and Lifeact-mRFP (pseudocolored green, F-actin). Projected multi-plane *en face* images **(B)** and side views at the cleavage plane (**B'**; yellow rectangle in the *en face* view) are shown. Note that the cytokinetic ring remains connected to adherens junctions throughout cytokinesis. For side views, top is apical and bottom is basal. Scale bars represent 10 µm.

Adherens junction proteins, but not tight junction proteins, are stabilized at the cleavage furrow of dividing cells

Although the overall structure of tight junctions and adherens junctions remains intact during cytokinesis, and both junctions appear to be connected to the ingressing contractile ring by fluorescence microscopy **(Fig. 2.2)**, it remained unclear whether the tension generated by the contractile ring affected the dynamics of individual junction proteins. To answer this question, I compared FRAP curves for the adherens junction proteins E-cadherin (E-cad-3xmChe) and β-catenin (β-catenin-GFP) and the tight junction proteins Claudin-6 (mCherry-Claudin-6) and ZO-1 (mRFP-ZO-1) in interphase cells and dividing cells at both the cleavage furrow and a polar region **(Fig. 2.3A and S2.1A)**. There were no significant differences in FRAP between interphase cells and the polar region of cells undergoing cytokinesis, indicating that junction protein dynamics are not globally changed in dividing cells **(Fig. 2.3B–2.3F and S1)**. Notably, the mobile fraction for E-cadherin was significantly reduced at the cleavage furrow compared with the polar region (41.0% ±2.2% versus 73.2% ± 2.6%, respectively; **Fig. 2.3B and 2.3C**), indicating that E-cadherin is stabilized at the cleavage furrow. Similar results were observed for β-catenin; the mobile fraction was strongly reduced at the cleavage furrow compared with the polar region (39.5% ± 4.4% versus 62.4% ± 2.0%, respectively; **Fig. 2.3D**). In contrast to the adherens junction proteins, the mobile fractions of Claudin-6 and ZO-1 were unchanged at the cleavage furrow compared with the polar region (Claudin, 39.8% ± 3.3% versus 34.6% ± 2.0%; ZO-1, 67.9% ± 0.7% versus 70.9% ±2.0%; **Fig. 2.3E, 2.3F, and S2.1**).

Figure 2.3: Adherens, but not tight junction proteins, are stabilized at the cleavage furrow of dividing cells

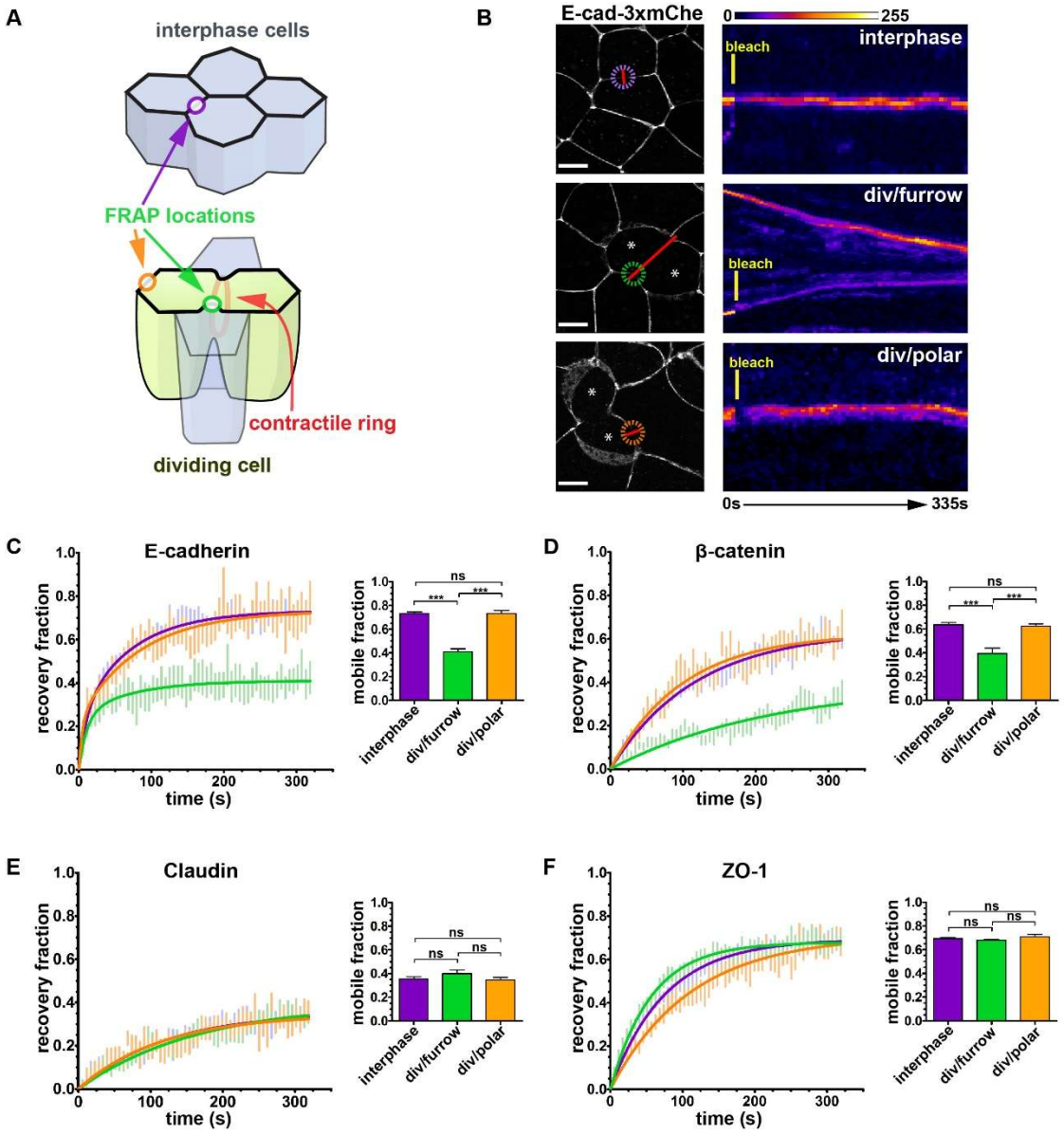

Figure 2.3: Adherens junction proteins, but not tight junction proteins, are stabilized at the cleavage furrow of dividing cells

A) Diagram depicting locations of FRAP measurements in interphase (purple circle) and dividing cells (green circle, cleavage furrow; orange circle, polar region). **B)** Representative examples of E-cad-3x mCherry FRAP. Cell images (left) show a frame taken from a time-lapse movie. The colored dashed circles indicate the bleached areas, the red lines indicate the locations used to generate the kymographs (right), and the white asterisks indicate the two daughter cells. A FIRE look up table was applied to the kymographs; time (horizontal axis) and bleach time points are indicated. Scale bars represent 10 um. **C)** E-cad-3xmCherry FRAP data fitted with a double exponential curve and graph of average mobile fractions. The numbers of cells (n) quantified are interphase cells (n = 23), dividing cells/furrow (n = 17), and dividing cells/polar (n = 12). **D–F)** FRAP data of β-catenin-GFP **(D)**, mCherry-Claudin-6 **(E)**, and mRFP-ZO-1 **(F)** fitted with a single exponential curve and graph of average mobile fractions. n = 21, 19, and 14 **(D)**; n = 23, 18, and 10 **(E)**; and n = 34, 34, and 21**(F)**.

Tension generated by the contractile ring stabilizes E-cadherin.

Our finding that adherens junction proteins are stabilized at the furrow during cytokinesis is consistent with previous studies showing that adherens junction proteins are stabilized under high tension and are more dynamic under reduced tension (Yonemura et al. 2010; Priya, Yap, and Gomez 2013; Ratheesh et al. 2012). We tested this idea in *Xenopus* embryos by using pharmacological approaches to globally increase or decrease tension **(Fig. 2.4)**. Interphase cells in embryos treated with the phosphatase inhibitor calyculin A, which increases tension (Fernandez-Gonzalez et al. 2009; Ishihara et al. 1989), exhibited stabilized junctional E-cadherin compared to controls (mobile fraction, 56.1% ± 3.4%versus 73.5% ± 3.1%; **Fig. 2.4A**). ZO-1 was stabilized in cells treated with calyculin A (mobile fraction, 62.8% ± 1.0% versus 75.5% ± 1.2%; **Fig. 2.4D**), but not at the furrow **(Fig. 2.3F)**, indicating that tension from the ingressing contractile ring is transmitted primarily to the adherens junction not the tight junction.

To reduce tension generated by the contractile ring, we injected embryos with the Rho-associated protein kinase (ROCK) inhibitor Y-27632 to reduce Myosin II activity (Narumiya, Ishizaki, and Ufhata 2000). E-cadherin was more dynamic at the cleavage furrow in Y-27632-treated cells compared to controls (mobile fraction, 59.3% ± 4.0% versus 40.3% ± 2.0%; **Fig. 2.4B**). Treatment with the same concentration of Y-27632 did not affect E-cadherin dynamics in interphase cells compared to controls (mobile fraction, 80.2% ± 2.3% versus 80.5% ± 1.1%; **Fig. 2.4C**). In line with our findings that E-cadherin is stabilized by tension from the contractile ring but ZO-1 is not, co-imaging of E-cad-3xGFP and mRFP-ZO-1 during cytokinesis also revealed that the adherens junction invaginated faster than the tight junction, with the tight junction

completing invagination around 10 min after the adherens junction **(Fig. S2.2A**). To confirm these results, we also examined GFP-Claudin-6 and E-cad-3xmCherry-expressing embryos **(Fig. S2.2B)**. The invagination of Claudin-6 was also delayed compared with invagination of E-cadherin **(Fig. S2.2B)**. Likewise, when cells in late cytokinesis were examined by immunofluorescence microscopy, endogenous β-catenin had ingressed farther than ZO-1 **(Fig. S2.2C)**. Together these data indicate that the adherens junction is the load-bearing junction for the contractile ring, and it completes invagination prior to the tight junction.

Figure 2.4: Tension generated by the contractile ring stabilizes E-cadherin

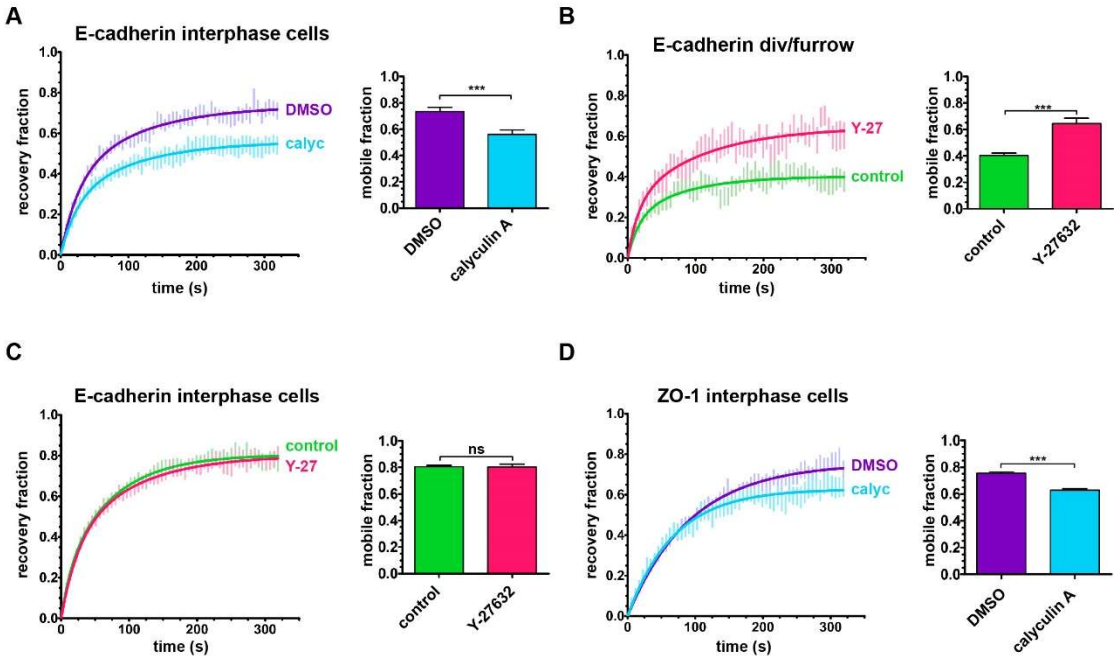

Figure 2.4: Tension generated by the contractile ring stabilizes E-cadherin
A) E-cadherin-3xmCherry FRAP data of interphase cells fitted with a double exponential curve and graph of average mobile fractions when treated with vehicle (dimethyl sulfoxide, DMSO) or 500 nM calyculin A. The number of cells (n) quantified is: DMSO (n=29), calyculin A (n=30). **B)** E-cadherin-3xmCherry FRAP data at the furrow of dividing cells fitted with a double exponential curve and graph of average mobile fractions when injected with H_2O (control) or 1 ng of Y-27632. The number of cells (n) quantified is: control (n=19), Y-27632 (n=20). **C)** E-cadherin-3xmCherry FRAP data of interphase cells fitted with a double exponential curve and graph of average mobile fractions when injected with H_2O (control) or 1 ng of Y-27632. The number of cells (n) quantified is: control (n=30), Y-27632 (n=29). **D)** mRFP-ZO-1 FRAP data of interphase cells fitted with a single exponential curve and graph of average mobile fractions when treated with vehicle (dimethyl sulfoxide, DMSO) or 500 nM calyculin A. The number of cells (n) quantified is: DMSO (n=35), calyculin A (n=26).

Tension generated by the contractile ring recruits Vinculin to the cleavage furrow.

The adherens junction protein α-catenin is known to act as a tension transducer that senses increased junctional tension generated by pulling forces from adjacent cells and responds by strengthening the junction (Yonemura et al. 2010; Leerberg et al. 2014). High tension induces a conformational change in α-catenin and recruitment of Vinculin to adherens junctions (Yonemura et al. 2010). To confirm that Vinculin-3xGFP is recruited to adherens junctions in response to increased tension in *Xenopus*, we increased junctional tension globally in two ways. First, embryos treated with calyculin A exhibited a ~2-fold increase in Vinculin-3xGFP recruitment to junctions, whereas the intensity of E-cad-3xmCherry was unchanged **(Fig. 2.5A)**. Second, upon addition of ATP, which also increases contractility (Joshi, von Dassow, and Davidson 2010; Kim et al. 2014), the embryo exhibited contraction within 60 s and a significant increase (~3-fold) in the intensity of Vinculin-3xGFP at junctions within minutes **(Fig. 2.5B)**. Next, we tested whether fluorescently-tagged Vinculin is recruited in response to increased junctional tension generated during cytokinesis. Vinculin-3xGFP was significantly increased specifically at the cleavage furrow **(Fig. 2.5C-J)**, whereas the intensity of a membrane marker **(Fig. 2.5C-F)** or a-catenin **(Fig. 2.5G-J)** was not. Together, these results suggest that elevated tension reinforces adherens junctions connected to the contractile ring by increasing the stability of individual adherens junction proteins and recruiting Vinculin to the cleavage furrow.

Figure 2.5: Tension generated by the contractile ring recruits Vinculin to the cleavage furrow

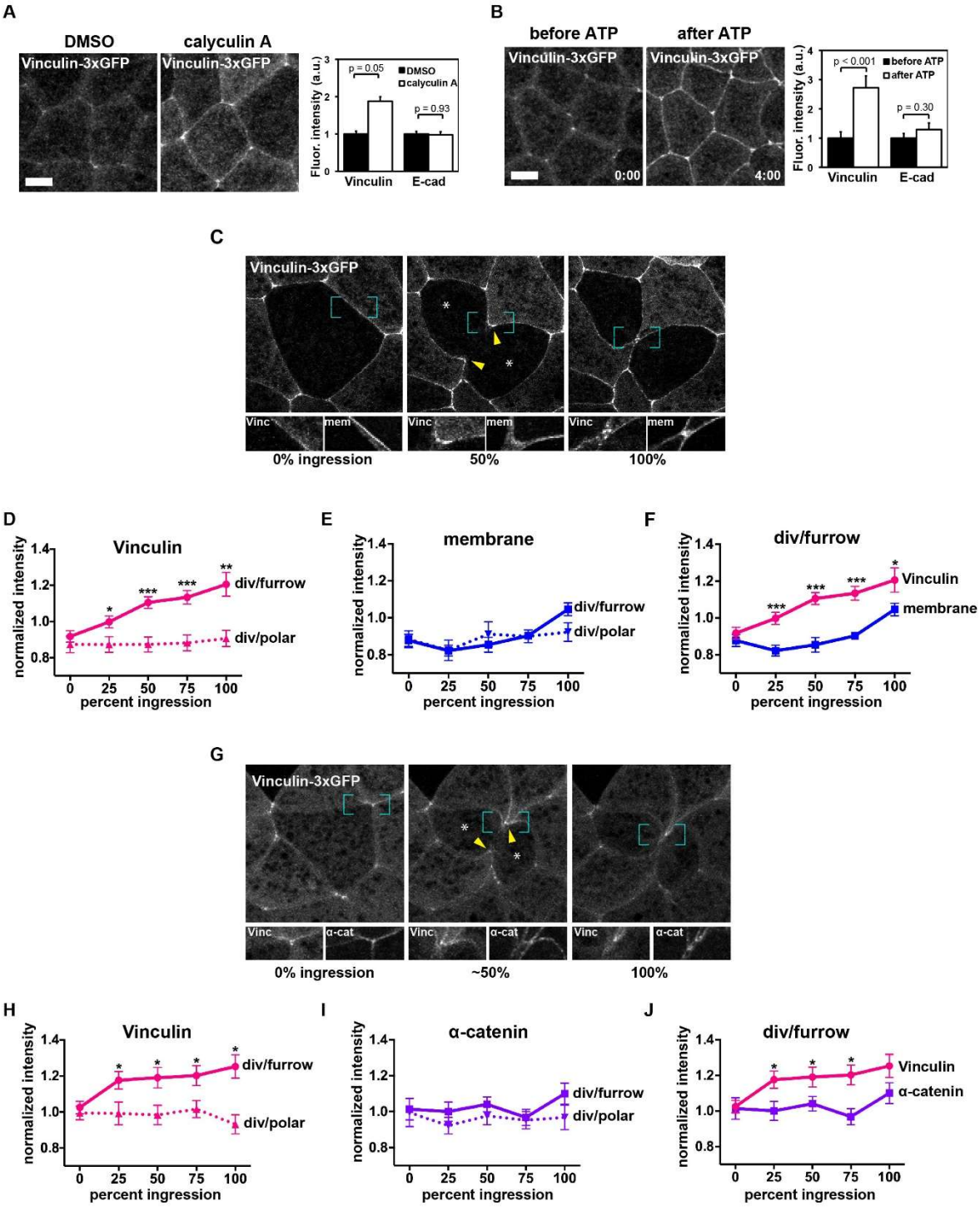

Figure 2.5: Tension generated by the contractile ring recruits Vinculin to the cleavage furrow
A) Vinculin-3xGFP in embryos treated with DMSO or calyculin A. Quantification of Vinculin recruitment to junctions and E-cadherin-3xmCherry intensity with calyculin A treatment. Scale bar, 10 µm. **B)** Vinculin-3xGFP before and after addition of extracellular ATP. Quantification of Vinculin recruitment to junctions and E-cadherin-3xmCherry intensity after ATP addition. Scale bar, 10 µm. **C)** Vinculin-3xGFP in a dividing cell. White asterisks indicate daughter cells, yellow arrowheads indicate accumulation of Vinculin-3xGFP at the cleavage furrow, and blue brackets indicate magnified areas of Vinculin-3xGFP and mCherry-membrane shown below the cell view. **D)** Quantification of Vinculin-3xGFP at the cleavage furrow and polar region of dividing cells. The number of cells quantified is: (n=14). **E)** Quantification of a fluorescent membrane marker, mCherry-farnesyl, at the cleavage furrow or polar region of dividing cells. The number of cells quantified is: (n=14). **F)** Quantification of Vinculin-3xGFP and mCherry-membrane intensity at the cleavage furrow of dividing cells (n = 14). Error bars represent SEM. **G)** Vinculin-3xGFP in a dividing cell. White asterisks indicate daughter cells, yellow arrowheads indicate accumulation of Vinculin-3xGFP at the cleavage furrow, and blue brackets indicate magnified areas of Vinculin-3xGFP and mCherry-α-catenin shown below the cell view. **H)** Quantification of Vinculin-3xGFP at the cleavage furrow and polar region of dividing cells. The number of cells quantified is: (n=9). **I)** Quantification of mCherry-α-catenin intensity at the cleavage furrow and polar regions of dividing cells. The number of cells quantified is: (n=9). **J)** Quantification of Vinculin-3xGFP and mCherry-α-catenin intensity at the cleavage furrow of dividing cells. The number of cells quantified is: (n=9) Error bars, S.E.M. Statistics, unpaired Student's t-test, *p<0.05, **p<0.001, ***p<0.0001

Dominant-negative Vinculin abolishes cell-cell junction reinforcement at the cleavage furrow and accelerates ingression

To test how reinforcement of adherens junctions at the cleavage furrow, in turn, affects the process of cytokinesis, we perturbed Vinculin-mediated adherens junction strengthening. For this purpose, we developed a dominant-negative Vinculin. Vinculin is localized at adherens junctions through interaction of its N-terminal D1 domain with α-catenin under tension, and Vinculin recruits F-actin through its C-terminal D5 domain **(Fig. 2.6A)** (Choi et al. 2012; Peng et al. 2012). We predicted that overexpression of the D1 domain alone, which localizes at adherens junctions **(Fig. S2.2D)**, would competitively interfere with recruitment of full-length Vinculin to adherens junctions and might abolish tension-mediated reinforcement of adherens junctions. We tested the dominant-negative effect of Vinculin D1 by expressing full-length Vinculin-3xGFP uniformly and untagged Vinculin D1 with an injection marker in a mosaic manner. As predicted, the localization of Vinculin-3xGFP at both bicellular and tricellular

junctions was drastically reduced in Vinculin-D1-expressing cells **(Fig. 2.6B)**. The recruitment of Vinculin-3xGFP to the cleavage furrow in dividing cells was also abolished when the cell neighboring the cleavage plane expressed Vinculin D1 **(Fig. 2.6C)**.

We examined the effect of Vinculin D1 on the behavior of adherens junctions and tight junctions during cytokinesis by imaging embryos co-expressing E-cad-3xGFP and mRFP-ZO-1 **(Fig. 2.6)**. In control cells, signal intensity for both adherens junctions and tight junctions was maintained at the cleavage furrow throughout cytokinesis **(Fig. 2.6D, 2.6D', and S2.2A)**. In fact, early in cytokinesis (25% ingression), the intensity of ZO-1 and E-cadherin at the cleavage furrow was slightly but significantly increased compared with a polar region **(Fig. 2.6H)**. In contrast, signal for both adherens junctions and tight junctions was reduced at the cleavage furrow in Vinculin-D1-expressing cells **(Fig. 2.6E, 2.6E', 2.6I, and S2.2E)**, suggesting that inhibition of Vinculin localization abolishes the reinforcement of adherens junctions at the cleavage furrow. Furthermore, Vinculin-D1-expressing cells ingressed much faster than control cells **(Fig. 2.6F and 2.6G)**, likely due to a lack of counteracting force from the cells neighboring the cleavage furrow. These data indicate that Vinculin-mediated adherens junction reinforcement is involved in maintenance of both adherens junctions and tight junctions at the cleavage furrow of dividing cells.

Figure 2.6: Dominant-negative Vinculin abolishes junction reinforcement at the cleavage furrow and accelerates ingression

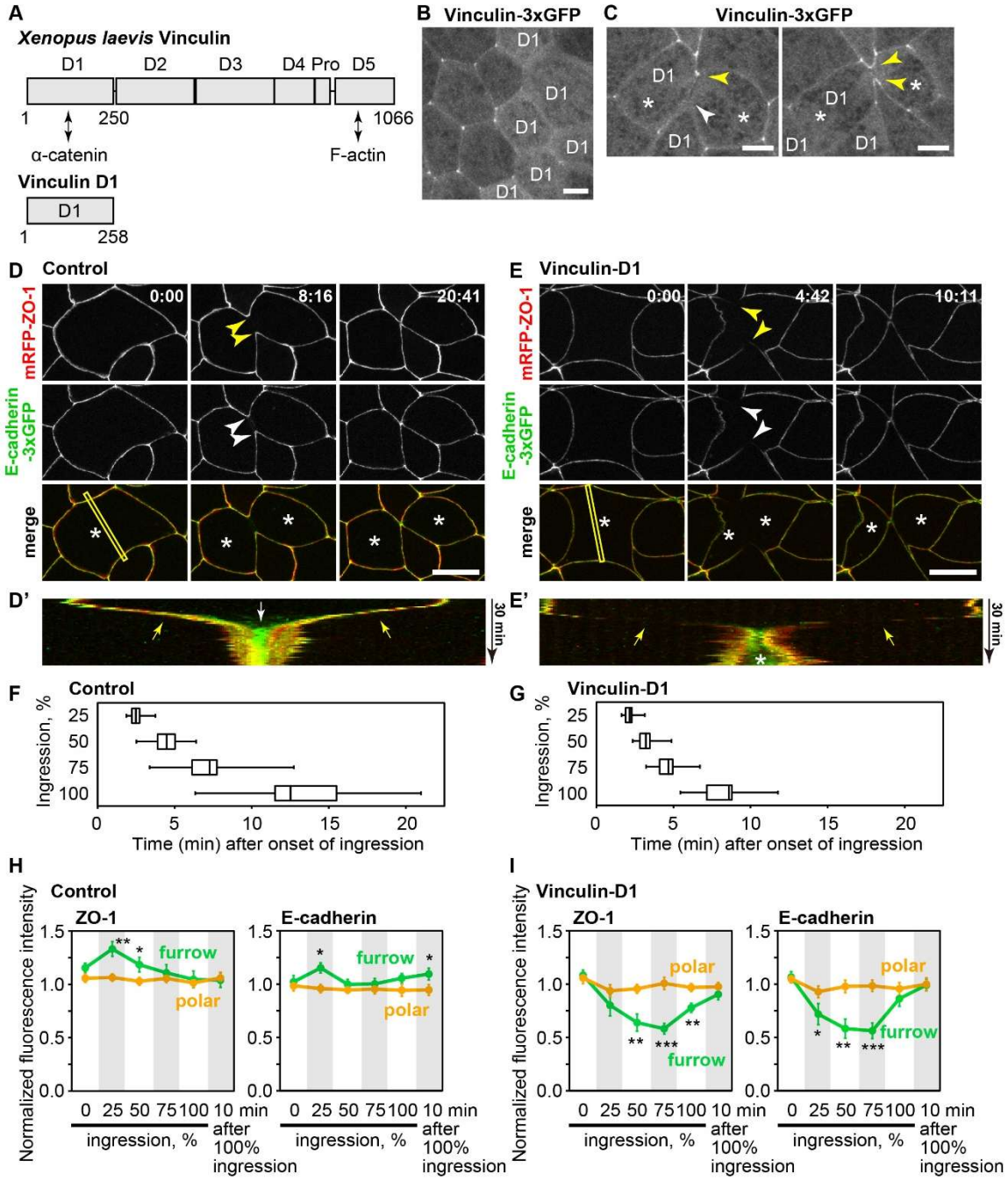

Figure 2.6: Dominant-negative Vinculin abolishes cell-cell junction reinforcement at the cleavage furrow and accelerates ingression

A) Domain structure of *Xenopus laevis* Vinculin. Pro, proline-rich region. **(B and C)** Live imaging of Vinculin-3xGFP in interphase **(B)** and dividing **(C)** cells of embryos expressing Vinculin D1 in a mosaic manner. D1 indicates Vinculin D1-expressing cells, which are identified with a lineage tracer (mCherry-H2B; not shown). Note that Vinculin-3xGFP intensity at bicellular and tricellular adherens junctions is reduced in **(B)**, and the localization of Vinculin at cleavage furrow (yellow arrowheads) is abolished when the neighbor cell expresses Vinculin D1 (white arrowhead). Asterisks in **(C)** indicate daughter cells. Scale bars represent 10 µm. **(D and E)** Live imaging of embryos expressing mRFP-ZO-1 (red, tight junctions) and E-cad-3xGFP (green, adherens junctions) without **(D)** or with **(E)** expression of Vinculin D1. Arrowheads show that ZO-1 (yellow arrowheads) and E-cadherin (white arrowheads) are maintained at the cleavage furrow in control cells **(D)** or reduced in Vinculin-D1-expressing cells **(E)**. Scale bars represent 20 µm. **(D' and E')** Kymographs of the furrow region shown by yellow rectangles in **(D)** and **(E)**. Note that E-cadherin (green) completes invagination (white arrow) before ZO-1 (red) in **(D')** and that both E-cadherin and ZO-1 are maintained **(D')** or reduced **(E')** at ingressing furrow region (yellow arrows). In (E 0), two vertices move apart after division (asterisk) because the dividing cell underwent a type I division (see Figure 7) (F and G) Time that it takes cells to reach 25%, 50%, 75%, and 100% ingression are shown for control **(F)** and Vinculin-D1-expressing **(G)** cells. Whiskers indicate the minimum and maximum, boxes indicate the 25 and 75 percentiles, and vertical line indicates the median. n = 12. **(H and I)** Normalized fluorescence intensity of mRFP-ZO-1 and E-cad-3xGFP at the furrow (green) and polar region (orange) in control **(H)** and Vinculin-D1-expressing cells **(I)**. n = 12. Error bars represent SEM. Statistics: two-tailed paired Student's t test. *p < 0.05; **p < 0.005; ***p < 0.0005.

Discussion

Cell-cell junctions are crucial for maintaining tissue integrity and barrier function. Cell division presents a striking example of epithelial remodeling, where the dividing cell must form a new cell-cell junction after cytokinesis as well as maintain and remodel existing junctions during the major shape changes associated with cytokinesis. Tight junctions and adherens junctions must be stable enough to promote barrier function and tissue integrity during epithelial homeostasis but plastic enough to remodel when necessary. It has been unclear how this balance is achieved during cell division. This study provides novel insights into how epithelial integrity and barrier function are maintained during cytokinesis invertebrate epithelial tissues **(Fig. 2.7)**. Our results indicate that elevated tension from the contractile ring reinforces the adherens junctions connected to the contractile ring by increasing the stability of individual adherens junction proteins and recruiting Vinculin to the cleavage furrow. The data

presented here also highlight important differences in how cell-cell junctions are remodeled during epithelial cell division in *Xenopus* versus *Drosophila*.

Figure 2.7: Model of epithelial cell cytokinesis in *Xenopus* and *Drosophila*

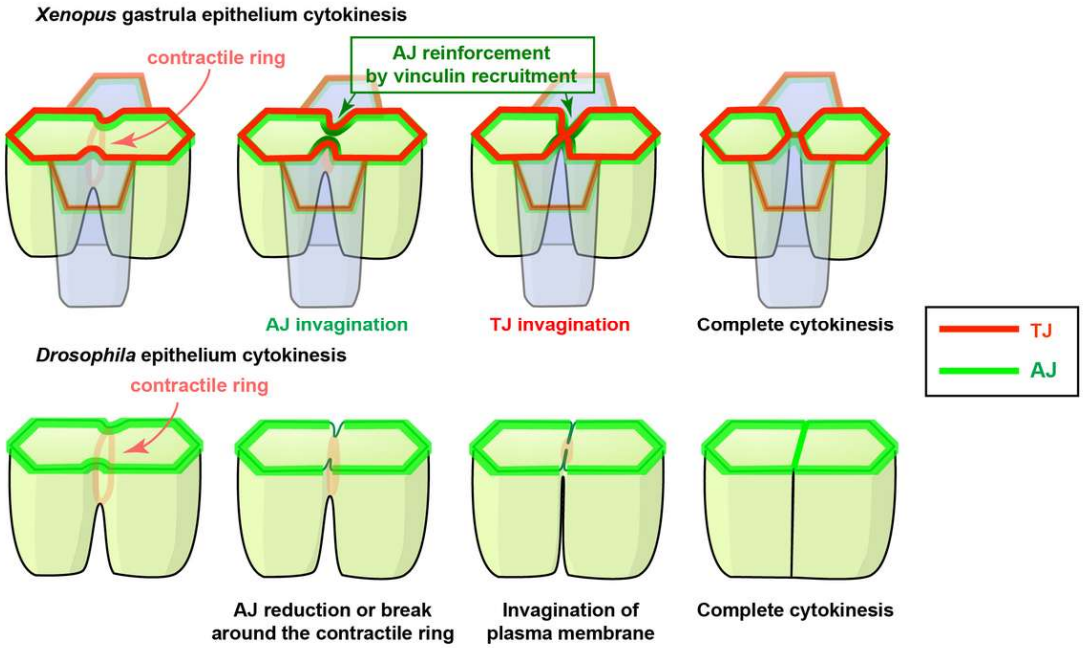

Figure 2.7: Model of epithelial cell cytokinesis in *Xenopus* and *Drosophila*
Model highlighting the difference in epithelial cytokinesis found in *Xenopus* (vertebrate) *Drosophila* (invertebrate).

Comparison of epithelial cytokinesis in vertebrates and invertebrates

Recently, three labs described adherens junction behaviors during cytokinesis in *Drosophila* epithelia using live imaging (Guillot and Lecuit 2013; Founounou, Loyer, and Le 2013; Herszterg et al. 2013). Notably, the structure and molecular composition of cell-cell junctions is distinct between vertebrates and invertebrates (Hartsock and Nelson 2008; Van Itallie and Anderson 2014; Tepass et al. 2001). Vertebrates, including *Xenopus*, have tight junctions and adherens junctions, whereas invertebrates, including *Drosophil*a, have adherens

junctions and septate junctions (Tepass et al. 2001; Furuse and Tsukita 2006), which serve an analogous function to tight junctions while differing in ultrastructure. We identified a number of striking differences in *Xenopus* epithelial cytokinesis compared with *Drosophila*.

First, adherens junctions and tight junctions are maintained throughout cytokinesis and are persistently connected to the contractile ring. In fact, we observed a slight increase in fluorescence intensity of ZO-1 and E-cadherin at the cleavage furrow early in cytokinesis and increased recruitment of Vinculin at the furrow throughout cytokinesis. These observations are in clear contrast to the behaviors of adherens junctions in the *Drosophila* embryonic epidermal epithelium (Guillot and Lecuit 2013) or the dorsal thorax pupal epithelium (Founounou, Loyer, and Le 2013; Herszterg et al. 2013) **(Fig. 2.7)**. In *Drosophila* epithelial cytokinesis, the adherens junction exhibits a break or reduction in E-cadherin at the point where the contractile ring connects to the adherens junction and then becomes disengaged from the contractile ring. In fact, in the embryonic epithelium, a gap appears between the dividing cell and its neighbors (Guillot and Lecuit 2013).

In *Xenopus*, inhibition of endogenous Vinculin recruitment to adherens junctions at the cleavage furrow by expressing dominant-negative Vinculin resulted in the reduction of both adherens junction and tight junction proteins at the cleavage furrow, mimicking the reduction of adherens junctions observed in *Drosophila* epithelial cytokinesis. The differences observed between the systems may arise from a unique adherens junction reinforcement mechanism present in the vertebrate epithelium. Notably, the *Drosophila* Vinculin gene is dispensable (Alatortsev et al. 1997), whereas Vinculin knockout mice have severe defects in heart and brain development, leading to embryonic lethality (Xu, Baribault, and Adamson

1998). It is possible that the adherens junction-reinforcing function of Vinculin may only be important in vertebrates, although further studies are required to directly test the function of Vinculin at adherens junctions in *Drosophila*.

Mechanics of cytokinesis

Cytokinesis is driven by the assembly and constriction of an actomyosin contractile ring. We investigated the impact of mechanical force generated by the contractile ring on junction protein dynamics. Our FRAP data indicate that the adherens junctions at the cleavage furrow respond to increased tension generated by the contractile ring by locally stabilizing E-cadherin and β-catenin. Furthermore, perturbation of Vinculin-dependent adherens junction reinforcement by expressing dominant-negative Vinculin significantly increased the ingression rate of contractile rings. This suggests that cells neighboring the cleavage furrow provide counteracting tension to the force generated by the contractile ring, which is transmitted through the reinforced adherens junctions at the cleavage furrow. Therefore, local strengthening of the adherens junction may be important for maintaining an adhesive connection as the neighbor cells are pulled in by the ingressing contractile ring.

Taken together, our data provide novel insights into how epithelial integrity and barrier function are maintained throughout cytokinesis in a vertebrate epithelial tissue. Our results highlight important differences in how cell-cell junctions are remodeled during cell division in the vertebrate *Xenopus* versus *Drosophila*. This work also raises multiple questions for future studies. For example, it will be important to examine whether the *Xenopus*-type division described here is common in other vertebrate epithelial tissues, both developing and adult tissues. Specifically, it will be interesting to test epithelial tissues that represent different

physical cellular properties, such as tissues that are under different amount of apical tension or have different tissue compliance, to determine whether junctions are maintained or disengaged at the furrow, the impact of contractile ring mechanics on individual junction protein dynamics, and the effect on cytokinesis success.

Materials and methods

***Xenopus* embryos and microinjection**

All studies conducted using Xenopus embryos strictly adhered to the compliance standards of the US Department of Health and Human Services Guide for the Care and Use of Laboratory Animals and were approved by the University of Michigan's Institutional Animal Care and Use Committee. *Xenopus* embryos were collected, *in vitro* fertilized, de-jellied, and microinjected with mRNAs for fluorescent probes using methods described previously (Breznau et al. 2015; Reyes et al. 2014). Embryos were injected at either the two-cell or the four-cell stage and allowed to develop to gastrula stage (Nieuwkoop and Faber stages 10 to 11).

DNA constructs, mRNA preparation

cDNAs encoding human ZO-1 (pSK/ZO-1, Addgene plasmid #30316) (Willott et al. 1993), *Xenopus laevis* E-cadherin (pCS2+/xE-cadherin-3HA; gift from P.D. McCrea, University of Texas MD Anderson Cancer Center), *Xenopus laevis* β-catenin (Addgene plasmid #16389) (Miller and Moon 1997), *Xenopus laevis* claudin-6 (gift from E.M. De Robertis, UCLA) (Brizuela, Wessely, and De 2001) were amplified using PCR. The Vinculin D1 fragment was amplified by PCR using full-length Vinculin as a template. The resulting PCR products were cloned into the pCS2+ vector with or without EGFP (GFP), mCherry, or monomeric red fluorescent protein 1 (mRFP) tags as indicated in figure legends. The sequences of all coding regions were verified by DNA sequencing (GENEWIZ, South Plainfield, NJ). Lifeact-EGFP and Lifeact-mRFP were a gift from W.M. Bement (University of Wisconsin, Madison), and mem (membrane; 2xmyristoylation signal)-TagBFP was a gift from J.B. Wallingford (University of Texas, Austin). MgcRacGAP-3xEGFP (Miller and Bement 2009) and mCherry-farnesyl (Reyes et al. 2014) were previously published. mRNAs were prepared as described previously [S5]. Linearization of plasmid DNA for *in*

vitro transcription was generally performed with NotI, except for mRFP-ZO-1, which was linearized with KpnI.

Microinjection of *Xenopus* embryos and mRNA concentrations used

Embryos were injected at either the 2-cell or the 4-cell stage and allowed to develop to gastrula- stage (Nieuwkoop and Faber stage 10-11). For mosaic expression of vinculin D1, vinculin-3xGFP was injected into both cells at the 2-cell stage and vinculin D1 was injected along with mChe-H2B (as a lineage marker) into two cells at the 4-cell stage such that vinculin D1-expressing cells could be compared to neighboring internal control cells. 5 nl of mRNA was injected into each cell at the following concentrations: mRFP-ZO-1 (50 μg/ml), GFP-claudin-6 (1 μg/ml), mCherry-claudin-6 (2 μg/ml), E-cadherin-3xGFP (5 μg/ml), E-cadherin-3xmCherry (10 μg/ml), GFP-β-catenin (8 μg/ml), α-catenin-mCherry (9 μg/ml), vinculin-3xGFP (10-25 μg/ml), vinculin D1-GFP (40 μg/ml), vinculin D1 (40 μg/ml), mCherry-farnesyl (6 μg/ml), GFP-tricellulin (0.4 μg/ml), mCherry-tricellulin (0.4 μg/ml), angulin-1-3xGFP (5 μg/ml), angulin-1-3xmCherry (5 μg/ml), Lifeact-GFP (5 μg/ml), Lifeact-mRFP (5 μg/ml), mem-TagBFP (10 μg/ml), GFP-H2B (5 μg/ml), mCherry-H2B (4 μg/ml), MgcRacGAP-3xGFP (0.4 μg/ml).

Barrier Assay

Gastrula-stage embryos expressing mRFP-ZO-1 and/or mCherry-H2B were mounted in 10 mM fluorescein (332 Da) and observed. As positive control of barrier failure, embryos were injected with 5 nl of 100 mM EGTA in 0.1X Marc's modified Ringer's (MMR) into the blastocoel and observed after 30 min.

Immunostaining

Gastrula-stage albino embryos were immunostained by methods described previously (Breznau et al. 2015; Reyes et al. 2014) with the following changes: embryos were fixed with 2% TCA (for staining of β-catenin and ZO-1) or 2% formaldehyde (for staining of Tricellulin, Angulin-1, and ZO-1) in 1X PBS for 2 hr, permeabilized with 2% Triton X-100 in PBS for 20 min, and blocked in Tris-buffered saline (50 mM Tris

and 150 mM NaCl [pH 7.4]) containing 10% fetal bovine serum (10082-139; Invitrogen) for 1 or 2 hr at room temperature. Embryos were incubated with 10 mg/ml DAPI (D1306; Life Technologies) and mounted in Vectashield mounting medium (H-1000; Vector Laboratories).

Antibodies

The rabbit anti-β-catenin antibody (ab2365) was purchased from Abcam (Cambridge, UK) and was used for immunostaining at 1:200. The mouse anti-ZO-1 antibody (T8-754) was a generous gift from Dr. Masahiko Itoh (Dokkyo Medical University, Japan) and was used for immunostaining at 1:500. Secondary antibodies used for immunostaining were Alexa Fluor 488-goat anti-rabbit IgG (A11008; Life Technologies) and Alexa Fluor 568-goat anti-mouse IgG (A11004; Life Technologies). Each secondary antibody was used for immunostaining at 1:500.

Live and fixed confocal microscopy

Fluorescent confocal images were collected on an inverted Olympus Fluoview1000 microscope equipped with a 60x super corrected PLAPON 60XOSCobjective (numerical aperture [NA] = 1.4; working distance = 0.12 mm) and FV10-ASW software. Live and fixed imaging was carried out as described previously (Breznau et al. 2015; Reyes et al. 2014).

FRAP

FRAP was performed on gastrula-stage albino embryos using the microscope described above. A 405-nm laser was pulsed in a circular region of interest (ROI) (35% laser power; 600 ms; diameter of 7.8 µm) to bleach junction proteins of interphase cells or the cleavage furrow or polar region of dividing cells. In dividing cells, bleaching was performed once the cleavage furrow was apparent, at ~10%–25% ingression. The apical surface (3 µm deep) of the embryos was imaged for all experiments. This allowed the tracking of the apical region of the cleavage furrow in the Z direction during cytokinesis.

Statistical analysis

A two-tailed paired Student's t test was used for statistical analysis unless otherwise specified. Statistical analysis of FRAP data was performed in GraphPad Prism version 6 (GraphPad Software). E-cadherin data were fit with a double exponential curve to derive the fast and slow halftime of recovery for FRAP($t_{1/2}$) and the plateau/mobile fraction. A single exponential curve was fit to data for β-catenin, Claudin-6, and ZO-1 to derive the $t_{1/2}$ and the plateau/mobile fraction. Curves were constrained to y = 0 and the plateau to be less than 1. An unpaired Student's t test with Welch's correction was used for statistical analysis, and data $\geq$1.1 or % $\leq$-0.1 were removed from statistical analysis.

FRAP image analysis

FRAP data were analyzed using FIJI. A FIRE look up table was applied to average intensity projections to allow for easy tracking of the bleached area of the junction. The fluorescence intensity of a small circular ROI (diameter of 0.6 µm) was measured in three areas of the cell: the bleached region of the junction, a reference junction, and background signal in the cytoplasm. Reference ROIs were chosen as follows: for interphase cells, a different bicellular junction; for the furrow of dividing cells, the unbleached furrow of the same cell; and for polar regions of dividing cells, the opposite polar region of the same cell. ROIs were moved manually to account for cell movements and were measured using a custom macro that measured and advanced frames. Measurements were imported into Microsoft Excel and normalized first to background signal and fluctuations in the reference points using the following equation:

$$I_{norm}(t) = \left(\frac{I_{ref\ pre}}{I_{ref}(t) - I_{back}(t)} \right) \left(\frac{I_{ref\ frap}(t) - I_{back}(t)}{I_{frap\ pre}} \right)$$

Where I_{frap} is the ROI tracking the bleached area, I_{ref} is the ROI tracking the reference area, and I_{back} is the ROI measuring the cytoplasmic background. (t) indicates the specific time point, and pre indicates the

average intensity pre bleach. Then, the values were constrained between 1 and 0 with the following equation:

$$I_{norm}(t) = \left(\frac{I_{norm}(t) - I_{back}(t_{bleach})}{I_{norm\ pre} - I_{nrom}(t_{bleach})} \right)$$

Where I_{norm} indicates the normalized values from the first equation, (t) indicates the specific time point, t_{bleach} indicates the bleached time point, and pre indicates the average intensity of the ROI pre bleach.

Image analysis of fluorescence intensity at cleavage furrow of dividing cells.

The fluorescence intensity of a linear ROI (width of 0.5 µm for ZO-1 and E-cadherin and 0.8 µm for vinculin, membrane, and α-catenin) was measured for each channel in three areas of the cell: cleavage furrow and polar region in the dividing cell and reference region in a non-dividing cell. The relative intensity at the cleavage furrow and polar regions was determined by dividing by the intensity at the reference region.

Image analysis of the duration of cytokinesis.

Relative furrow ingression percent at each time point after the onset of ingression was determined by dividing the distance between adherens junctions on either side of the furrow by the cell width prior to ingression. The time that it takes to achieve 25%, 50%, and 75% ingression was determined by curve fitting using the Rodbard option in ImageJ.

Supplemental figures

Figure S2.1: Adherens, but not tight junction proteins, are stabilized at the cleavage furrow of dividing cells

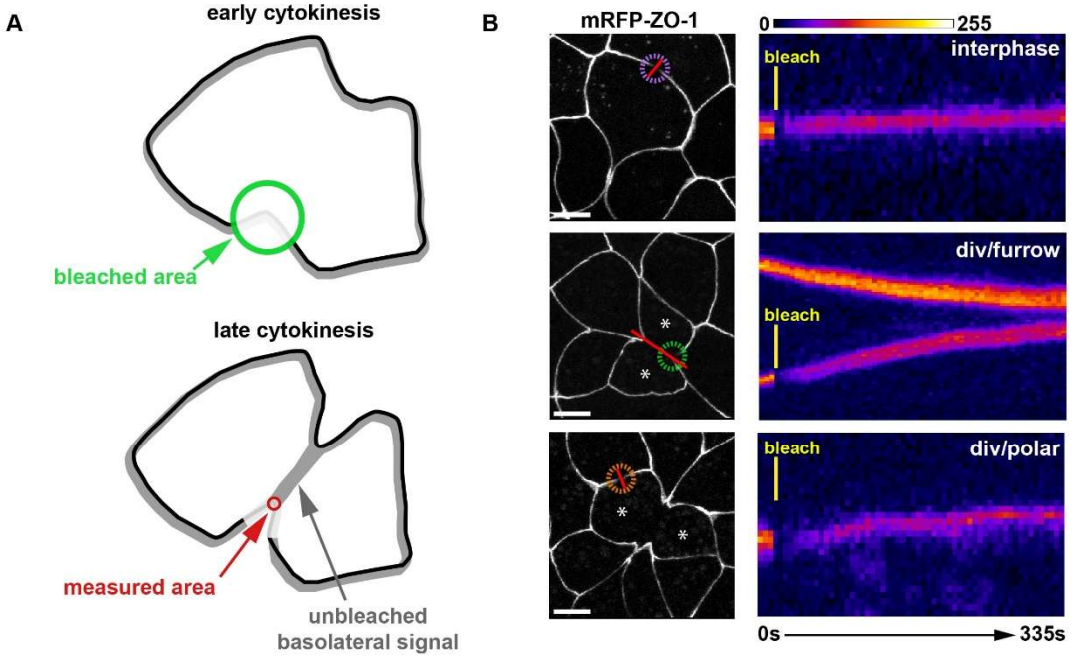

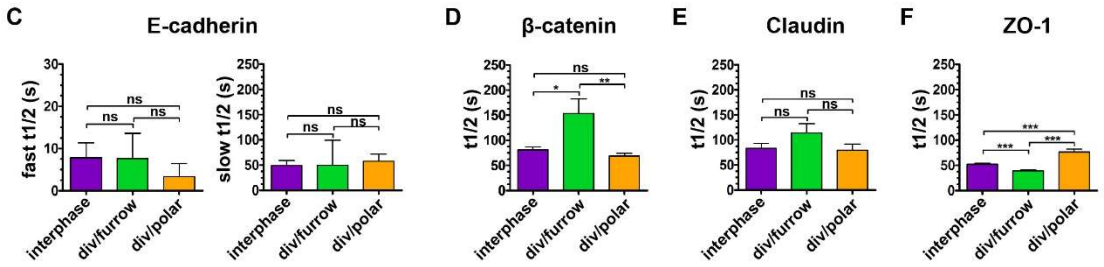

G

E-cadherin	mobile fraction	fast t1/2	slow t1/2
interphase	73.2 ± 1.3%	7.4 ± 3.6s	49.5 ± 9.9s
div/furrow	41.0 ± 2.2%	7.6 ± 6.0s	50.1 ± 49.2s
div/polar	73.2 ± 2.6%	3.4 ± 3.0s	58.0 ± 14.1s

E-cadherin	mobile fraction	fast t1/2	slow t1/2
interphase (DMSO)	73.5 ± 3.1%	17.8 ± 7.3s	72.4 ± 36.5s
interphase (calyculin A)	56.1 ± 3.4%	16.3 ± 10.7s	70.7 ± 48.8s

E-cadherin	mobile fraction	fast t1/2	slow t1/2
div/furrow	40.3 ± 2.0%	11.3 ± 9.4s	55.1 ± 39.8s
div/furrow (Y-27632)	59.3 ± 4.0%	11.0 ± 7.1s	73.3 ± 37.8s

E-cadherin	mobile fraction	fast t1/2	slow t1/2
interphase	80.5 ± 1.1%	9.7 ± 4.8s	49.6 ± 7.2s
interphase (Y-27632)	80.2 ± 2.3%	16.8 ± 6.3s	66.3 ± 23.7s

β-catenin	mobile fraction	t1/2
interphase	63.8 ± 1.8%	81.4 ± 5.6s
div/furrow	39.5 ± 4.4%	153.7 ± 28.8s
div/polar	62.4 ± 2.0%	69.0 ± 5.9s

Claudin	mobile fraction	t1/2
interphase	35.5 ± 1.8%	83.0 ± 10.0s
div/furrow	39.8 ± 3.3%	113.7 ± 18.7s
div/polar	34.6 ± 2.0%	79.4 ± 11.8s

ZO-1	mobile fraction	t1/2
interphase	69.3 ± 0.7%	52.3 ± 1.7s
div/furrow	67.9 ± 0.7%	39.2 ± 1.6s
div/polar	70.9 ± 2.0%	76.8 ± 5.6s

ZO-1	mobile fraction	t1/2
interphase (DMSO)	75.5 ± 1.2%	64.1 ± 2.9s
interphase (calyculin A)	62.8 ± 1.0%	47.2 ± 2.7s

Figure S2.1: Adherens junction proteins, but not tight junction proteins, are stabilized at the cleavage furrow of dividing cells

A) Diagram depicting the approach used to measure FRAP at the furrow of dividing cells. This strategy was chosen to ensure that measured recovery was of the bleached region and not due to signal from either side of the furrow or due to basolateral signal coming into the focal plane. A circular ROI with a diameter of 7.8 μm (green circle) was used to bleach the furrow; a circular ROI with a diameter of 0.6 μm (red circle) was used to measure recovery during analysis. FRAP in interphase cells and the polar region of dividing cells was measured using the same method. **B)** Cell view and kymographs of mRFP-ZO-1 FRAP. Colored dashed circles indicate the bleached area, red line indicates the location used to generate the kymographs, and the white asterisks indicate the two daughter cells. A FIRE lookup table (above kymographs) was applied to the kymographs; time (horizontal axis) and bleach time points are indicated. Scale bars, 10 μm. **C)** E-cadherin-3xmCherry FRAP fast and slow $t_{1/2}$s derived from the double exponential curve that was fitted to the data. The number of cells (n) quantified is: interphase cells (n=23), dividing cells/furrow (n=17), dividing cells/polar (n=12). **D)** β-catenin-GFP FRAP t1/2s. n=21, 19, 14. **E)** mCherry-Claudin-6 FRAP t1/2s. n=23, 18, 10. **F)** mRFP-ZO-1 FRAP $t_{1/2}$s. n=34, 34, 21. **G)** Table of mobile fraction and $t_{1/2}$ values of measured junction proteins. Error bars, S.E.M. Statistics, unpaired t-test, *p=0.014, **p=0.004, ***p<0.0001.

Figure S2.2: Adherens junctions complete invagination before tight junctions and Dominant-negative Vinculin abolishes cell-cell junction reinforcement at the cleavage furrow

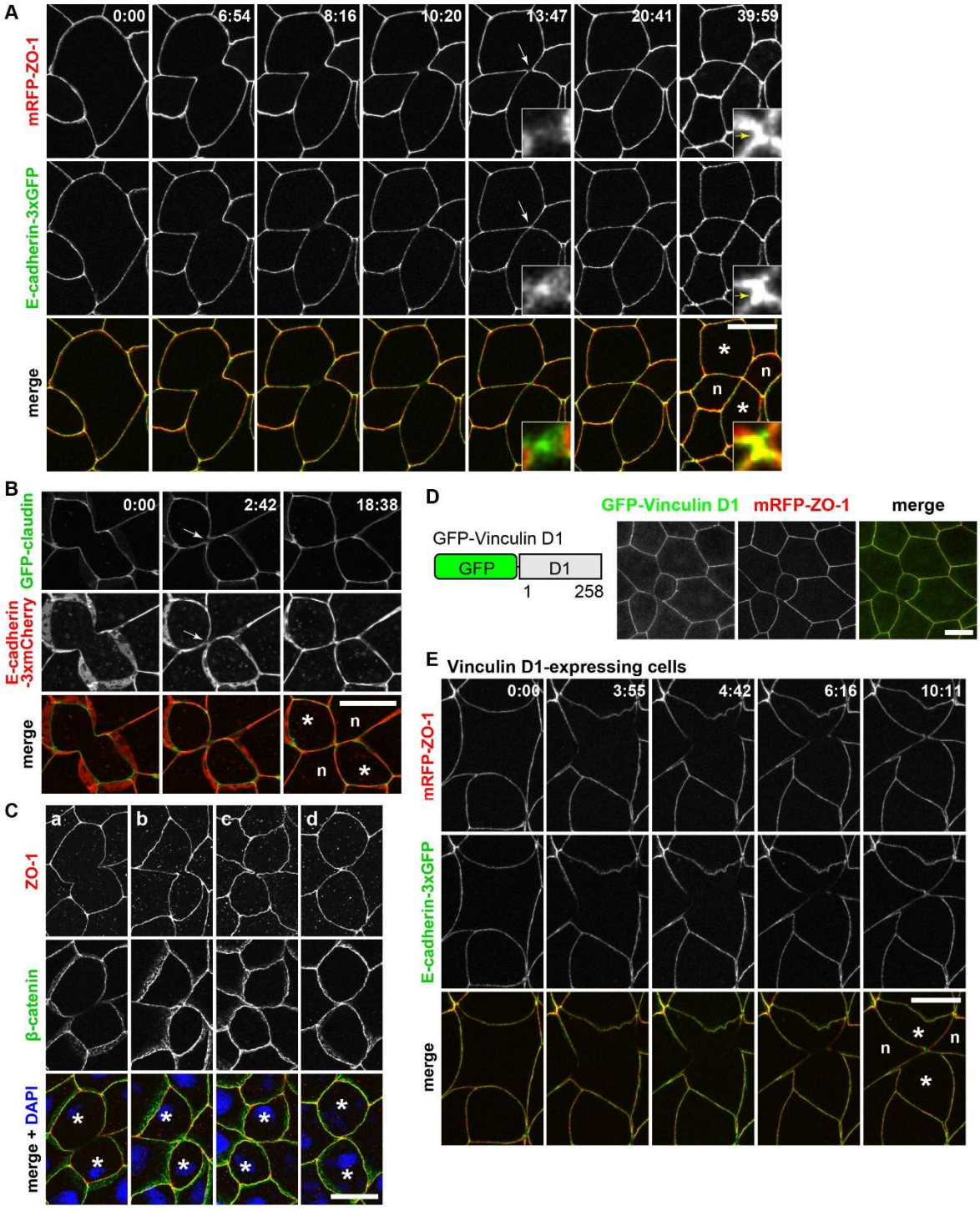

Figure S2.2: Adherens junction complete invagination before tight junction and dominant-negative Vinculin abolishes cell-cell junction reinforcement at the cleavage furrow

A and E). Detailed montage of the dividing control **(A)** and Vinculin D1-expressing **(E)** cells shown in Figures 6D and 6E. Note that the adherens junction has completed invagination, whereas the tight junction is still apart at 13:47 (white arrows) in A. Insets in A: Higher magnification of new interface between neighbor cells (yellow arrows). **B)** Live imaging of a gastrula-stage embryo expressing GFP-Claudin-6 (green, tight junction marker) and E-cadherin-3xmCherry (red, adherens junction marker). Note that the invagination of the adherens junction precedes the tight junction. **C)** Immunofluorescence staining of four representative cells in gastrula-stage embryos using anti-ZO-1 (tight junction marker, red), anti-β-catenin (adherens junction marker, green) and DAPI (DNA marker, blue). Note that adherens junction has invaginated further than tight junction (see cells b and c), supporting the live imaging results. **D)** Live imaging of an embryo expressing Vinculin D1-GFP and mRFP-ZO-1. Note that Vinculin D1-GFP uniformly labels cell-cell junctions. Asterisks and "n"s indicate daughter cells and neighbor cells, respectively. Scale bars, 20 μm.

References

Alatortsev, VE, IA Kramerova, MV Frolov, SA Lavrov, and ED Westphal. 1997. “Vinculingene Is Non-Essential InDrosophila Melanogaster”. *FEBS Letters* 413 (2). Wiley: 197–201. doi:10.1016/s0014-5793(97)00901-0.

Baker, J, and D Garrod. 1993. “Epithelial Cells Retain Junctions during Mitosis”. *J Cell Sci* 104 (Pt 2): 415–25.

Breznau, EB, AC Semack, T Higashi, and AL Miller. 2015. “MgcRacGAP Restricts Active RhoA at the Cytokinetic Furrow and Both RhoA and Rac1 at Cell-Cell Junctions in Epithelial Cells”. *Mol Biol Cell* 26: 2439–55.

Brizuela, BJ, O Wessely, and EM De Robertis. 2001. “Overexpression of the Xenopus Tight-Junction Protein Claudin Causes Randomization of the Left-Right Body Axis”. *Dev Biol* 230: 217–29.

Buckley, CD, J Tan, KL Anderson, D Hanein, N Volkmann, WI Weis, WJ Nelson, and AR Dunn. 2015. “The Minimal Cadherin-Catenin Complex Binds to Actin Filaments under Force”. *Biophysical Journal* 108 (2). Elsevier BV: 11a. doi:10.1016/j.bpj.2014.11.088.

Choi, HJ, S Pokutta, GW Cadwell, AA Bobkov, LA Bankston, RC Liddington, and WI Weis. 2012. “Alpha-E-Catenin Is an Autoinhibited Molecule That Co-Activates Vinculin”. Protein Data Bank Rutgers University. doi:10.2210/pdb4e18/pdb.

Choi, W, BR Acharya, G Peyret, M Fardin, R Mège, B Ladoux, AS Yap, AS Fanning, and M Peifer. 2016. “Remodeling the Zonula Adherens in Response to Tension and the Role of Afadin in This Response”. *The Journal of Cell Biology* 213 (2). Rockefeller University Press: 243–60. doi:10.1083/jcb.201506115.

Eisenhoffer, GT, and J Rosenblatt. 2013. “Bringing Balance by Force: Live Cell Extrusion Controls Epithelial Cell Numbers”. *Trends Cell Biol* 23: 185–92.

Fededa, JP, and DW Gerlich. 2012. “Molecular Control of Animal Cell Cytokinesis”. *Nature Cell Biology* 14 (5). Springer Nature: 440–47. doi:10.1038/ncb2482.

Fernandez-Gonzalez, R, SSM Simoes, JC Röper, S Eaton, and JA Zallen. 2009. “Myosin II Dynamics Are Regulated by Tension in Intercalating Cells”. *Developmental Cell* 17 (5). Elsevier BV: 736–43. doi:10.1016/j.devcel.2009.09.003.

Founounou, N, N Loyer, and R Le Borgne. 2013. “Septins Regulate the Contractility of the Actomyosin Ring to Enable Adherens Junction Remodeling during Cytokinesis of Epithelial Cells”. *Dev Cell* 24: 242–55.

Furuse, M, and S Tsukita. 2006. “Claudins in Occluding Junctions of Humans and Flies”. *Trends in Cell Biology* 16 (4). Elsevier BV: 181–88. doi:10.1016/j.tcb.2006.02.006.

Furuse, M, H Sasaki, K Fujimoto, and S Tsukita. 1998. “A Single Gene Product Claudin-1 or -2, Reconstitutes Tight Junction Strands and Recruits Occludin in Fibroblasts”. *The Journal of Cell Biology* 143 (2). Rockefeller University Press: 391–401. doi:10.1083/jcb.143.2.391.

Gibson, MC, AB Patel, R Nagpal, and N Perrimon. 2006. “The Emergence of Geometric Order in Proliferating Metazoan Epithelia”. *Nature* 442: 1038–41.

Green, KJ. S Getsios, S Troyanovsky, and LM Godsel. 2009. “Intercellular Junction Assembly Dynamics, and Homeostasis”. *Cold Spring Harbor Perspectives in Biology* 2 (2). Cold Spring Harbor Laboratory: a000125–a000125. doi:10.1101/cshperspect.a000125.

Green, RA. E Paluch, and K Oegema. 2012. “Cytokinesis in Animal Cells”. *Annual Review of Cell and Developmental Biology* 28 (1). Annual Reviews: 29–58. doi:10.1146/annurev-cellbio-101011-155718.

Guillot, C, and T Lecuit. 2013. “Adhesion Disengagement Uncouples Intrinsic and Extrinsic Forces to Drive Cytokinesis in Epithelial Tissues”. *Dev Cell* 24: 227–41.

Guillot, C, and T Lecuit. 2013. “Mechanics of Epithelial Tissue Homeostasis and Morphogenesis”. *Science* 340 (6137). American Association for the Advancement of Science (AAAS): 1185–89. doi:10.1126/science.1235249.

Hartsock, Andrea, and WJ Nelson. 2008. “Adherens and Tight Junctions: Structure Function and Connections to the Actin Cytoskeleton”. *Biochimica Et Biophysica Acta (BBA) - Biomembranes* 1778 (3). Elsevier BV: 660–69. doi:10.1016/j.bbamem.2007.07.012.

Herszterg, S, A Leibfried, F Bosveld, C Martin, and Y Bellaiche. 2013. “Interplay between the Dividing Cell and Its Neighbors Regulates Adherens Junction Formation during Cytokinesis in Epithelial Tissue”. *Dev Cell* 24: 256–70.

Higashi, T, TR Arnold, RE Stephenson, KM Dinshaw, AL Miller. “Maintenance of the Epithelial Barrier and Remodeling of Cell-Cell Junctions during Cytokinesis.” *Current Biology* **26**, 1829–1842 Elsevier BV, 2016

Huang, J, L Huang, YJ Chen, E Austin, CE Devor, F Roegiers, and Y Hong. 2011. “Differential Regulation of Adherens Junction Dynamics during Apical-Basal Polarization”. *Journal of Cell Science* 124 (23). The Company of Biologists: 4001–13. doi:10.1242/jcs.086694.

Huveneers, S, J Oldenburg, E Spanjaard, G van der Krogt, I Grigoriev, A Akhmanova, H Rehmann, and J de Rooij. 2012. “Vinculin Associates with Endothelial VE-Cadherin Junctions to Control Force-Dependent Remodeling”. *The Journal of Experimental Medicine* 209 (3). Rockefeller University Press: i3–i3. doi:10.1084/jem2093oia3.

Ishihara, H, BL Martin, DL Brautigan, H Karaki, H Ozaki, Y Kato, N Fusetani, S Watabe, K Hashimoto, D Uemura. 1989. “Calyculin A and Okadaic Acid: Inhibitors of Protein Phosphatase Activity”. *Biochemical and Biophysical Research Communications* 159 (3). Elsevier BV: 871–77. doi:10.1016/0006-291x(89)92189-x.

Itoh, M, K Morita, and S Tsukita. 1999. “Characterization of ZO-2 as a MAGUK Family Member Associated with Tight as Well as Adherens Junctions with a Binding Affinity to Occludin and alpha-Catenin”. *Journal of Biological Chemistry* 274 (9). American Society for Biochemistry & Molecular Biology (ASBMB): 5981–86. doi:10.1074/jbc.274.9.5981.

Jinguji, Y, and H Ishikawa. 1992. “Electron Microscopic Observations on the Maintenance of the Tight Junction during Cell Division in the Epithelium of the Mouse Small Intestine”. *Cell Structure and Function* 17 (1). Japan Society for Cell Biology: 27–37. doi:10.1247/csf.17.27.

Joshi, SD, Michelangelo von Dassow, and Lance. A. Davidson. 2010. “Experimental Control of Excitable Embryonic Tissues: Three Stimuli Induce Rapid Epithelial Contraction”. *Experimental Cell Research* 316 (1). Elsevier BV: 103–14. doi:10.1016/j.yexcr.2009.08.005.

Kim, YT, M Hazar, DS Vijayraghavan, J Song, TR Jackson, SD Joshi, WC Messner, LA Davidson, and Philip R. LeDuc. 2014. “Mechanochemical Actuators of Embryonic Epithelial Contractility”. *Proceedings of the National Academy of Sciences* 111 (40). Proceedings of the National Academy of Sciences: 14366–71.

Le Page, Y, I Chartrain, C Badouel, and JP Tassan. 2011. “A Functional Analysis of MELK in Cell Division Reveals a Transition in the Mode of Cytokinesis during Xenopus Development”. *J Cell Sci* 124: 958–68. doi: 10.1242/jcs.069567

Lecuit, T, and AS Yap. 2015. “E-Cadherin Junctions as Active Mechanical Integrators in Tissue Dynamics”. *Nature Cell Biology* 17 (5). Springer Nature: 533–39. doi:10.1038/ncb3136.

Leerberg, JM., GA Gomez, S Verma, EJ Moussa, SK Wu, R Priya, BD Hoffman, C Grashoff, MA Schwartz, and AS Yap. 2014. “Tension-Sensitive Actin Assembly Supports Contractility at the Epithelial Zonula Adherens”. *Current Biology* 24 (15). Elsevier BV: 1689–99. doi:10.1016/j.cub.2014.06.028.

Liu, KC, and RE Cheney. 2012. “Myosins in Cell Junctions”. *BioArchitecture* 2 (5). Informa UK Limited: 158–70. doi:10.4161/bioa.21791.

Miller, AL, and WM Bement. 2009. “Regulation of Cytokinesis by Rho GTPase Flux”. *Nat Cell Biol* 11: 71–77. doi: 10.1038/ncb1814

Miller, JR, and RT Moon. 1997. “Analysis of the Signaling Activities of Localization Mutants of Beta-Catenin during Axis Specification in Xenopus”. *J Cell Biol* 139: 229–43.

Narumiya, S, T Ishizaki, and M Ufhata. 2000. “Use and Properties of ROCK-Specific Inhibitor Y-27632”. In *Methods in Enzymology*, 273–84. Elsevier. doi:10.1016/s0076-6879(00)25449-9.

Nowotarski, SH, and M Peifer. 2014. “Cell Biology: A Tense but Good Day for Actin at CellCell Junctions”. *Current Biology* 24 (15). Elsevier BV: R688–R690. doi:10.1016/j.cub.2014.06.063.

Peng, X, JL Maiers, D Choudhury, SW Craig, and KA DeMali. 2012. “alpha-Catenin Uses a Novel Mechanism to Activate Vinculin”. *Journal of Biological Chemistry* 287 (10). American Society for Biochemistry & Molecular Biology (ASBMB): 7728–37. doi:10.1074/jbc.m111.297481.

Priya, R, A S Yap, and GA Gomez. 2013. “E-Cadherin Supports Steady-State Rho Signaling at the Epithelial Zonula Adherens”. *Differentiation* 86 (3). Elsevier BV: 133–40. doi:10.1016/j.diff.2013.01.002.

Ratheesh, A, and AS Yap. 2012. “A Bigger Picture: Classical Cadherins and the Dynamic Actin Cytoskeleton”. *Nature Reviews Molecular Cell Biology* 13 (10). Springer Nature: 673–79. doi:10.1038/nrm3431.

Ratheesh, A, GA Gomez, R Priya, S Verma, EM Kovacs, K Jiang, NH Brown, AA, Samantha J Stehbens, and AS Yap. 2012. “Centralspindlin and $\Upalpha$-Catenin Regulate Rho Signalling at the Epithelial Zonula Adherens”. *Nature Cell Biology* 14 (8). Springer Nature: 818–28. doi:10.1038/ncb2532.

Reinsch, S, and E Karsenti. 1994. “Orientation of Spindle Axis and Distribution of Plasma Membrane Proteins during Cell Division in Polarized MDCKII Cells”. *J Cell Biol* 126: 1509–26.

Reyes, CC, M Jin, EB Breznau, R Espino, R Delgado-Gonzalo, AB Goryachev, and AL Miller. 2014. “Anillin Regulates Cell-Cell Junction Integrity by Organizing Junctional Accumulation of Rho-GTP and Actomyosin”. *Curr Biol* 24: 1263–70. doi: 10.1016/j.cub.2014.04.021

Rodgers, LS., and AS Fanning. 2011. “Regulation of Epithelial Permeability by the Actin Cytoskeleton”. *Cytoskeleton* 68 (12). Wiley: 653–60. doi:10.1002/cm.20547.

Sasaki, H, C Matsui, K Furuse, Y Mimori-Kiyosue, M Furuse, and S Tsukita. 2003. “Dynamic Behavior of Paired Claudin Strands within Apposing Plasma Membranes”. *Proc Natl Acad Sci USA* 100: 3971–76.

Shen, L, CR Weber, and JR Turner. 2008. “The Tight Junction Protein Complex Undergoes Rapid and Continuous Molecular Remodeling at Steady State”. *The Journal of Cell Biology* 181 (4). Rockefeller University Press: 683–95. doi:10.1083/jcb.200711165.

Takeichi, M. 1995. “Morphogenetic Roles of Classic Cadherins”. *Current Opinion in Cell Biology* 7 (5). Elsevier BV: 619–27. doi:10.1016/0955-0674(95)80102-2.

Tepass, U, G Tanentzapf, R Ward, and R Fehon. 2001. “Epithelial Cell Polarity and Cell Junctions in Drosophila”. *Annual Review of Genetics* 35 (1). Annual Reviews: 747–84. doi:10.1146/annurev.genet.35.102401.091415.

Van Itallie, CM. and JM Anderson. 2014. “Architecture of Tight Junctions and Principles of Molecular Composition”. *Seminars in Cell & Developmental Biology* 36 (December). Elsevier BV: 157–65. doi:10.1016/j.semcdb.2014.08.011.

Willott, E, MS Balda, AS Fanning, B Jameson, C Van Itallie, and JM Anderson. 1993. “The Tight Junction Protein ZO-1 Is Homologous to the Drosophila Discs-Large Tumor Suppressor Protein of Septate Junctions”. *Proc Natl Acad Sci USA* 90: 7834–38.

Xu, W, H Baribault, and ED Adamson. 1998. “Vinculin Knockout Results in Heart and Brain Defects during Embryonic Development”. *Development* 125: 327–37.

Yamada, S, S Pokutta, F Drees, WI Weis, and WJ Nelson. 2005. “Deconstructing the Cadherin-Catenin-Actin Complex”. *Cell* 123: 889–901.

Yonemura, S, Y Wada, T Watanabe, A Nagafuchi, and M Shibata. 2010. “Alpha-Catenin as a Tension Transducer That Induces Adherens Junction Development”. *Nat Cell Biol* 12: 533–42. doi: 10.1038/ncb2055

Yu, D, AM Marchiando, CR Weber, DR Raleigh, Y Wang, L Shen, and JR Turner. 2010. “MLCK-Dependent Exchange and Actin Binding Region-Dependent Anchoring of ZO-1 Regulate Tight Junction Barrier Function”. *Proc Natl Acad Sci USA* 107: 8237–41. doi: 10.1073/pnas.0908869107

Chapter 3

Anillin regulates epithelial cell mechanics by structuring the medial-apical actomyosin network

Abstract

Mechanical forces from cells sculpt organisms during development, while misregulation of cellular mechanics can influence disease progression. Here, we investigate how the actomyosin scaffold protein Anillin contributes to epithelial mechanics in developing *Xenopus laevis* embryos. We find that junctional mechanosensitive recruitment of Vinculin is reduced when Anillin is depleted and increased when Anillin is overexpressed, suggesting that Anillin promotes junctional tension. Using junction recoil following laser ablation as a readout for the forces exerted on junctions, we show, unexpectedly, that junctions recoil faster when Anillin is depleted and slower when Anillin is overexpressed. Unifying these findings, we demonstrate that Anillin organizes and stabilizes the medial-apical actomyosin network. Finally, we show that Anillin's effects on cellular mechanics impact tissue-wide mechanics. Together, these results reveal Anillin as a key regulator of epithelial mechanics and lay the groundwork for future studies on how Anillin may contribute to mechanical events in development and disease.

Introduction

During development, an organism takes its shape by generating forces and establishing mechanical properties at the cellular level (Davidson 2012). Forces produced by the contractile actomyosin cytoskeleton within cells are transmitted via mechanical properties between cells and through the tissue via cell-cell junctions. By coordinating which cells are contracting, elongating, or rearranging, tissues can bend, fold, or elongate allowing for the complex tissue organization found in many multicellular organisms. Understanding how cell-scale mechanical inputs result in tissue-scale changes requires a comprehensive knowledge of the proteins involved in controlling cellular mechanics.

Anillin is a scaffolding protein that was first characterized for its role in cell division (Field and Alberts 1995) and has since been shown to regulate cytokinesis in organisms ranging from yeast to humans (Piekny and Maddox 2010). Anillin localizes to the actomyosin contractile ring during cytokinesis and primarily to the nucleus during interphase (Field and Alberts 1995; Oegema et al. 2000; D'Avino 2009). Anillin anchors the contractile ring to the plasma membrane by binding to actomyosin through its N-terminal Myosin- and F-actin-binding domains and to lipids through its C-terminal C2 and PH domains (Straight, Field, and Mitchison 2005; Piekny and Glotzer 2008; Liu et al. 2012; Sun et al. 2015). Anillin can both enhance and limit contractility during cytokinesis through binding to active RhoA, several of Rho's positive and negative regulators, and by crosslinking F-actin (Piekny and Glotzer 2008; Frenette et al. 2012; Manukyan et al. 2015; Descovich et al. 2017). Anillin promotes RhoA activity by binding to active RhoA (Piekny and Glotzer 2008; Sun et al. 2015) and the positive regulator of RhoA Ect2 (Frenette et al. 2012) and high contractility in the contractile ring promotes the interaction

between the negative regulator of RhoA P190RhoGAP-A and Anillin which in turn limits RhoA activity (Manukyan et al. 2015).

Recently, novel roles for Anillin in regulating epithelial cell-cell junctions have been reported. Our group showed that Anillin is localized to cell-cell junctions in frog embryos where it regulates cell-cell junction integrity, as both tight junctions and adherens junctions were disrupted when Anillin was knocked down (Reyes et al. 2014). Furthermore, we showed that Anillin scaffolds the contractile actomyosin machinery connected to epithelial cell-cell junctions (Reyes et al. 2014). Proteomic studies supported Anillin's association with cadherin-mediated adhesions in fly and human cells (Guo et al. 2014; Toret et al. 2014). Studies in human epithelial cells confirmed and expanded our understanding of Anillin's function at cell-cell junctions. Anillin knockdown in cultured human epithelial cells resulted in junction disassembly and disorganized junctional F-actin and Myosin II (Wang et al. 2015). A recent study reported that Myosin II anchors Anillin to the apical cell cortex, and cycles of binding and unbinding to Anillin stabilize active RhoA by increasing its cortical residence time, thus promoting junctional actomyosin contractility (Budnar et al. 2018). Finally, *in vivo* studies in zebrafish demonstrated that barrier function in the kidney, which is mediated by tight junctions, was compromised by a mutation in Anillin that causes Focal Segmental Glomerulosclerosis, a leading cause of kidney failure (Gbadegesin et al. 2014).

Despite these emerging roles for Anillin in regulating actomyosin-mediated cell-cell junction contractility, very little is known about how Anillin contributes to the mechanical properties of epithelial tissues in development and disease. Notably, Anillin is expressed during developmental events that are controlled by mechanical inputs from cells and tissues, including

gastrulation and neurulation. Anillin is also overexpressed in multiple human cancers (Hall et al. 2005). Increased tissue stiffness is frequently observed during tumorigenesis; tumor growth and metastases are sensitive to mechanical cues, which significantly affect cancer prognosis (Kumar and Weaver 2009). Changes in mechanical properties can be mediated by changes in the composition of the extracellular matrix as well as changes in the organization of the intracellular cytoskeleton. Changes in the actomyosin cytoskeleton are associated with increased expression or activity of proteins that promote intracellular contractility, such as RhoA and its downstream effector ROCK (Rho-associated protein kinase) (Butcher, Alliston, and Weaver 2009). Although there is little research on how Anillin may contribute to the mechanical properties of cancer, it is becoming clear that Anillin's function goes beyond cytokinesis. Anillin resides not only in the nucleus of interphase cancer cells, but also in the cytoplasm, and Anillin expression can have either positive or negative outcomes for patients depending on the cancer type and Anillin's subcellular localization (Hall et al. 2005; Suzuki et al. 2005; Ronkainen et al. 2011; Liang et al. 2015; Magnusson et al. 2016; Wang et al. 2016; Idichi et al. 2017; Zhang et al. 2017). Based on Anillin's demonstrated role in regulating cell-cell junction contractility and potential involvement in regulating development and disease, we sought to test whether Anillin affects epithelial cell and tissue mechanics.

In order to characterize how Anillin affects cell and tissue mechanics, we used the animal cap epithelium of developing *Xenopus laevis* embryos as a model vertebrate epithelial tissue. We identified a new role for Anillin in organizing F-actin and Myosin II at the medial-apical surface of epithelial cells. The medial-apical population of actomyosin has previously been characterized, particularly in flies, and is critical for constricting the apical surface of

epithelial cells to drive tissue bending during embryonic development (Dawes-Hoang et al. 2005; Martin, Kaschube, and Wieschaus 2009; Plageman et al. 2011; Martin and Goldstein 2014). Here, we show that Anillin promotes a contractile medial-apical actomyosin network, which produces tensile forces that are transmitted between cells via cell-cell junctions. When Anillin is knocked down, medial-apical actomyosin is reduced and no longer forms a functional contractile network. When Anillin is overexpressed, medial-apical actomyosin is reorganized into thick bundles that span the apical surface. These bundles are contractile and increase the forces generated across the apical surface of epithelial cells. Finally, we show that cell-scale mechanical changes caused by modulating Anillin expression result in tissue-scale changes, as Anillin knockdown reduces tissue stiffness. Together, these results reveal that the scaffolding protein Anillin regulates epithelial mechanics.

Results

Anillin increases junctional tension but reduces recoil of junction vertices after laser ablation

Since Anillin can both promote and limit contractility at the cytokinetic contractile ring (Piekny and Glotzer 2008; Manukyan et al. 2015; Descovich et al. 2017), and Anillin localizes to cell-cell junctions where it maintains F-actin, Myosin II, and proper active RhoA distribution (Reyes et al. 2014), we sought to test whether Anillin affects junctional tension. As a readout of relative tension on junctions, we quantified the junctional accumulation of Vinculin-mNeon. High junctional tension induces a conformational change in α-catenin, which recruits Vinculin to adherens junctions to reinforce the connection to the actin cytoskeleton (Yonemura et al. 2010). We have previously vetted a tagged Vinculin probe in *Xenopus laevis* and used it to show that the cytokinetic contractile ring applies increased

tension on adherens junctions (Higashi et al. 2016). To test how Anillin affects junctional Vinculin recruitment, we knocked down Anillin with a previously characterized morpholino oligonucleotide (Reyes et al. 2014) or overexpressed a tagged version of Anillin (Anillin-3xmCherry). In control embryos, Vinculin-mNeon accumulated weakly along bicellular junctions and strongly at tricellular contacts, which are sites of higher tension **(Fig. 3.1 A)** (Choi et al. 2016; Higashi and Miller 2017). When Anillin was knocked down, the intensity of Vinculin-mNeon was reduced at junctions **(Fig. 3.1 A, B)**. We also examined α-catenin-mCherry intensity because Vinculin intensity could vary based on the amount of its binding partner α-catenin available at junctions **(Fig. S3.1 A-C)**. When Anillin was knocked down, α-catenin-mCherry was strongly reduced at junctions; therefore, the reduced Vinculin-mNeon intensity **(Fig. 3.1 A, B, S3.1 A, B)** does not simply indicate reduced tension, but also reduced α-catenin. Notably, when Anillin was overexpressed, the intensity of Vinculin-mNeon was significantly elevated **(Fig. 3.1 A, B, S3.1 A, B)**, and the intensity of α-catenin-mCherry was unchanged **(Fig. S3.1 A, C)**, indicating that increased Vinculin-mNeon recruitment was due to a tension-induced conformation change in α-catenin.

Changes in cell shape also supported the conclusion that Anillin affects junctional tension. When Anillin was knocked down, cells became less polygonal and more rounded **(Fig. 3.1 A)**, a hallmark of reduced tension (Yonemura et al. 2010). This is consistent with our previous report that Anillin knockdown leads to effects associated with reduced tension including cell rounding, apical doming, and loss of F-actin and Myosin II from junctions (Reyes et al. 2014). In contrast, when Anillin was overexpressed, junctions exhibited a wavy, distorted shape compared to more linear control junctions **(Fig. 3.1 A)**. Interestingly wavy junctions can

indicate either unbalanced high tension (Tokuda, Higashi, and Furuse 2014; Nowotarski and Peifer 2014), or uniform low tension along the junction (Nowotarski and Peifer 2014; Choi et al. 2016).

As a complementary approach to test whether Anillin promotes junctional tension, we measured junction recoil after laser ablation. The amount of junction recoil (measured as distance between cell vertices over time) is reported to correlate with the relative junctional tension such that a junction under high tension will exhibit enhanced recoil (Farhadifar et al. 2007; Fernandez-Gonzalez et al. 2009). We used a 2-photon laser to ablate a local site in the center of a bicellular junction in embryos expressing E-cadherin-3xGFP. To avoid potential contributions of junction length to recoil, junctions of a similar length were selected for ablation in controls, Anillin knockdown, and Anillin overexpression **(Fig. 3.1 E)**. After laser ablation, control junctions recoiled 2.8 ± 0.2 µm after 18 s **(Fig. 3.1 C, D)**. Based on our hypothesis that Anillin promotes junctional tension, we expected to see reduced junction recoil when Anillin was knocked down; however, recoil increased to 4.1 ± 0.4 µm after 18 s **(Fig. 3.1 C, D & S3.1)**. When Anillin was overexpressed, we expected to see increased recoil; however, the recoil decreased to 1.6 ± 0.4 µm after 18 s **(Fig. 3.1 C, D)**.

Taken together, the Vinculin recruitment data indicated that Anillin increased junctional tension, whereas the laser ablation showed that Anillin reduces junction recoil, which would be consistent with reduced junctional tension. Although the Vinculin recruitment and laser ablation results initially seemed to be at odds with one another, an interesting phenotype emerged in the laser ablation data when we observed the Anillin-3xmCherry channel in Anillin overexpression embryos, as Anillin highlights the apical surface of the cells as well as the cell-

cell junctions. In several instances, we saw that the two cells adjacent to the junction that was ablated lost adhesion and recoiled *perpendicular* to the junction instead of in the expected recoil *parallel* to the junction **(Fig. 3.1F, S3.1D)**. This unexpected result lead us to hypothesize that Anillin was somehow responsible for exerting forces perpendicular to the junction, possibly through the medial-apical cortex, which could both increase Vinculin intensity at junctions and reduce recoil after laser ablation in the expected parallel direction.

Figure 3.1: Anillin increases junctional Vinculin recruitment but reduces recoil of junction vertices after laser ablation

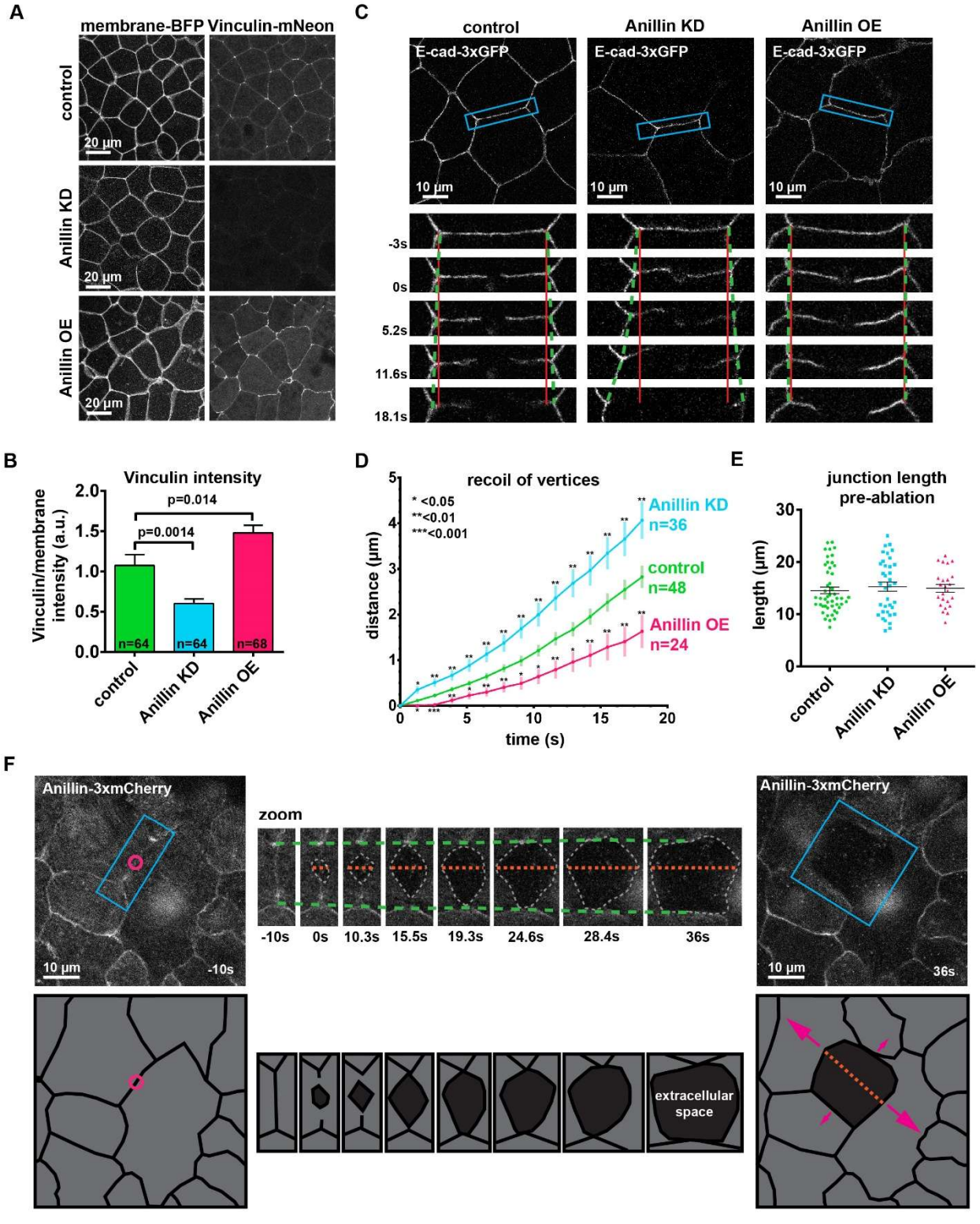

Figure 3.1: Anillin increases junctional Vinculin recruitment but reduces recoil of junction vertices after laser ablation

A) Confocal images of live epithelial cells in gastrula-stage *Xenopus laevis* embryos with a probe for the plasma membrane (2x membrane localization signal of Src family tyrosine kinase Lyn tagged with TagBFP at its C-terminus) and Vinculin-mNeon when Anillin is knocked down (KD) or overexpressed (OE). **B)** Quantification of Vinculin intensity as a ratio to membrane intensity. Measurements were taken by tracing a bicelllular junction from vertex to vertex. Error bars, S.E.M. Statistics, unpaired t-test, n=number of junctions. **C)** Cell view images showing E-cadherin tagged with 3xGFP prior to junction laser ablation. Blue boxes show the zoomed area for the ablation montage. Red lines indicate the initial location of junction vertices, green dashed lines indicate the location of junction vertices after ablation. **D)** Quantification of junction vertex separation over time during ablation experiments. Error bars, S.E.M. Statistics, unpaired t-test, n=number of junctions. **E)** Quantification of initial junction length from vertex to vertex for ablation experiments. Error bars, S.E.M. Unpaired t-tests between control and Anillin KD or Anillin OE resulted in no statistical significance, Control vs. KD p=0.49, Control vs OE p=0.69. **F)** Cell view of embryo overexpressing Anillin tagged with 3xmCherry. Blue boxes show the zoomed area for the ablation montage. Green dashed lines indicate the location of junction vertices during ablation, orange dashed line indicates the perpendicular separation between the two cells, and the grey dashed outline indicates the space forming between the two cells. Cartoon traces of the ablation data depicting the events during ablation are shown below. Pink circle indicates the site of laser ablation, orange line indicates perpendicular separation between cells, and pink arrows represent direction and intensity of forces where larger arrows represent larger forces. (Unannotated data can be found Supplemental Fig. 3.1 D).

Anillin structures medial-apical F-actin and Myosin II

Based on our finding that Anillin promotes contractile forces perpendicular to the junction, we next tested whether Anillin affects the medial-apical population of F-actin and Myosin II, which could generate these perpendicular forces. To observe medial-apical F-actin, we optimized our fixation conditions to preserve this delicate network of F-actin and stained it with phalloidin. In control cells, we observed a dense meshwork of thin filaments of medial-apical actin. Knocking down Anillin reduced the intensity of this network, while overexpressing Anillin drastically reorganized this network into thick bundles of F-actin that could span the entire surface of the cells **(Fig. 3.2 A, E)**. We also observed thick medial-apical bundles of F-actin in live cells overexpressing Anillin using a probe for F-actin (Lifeact-GFP) and Anillin-3xmCherry colocalized with the F-actin bundles **(Fig. 3.2 B)**. Varied F-actin bundle organization and dynamics were observed including linear arrays that spanned the apical surface of the cells,

aster like structures, and circular bundles that rotated or flowed from the junction towards the center of the cell **(Fig. 3.2 A, B)**.

To determine whether these medial-apical F-actin bundles were decorated with Myosin II, we performed live imaging with a probe for Myosin II, the SF9 intrabody (Nizak et al. 2003; Vielemeyer et al. 2010; Hashimoto et al. 2015), which we tagged with mNeon. In controls, Myosin II accumulated on the medial-apical surface in patches that resemble previously described cortical waves of F-actin (Bement et al. 2015) **(Fig. 3.2 C)**. Knocking down Anillin resulted in almost a complete loss of Myosin II from the apical surface of epithelial cells, and when Anillin was overexpressed Myosin II increased and decorated the large bundles of F-actin that formed **(Fig. 3.2 C, D, & F)**. These data identify a new role for Anillin in establishing and structuring proper medial-apical F-actin and Myosin II, which may be important for epithelial cell mechanics.

Figure 3.2: Anillin structures medial-apical F-actin and Myosin II

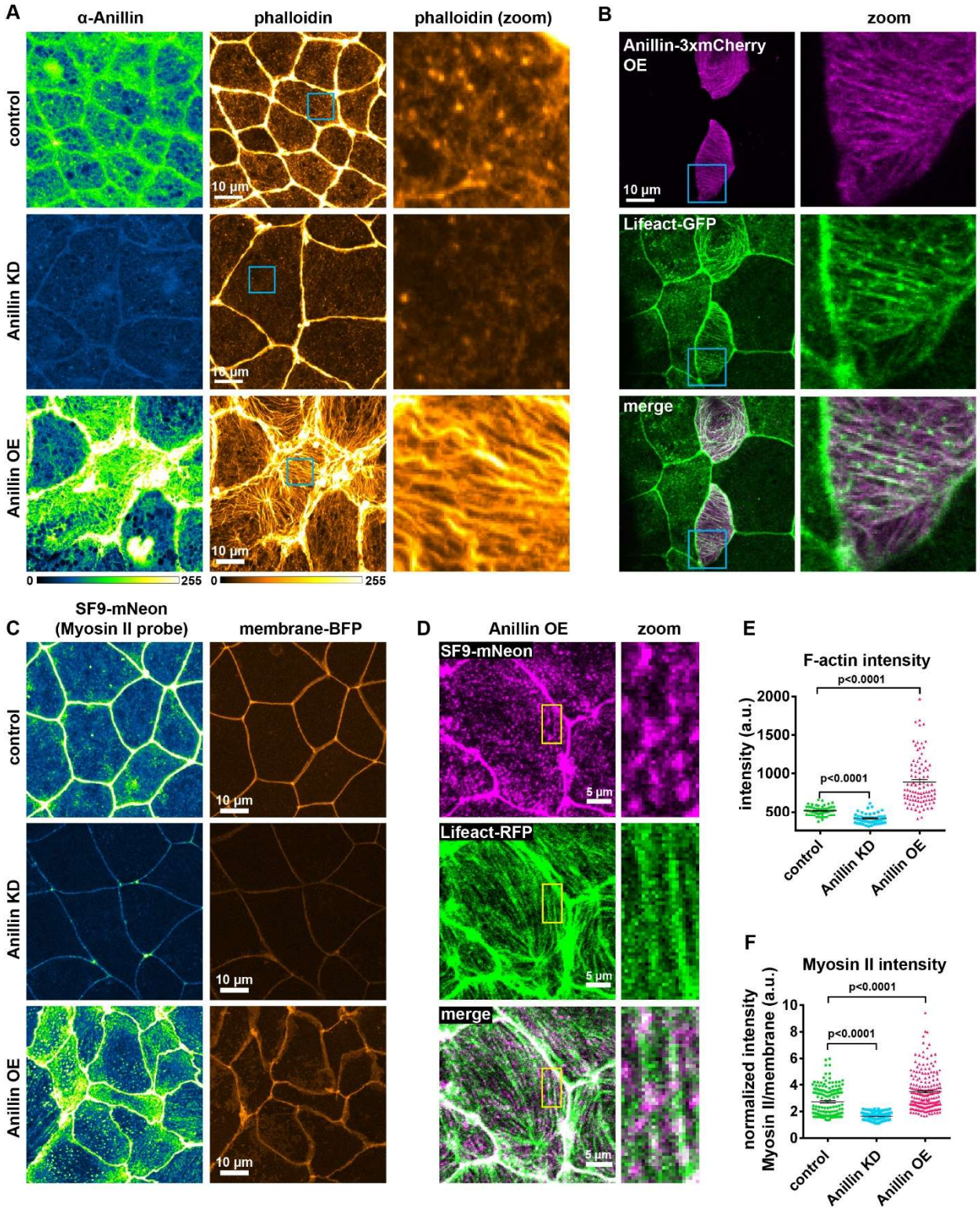

Figure 3.2: Anillin structures medial-apical F-actin and Myosin II
A) Confocal images of fixed epithelial cells from gastrula-stage *Xenopus laevis* embryos stained for Anillin (α-Anillin) and F-actin (Alexa Fluor 488 phalloidin). Blue boxes show zoomed in areas. **B)** Confocal images of live epithelial cells expressing Anillin-3xmCherry and Lifeact-GFP to probe for F-actin. Blue boxes show zoomed in areas. **C)** Confocal images of live epithelial cells expressing probes for Myosin II (SF9-mNeon) and membrane (membrane-TagBFP). **D)** Confocal images of live epithelial cells expressing probes for Myosin II (SF9-mNeon) and F-actin (Lifeact-RFP). Yellow boxes show zoomed in area. Notice how medial-apical Myosin II decorates the F-actin bundles. **E)** Quantification of medial-apical F-actin intensity from fixed embryos measured by a circular ROI 10 µm in diameter in the center of each cell. Error bars, S.E.M. Statistics, unpaired t-test. **F)** Quantification of medial-apical Myosin II intensity measured by a circular ROI 10 µm in diameter in the center of each cell. Medial-apical Myosin II intensity was normalized by dividing by junctional membrane intensity. Error bars, S.E.M. Statistics, unpaired t-test.

Anillin establishes a contractile medial-apical actomyosin network

When Anillin is knocked down, medial-apical actomyosin is dramatically reduced, and when Anillin is overexpressed, actomyosin is reorganized into large bundles, so we wanted to determine whether these populations of actomyosin are contractile. We added extracellular ATP, which leads to whole-embryo contraction driven by constriction of the apical surface of cells (Joshi, von, and Davidson 2010; Kim et al. 2014; Higashi et al. 2016) **(Fig. 3.3 A)**, making this an effective method to test whether the medial-apical actomyosin is contractile when Anillin is perturbed. When ATP was added to one side of the animal hemisphere, control embryos contracted towards the site of ATP addition **(Fig. 3.3 B)**. The contractile response could be observed and quantified in kymographs as a shift of the pigment towards the site of ATP addition **(Fig. 3.3 B)**. When Anillin was knocked down, the contractile response was attenuated, and when Anillin was overexpressed, the contractile response lasted longer **(Fig. 3.3 B & C)**.

At the cellular level, addition of ATP to control embryos resulted in a large burst of F-actin across the medial-apical surface that dissipated over time **(Fig. 3.3 D)**. The burst of F-actin initially accumulated near the junctions then spread toward the center of the cell **(Fig. S3.2 A &**

B). When Anillin was knocked down, F-actin accumulated transient and locally at junctions, which we have previously reported as flares of active RhoA associated with local actin accumulation (Reyes et al. 2014). However, these local actin accumulations did not propagate onto the medial-apical surface and resulted in local junction contraction, but not whole-cell or whole-embryo contraction **(Fig. 3.3 D-F)**. When Anillin was overexpressed, a burst of medial-apical F-actin similar to controls was observed; however, the large bundles of F-actin appeared thicker and more dynamic **(Fig. 3.3 D-F)**. When comparing the change in medial-apical F-actin before and after ATP (baseline and peak), knocking down Anillin significantly reduced the amount of F-actin accumulation compared to controls, while overexpressing Anillin resulted in no significant change in the amount of F-actin accumulation **(Fig. 3.3 D & E)**. Of note, medial-apical F-actin is already very high in Anillin overexpressing cells compared with controls before ATP addition, so it may not be possible to achieve a significant increase in F-actin above the already elevated level. Using another method to support Anillin's role in organizing a contractile medial-apical actomyosin network, we induced apical constriction by overexpressing Shroom 3, which induces apical constriction events during neurulation (Haigo et al. 2003; Itoh, Ossipova, and Sokol 2014). In cells induced to apically constrict by Shroom 3 overexpression Anillin accumulated across the apical surface of the cell, first near junctions then emanating towards the center of the cell **(Fig. S3.2 C)**. Taken together, these data support the idea that Anillin is required to establish a contractile medial-apical network. When Anillin is depleted, this network is not able to properly contract, and when Anillin is overexpressed, large bundles of actomyosin enhance whole-embryo contraction.

Figure 3.3: Anillin establishes a contractile medial-apical actomyosin network

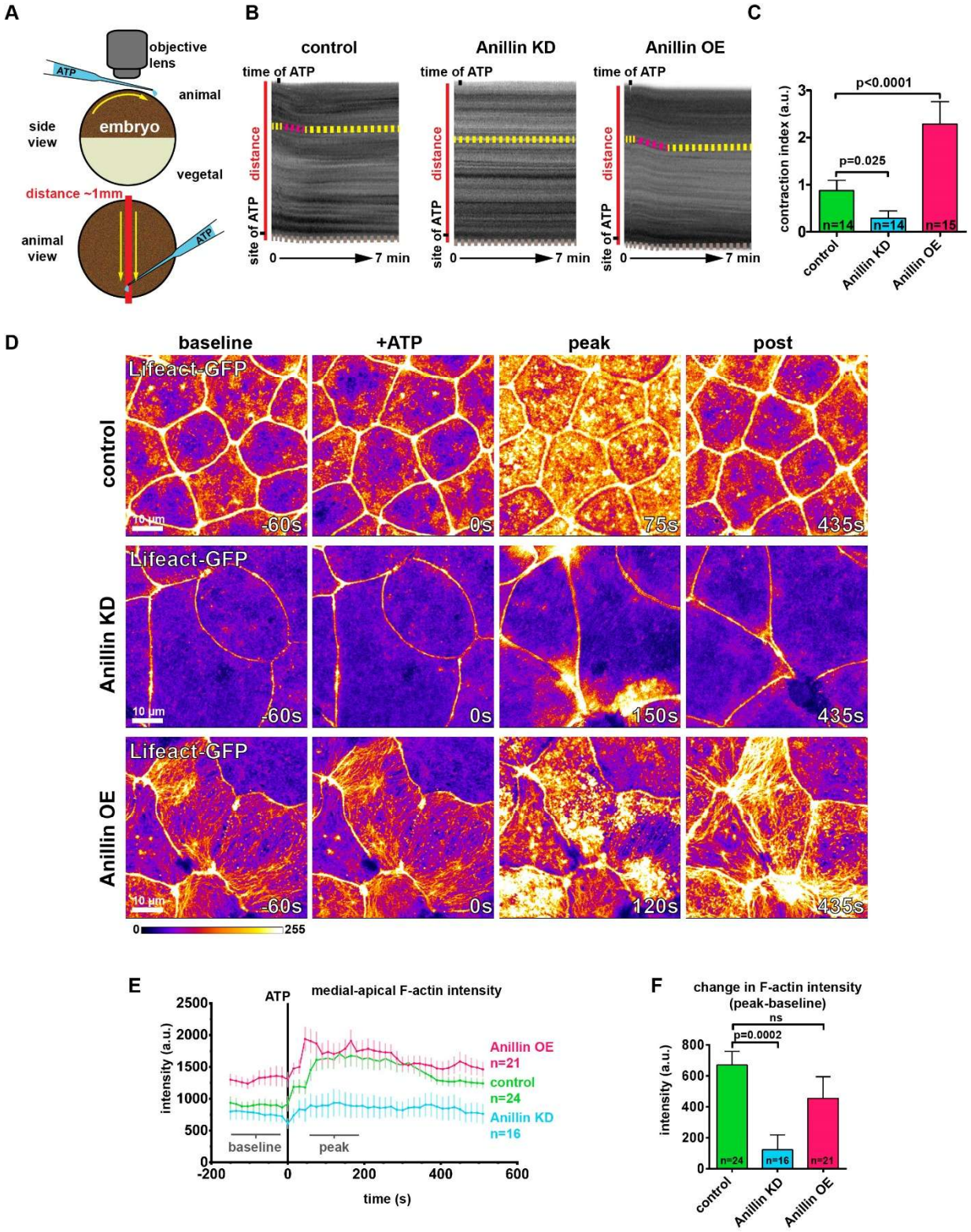

Figure 3.3: Anillin establishes a contractile medial-apical actomyosin network
A) Diagram of whole embryo extracellular ATP addition experiments. 40 nl of 50 mM ATP was micropipetted onto one side of the animal hemisphere of gastrula stage embryos. A video was captured of the embryo over time and kymographs were generated by drawing a line across the entire embryo (red line). Black arrows represent the direction of contraction towards the site of ATP addition. B) Kymographs of the animal hemisphere generated from light microscopy videos. The fluctuations in grey scale intensity are caused by the variations in pigment of the embryos. Contraction towards the site of ATP can be observed as a shift in the embryo's pigment towards the site of ATP addition. Yellow dashed lines represent periods of no contraction, and pink dashed lines represent contraction events. Brown dashed lines at the bottom of the kymograph represent movement of the whole embryo. C) Quantification of the contraction index measured from kymographs. Contraction index is the difference between the shift in a pigment over time (sum of the length of yellow and pink dashed lines in B) and the movement of the whole embryo over time (brown line in B). Statistics, unpaired t-test, n=number of embryos. D) Confocal images of live epithelial cells with F-actin probe Lifeact-GFP. After the addition of 500 µM ATP, notice the accumulation of medial-apical F-actin in controls and Anillin overexpressing cells, while F-actin only increases near the junctions in Anillin knockdown cells. The movement of cells across the field of view in controls and Anillin knockdown was caused by flow of solution when ATP was added. E) Quantification of medial-apical F-actin (Lifeact-GFP) intensity over time measured by a circular ROI 10 µm in diameter in the center of each cell. Statistics, unpaired t-test, n=number of cells. F) Comparison of the change in medial-apical F-actin (Lifeact-GFP) intensity before and after ATP addition. The difference between peak and baseline F-actin intensity was measured for each embryo by averaging the peak 10 frames (from 60s to 195s) and subtracting the baseline 10 frames (-15s to -150s). Statistics, unpaired t-test, n=number of cells.

Taken together, our results indicate that Anillin not only regulates junctional actomyosin (Reyes et al. 2014), but also organizes a medial-apical contractile actomyosin network that, when mechanically integrated across cells in an epithelial tissue (the animal cap epithelium), can affect tissue-level contraction (**Fig. 3.1-3)**. Based on our data, we speculate that Anillin can regulate the orientation of tensile forces applied on cell-cell junctions as shown in the model in Fig. 3.4. This model reconciles our initially surprising results that knocking down Anillin leads to *decreased* junctional Vinculin recruitment but *increased* recoil after laser ablation **(Fig. 3.1 A-D)**. We propose that Anillin knock down weakens medial-apical actomyosin to the point where it is no longer a contractile network **(Fig. 3.4 A)**. This results in decreased pulling forces perpendicular to junctions, allowing the parallel forces generated by junctional actomyosin to dominate **(Fig. 3.4 B)**. In contrast, overexpressing Anillin results in increased medial-apical actomyosin and reorganizes the actin into thick bundles that connect perpendicular to the junction **(Fig. 3.4 A)**. These actomyosin bundles are contractile and make

perpendicular forces on junctions dominant **(Fig. 3.4B)**, consistent with our data that when Anillin is overexpressed, Vinculin recruitment is *increased*, and following laser ablation, vertex separation is *reduced* but separation in the direction perpendicular to the junction occurs. Thus, our model suggests that the level of Anillin expression regulates if junctional or medial-apical actomyosin is the primary load-bearing structure on the apical surface of epithelial cells.

Figure 3.4: Model of how Anillin organizes medial-apical F-actin and regulates apical forces on junctions

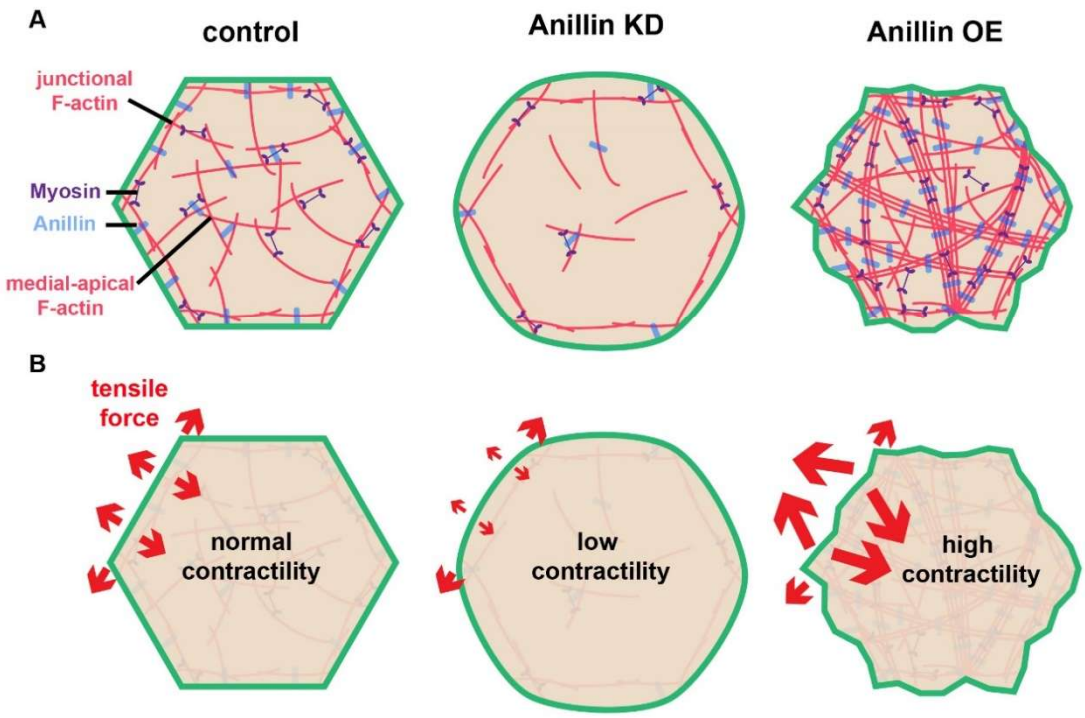

Figure 3.4: Model of how Anillin organizes medial-apical actomyosin contractility and regulates the orientation of tensile forces applied on junctions
A) Diagram of the apical surface of epithelial cells showing junctional and medial-apical F-actin and Anillin in control embryos or when levels of Anillin are perturbed. When Anillin is knocked down, medial-apical F-actin is strongly reduced, and when Anillin is overexpressed, medial-apical F-actin is reorganized into thick bundles decorated with Myosin II that span the apical surface. **B)** Diagram depicting the changes in the orientation of actomyosin-mediated forces applied on cell-cell junctions when Anillin is perturbed. When Anillin is knocked down, the medial-apical actomyosin is not robustly contractile, reducing forces perpendicular to the junction. When Anillin is overexpressed, perpendicular forces on cell-cell junctions are increased due to the large contractile bundles of F-actin that connect perpendicular to the junction.

Anillin's F-actin-binding domain and C-terminal domains are necessary for restructuring the medial-apical F-actin network

In order to build upon our proposed model **(Fig. 3.4)**, we examined which of Anillin's N-terminal functional domains are necessary for organizing medial-apical F-actin. We made Anillin mutants that lacked the Myosin II-binding domain (Δmyo), the F-actin-binding domain (Δact), or both the Myosin II- and F-actin-binding domains (Δmyoact) **(Fig. 3.5 A)**. When overexpressed, full length Anillin, and less intensely Δmyo localized to the medial-apical surface and Δmyo reorganized F-actin into long bundles that spanned the apical surface **(Fig. 3.5 B-D)**. When overexpressed, Δact localized medial-apically but only reorganize F-actin into short bundles or no bundles at all **(Fig. 3.5 B-D)**. Δmyoact did not localize medial-apically or reorganize F-actin robustly **(Fig. 3.5 B-D)**. These results indicate that both the Myosin II and F-actin-binding domains contribute to localizing Anillin to the medial-apical surface, and the F-actin-binding domain is necessary for reorganizing medial-apical F-actin into long bundles.

We next examined which of Anillin's functional C-terminal domains are necessary for reorganizing medial-apical F-actin. We made Anillin mutants that lacked the active RhoA binding domain (ΔRBD), the C2 domain which binds to the membrane and regulators of RhoA (ΔC2), and the PH domain which binds the membrane, septins, and regulators of RhoA (ΔPH) **(Fig. 3.5 E)**. When overexpressed both full length and ΔRBD were able to robustly localize to the medial-apical surface while medial-apical localization of the ΔC2 and ΔPH was reduced **(Fig. 3.5 F, G)**. Overexpression of ΔRBD, ΔC2, and ΔPH did not result in restructuring of medial-apical F-actin into long or short bundles **(Fig. 3.5 F, H)**. Together these results indicate that Anillin's F-actin binding domain and C-terminal domains are required for restructuring

medial-apical F-actin into long bundles that span the apical surface and Anillin's medial-apical localization is facilitated by actomyosin binding with possible contributions from binding to the membrane, regulators of RhoA, or Septins.

Figure 3.5: Anillin' s F-actin and C-terminal domains are requried for restructuring medial-apical F-actin

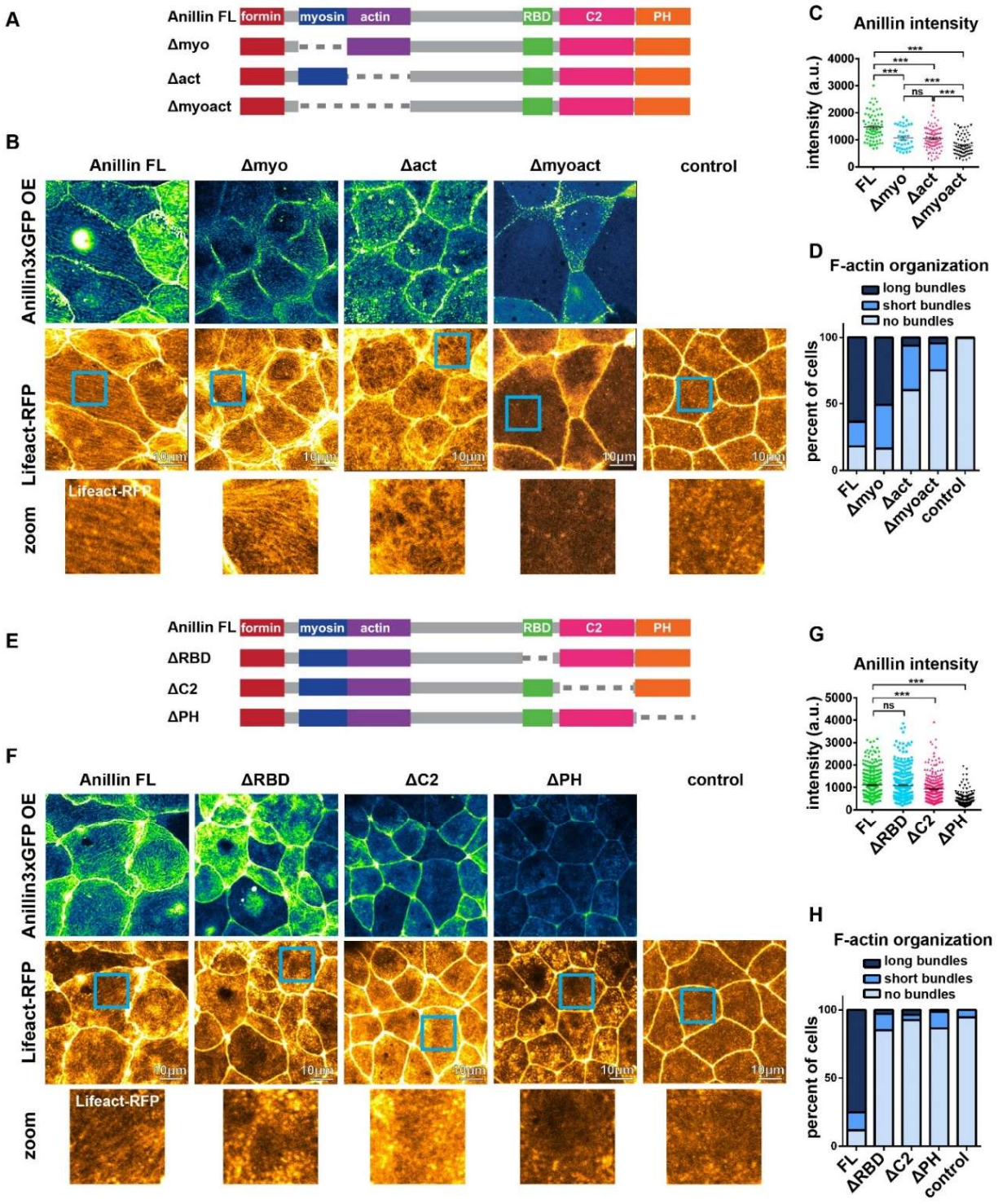

Figure 3.5: Anillin's F-actin-binding domain and C-terminal domains are necessary for structuring the medial-apical F-actin network

A) Domain diagram of full length Anillin and N-terminal domain deletions. Full Length (FL), Rho Binding Domain (RBD), Pleckstrin Homology (PH). **B)** Confocal images of live epithelial cells from gastrula stage *Xenopus laevis* embryos expressing either full length Anillin or Anillin domain deletions tagged with 3xGFP and Lifeact-RFP to probe for F-actin. Blue boxes show zoomed in area. **C)** Quantification of Anillin construct intensity measured by a circular ROI 10 µm in diameter in the center of each cell. Statistics, unpaired t-test, *** = <0.001, n=number of cells **D)** Blinded categorization of medial-apical F-actin bundles organization in cells. FL, n=306; Δmyo, n=112; Δact, n=61; Δmyoact, n=57; control, n=110 cells. **E)** Domain diagram of full length Anillin and C-terminal domain deletions. Full Length (FL), Rho Binding Domain (RBD), Pleckstrin Homology (PH). **F)** Confocal images of live epithelial cells from gastrula stage *Xenopus laevis* embryos expressing either full length Anillin or Anillin domain deletions tagged with 3xGFP and Lifeact-RFP to probe for F-actin. **G)** Quantification of Anillin construct intensity measured by a circular ROI 10 µm in diameter in the center of each cell. Statistics, unpaired t-test, *** = <0.001, n=number of cells **H)** Blinded categorization of medial-apical F-actin bundles in cells. FL, n= 395; ΔRBD, n= 352; ΔC2, n= 332; ΔPH, n=287; control, n=109 cells.

Anillin regulates epithelial cell mechanics by stabilizing medial apical F-actin

Our findings demonstrated that Anillin's actin-binding function is necessary to reorganize medial-apical F-actin, and previous work has shown that Anillin stabilizes F-actin by preventing Cofilin severing of actin filaments (Tian et al. 2015). This led us to ask if Anillin stabilizes medial-apical F-actin, and whether actin stabilization contributes to changes in epithelial cell mechanics. To test if Anillin stabilizes F-actin, we used Fluorescence Recovery After Photobleaching (FRAP) of actin-mNeon in controls cells and in cells overexpressing Anillin **(Fig. 3.6 A)**. After photobleaching in control cells, actin-mNeon recovered to 81 ± 2%, whereas in cells overexpressing Anillin, actin-mNeon recovered to 66 ± 2% **(Fig 3.6. A-C)**, indicating that Anillin stabilizes actin filaments. We attempted to perform FRAP of actin-mNeon when Anillin was knocked down, but because Anillin knockdown drastically reduces medial-apical F-actin, we had to inject excessive amounts of actin-mNeon mRNA in order to visualize medial-apical F-actin. This high level of actin-mNeon led to abnormal cell and embryo morphology in control and Anillin overexpression embryos. In Anillin knockdown cells, the overexpressed actin-mNeon recovered to 96 ± 8%; however, these data cannot be directly

compared with control and Anillin overexpression data because of the differing levels of actin-mNeon expression **(Fig. S3.3 A)**.

Because the FRAP data revealed that Anillin not only reorganizes F-actin, but also stabilizes actin filament dynamics, we hypothesized that stabilizing F-actin using the drug jasplakinolide (Holzinger 2001) could produce changes in cell mechanics similar to Anillin overexpression. After treating embryos with jasplakinolide (20 µM, 1 hr), we observed increased F-actin bundles at the medial-apical surface **(Fig. 3.6 D)**. These actin bundles were shorter than those observed when Anillin was overexpressed, didn't span the apical surface, and didn't flow towards the center of the cell **(Fig. 3.6 D)**. We performed junctional laser ablation to test whether the effect observed when F-actin was stabilized by jasplakinolide would recapitulate Anillin overexpression (reduced parallel recoil and increased perpendicular recoil). Indeed, jasplakinolide treatment strongly reduced parallel recoil, from 2.7 ± 0.3 µm after 18 s in controls to 0.2 ± 0.1 µm after 18 s **(Fig. 3.6 E & F)**. In support, jasplakinolide treatment of Anillin knock down embryos also reduced junction recoil after laser ablation **(Fig. S3.3 B)**. Remarkably, following jasplakinolide treatment of control embryos, we observed several examples of increased cell separation perpendicular to the junction, similar to the effect when Anillin was overexpressed **(Fig. 3.6 G)**. In some cases, for both jasplakinolide treated cells and Anillin-overexpressing cells, we observed that parallel vertex separation only occurred after perpendicular separation near the vertex occurred **(Fig. 3.6 G, S3.3 C-E)**, indicating that forces perpendicular to these junctions were maintaining cell shape after laser ablation. Together, these results demonstrate that Anillin stabilizes medial-apical F-actin and suggest that F-actin

stability contributes to the mechanical changes observed in epithelial cells when Anillin is perturbed.

Figure 3.6: Anillin regulates epithelial cell mechanics by stabilizing medial-apical F-actin

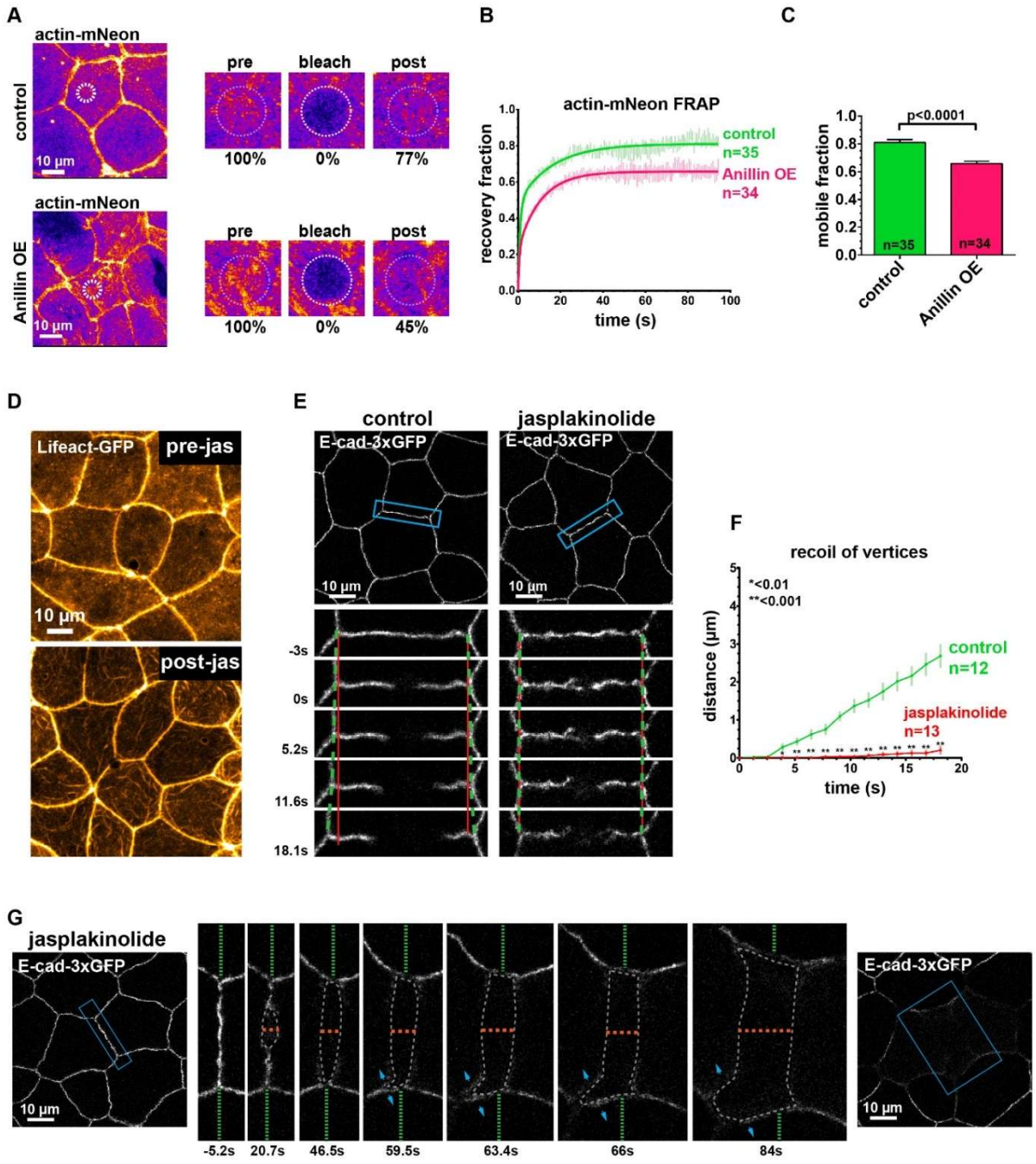

Figure 3.6: Anillin regulates epithelial cell mechanics by stabilizing medial-apical F-actin
A) Single plane confocal images of live epithelial cells from gastrula stage *Xenopus laevis* embryos expressing *Xenopus laevis* actin tagged with mNeon (actin-mNeon) in control or Anillin overexpressing embryos. White dashed circle shows the medial-apical area bleached in the zoomed view montages on the right. Normalized percent of original fluorescence intensity is indicated for the zoomed view. **B)** Medial-apical actin-mNeon Fluorescence Recovery After Photobleaching (FRAP) data fitted with a two phase association curve. n=number of cells. **C)** Mobile fractions from FRAP data. Error bars, S.E.M. Statistics, unpaired t-test, n=number of cells. **D)** Confocal images of live epithelial cells expressing a probe for F-actin (Lifeact-GFP). Top image was taken before the addition of 20 µm jasplakinolide. The bottom image of the same field of view was taken 1 hour after the addition of jasplakinolide. **E)** Single plane confocal images showing E-cadherin tagged with 3xGFP (E-cad-3xGFP) prior to junction laser ablation for a control embryo (2% EtOH) and an embryo treated with 20 µm jasplakinolide. Blue boxes show the zoomed area for the ablation montage. Red lines indicate the initial location of junction vertices, green dashed lines indicate the location of junction vertices after ablation. **F)** Quantification of vertex separation over time after ablation. Error bars, S.E.M. Statistics, unpaired t-test, n=number of cells **G)** Confocal images of an embryo expressing E-cad-3xGFP and treated with 20 µm jasplakinolide before and after laser ablation. Blue boxes show the zoomed area for the ablation montage. Green dashed lines indicate the position of the vertices relative to the edge of the image, orange dashed line indicates the perpendicular separation between the two cells, grey dashed line indicates the space forming between the two cells, and blue arrows represent forces on junctions adjacent to the lower cell vertex. Notice that the lower vertex only begins to separate in the parallel direction after the forces perpendicular to the adjacent junction (blue arrows) lead to loss of adhesion between the two cells.

Anillin promotes tissue stiffness

Since Anillin promotes medial-apical actin stability, and reduces junction recoil after laser ablation, we next asked whether Anillin promotes tissue-wide stiffness. To measure the effect that Anillin has on tissue stiffness, we utilized dorsal isolates from neurula stage (Nieuwkoop and Faber stage 15) *Xenopus laevis* embryos, as they are amenable to measuring tissue stiffness **(Fig. 3.7 A)** (Zhou, Kim, and Davidson 2009). First, we characterized the effects of Anillin knockdown on F-actin in the dorsal isolates by knocking down Anillin in half of the embryo, leaving the other half of the embryo as an internal control. Similar to our results in the gastrula stage animal cap epithelium **(Fig. 3.2 A & E)**, regions of the dorsal isolates where Anillin was knocked down showed a marked reduction in junctional and medial-apical F-actin compared with internal control regions **(Fig. 3.7 B,C & S3.4)**. Interestingly, transverse sections of dorsal isolates revealed that Anillin knockdown not only reduced apical F-actin but also enhanced accumulation of F-actin at the basal surface of these epithelial cells **(Fig. 3.7 C &**

S3.4). At the cellular scale, Anillin knockdown led to apical doming, similar to our previous report in gastrula stage epithelial cells **(Fig. 3.7 C & S3.4) (Reyes et al. 2014)**. At the tissue level, defects in the morphology of presomitic mesoderm, notochord, and endoderm were observed upon Anillin knockdown **(Fig. 3.7 A, C & S3.4)**.

To test whether Anillin promotes tissue stiffness, Anillin was knocked down throughout the embryo. Despite delayed gastrulation, the Anillin knock down embryos were able to develop to stage 15, and dorsal isolates were loaded onto a nanoNewton Force Measurement Device, which measures resistive forces generated by the dorsal isolate in response to compression **(Fig. 3.7 D)** (Zhou, Kim, and Davidson 2009). Stiffness (defined as the elastic modulus after 180 seconds of unconfined compression) is calculated using measured resistive force, compressive strain, and the dorsal isolate cross-sectional area **(Fig. 3.7 D)** (Zhou, Kim, and Davidson 2009). There was a significant reduction in the stiffness of dorsal isolates when Anillin was knocked down compared with controls **(Fig. 3.7 E)**. Taken together, these results indicate that Anillin promotes tissue stiffness, which may be due to the strong reduction in medial-apical F-actin. It should be noted, however, that the loss of junctional F-actin or the defects in presomitic mesoderm, notochord, or endoderm may also contribute to the measured change in tissue stiffness.

Figure 3.7: Anillin promotes tissue stiffness

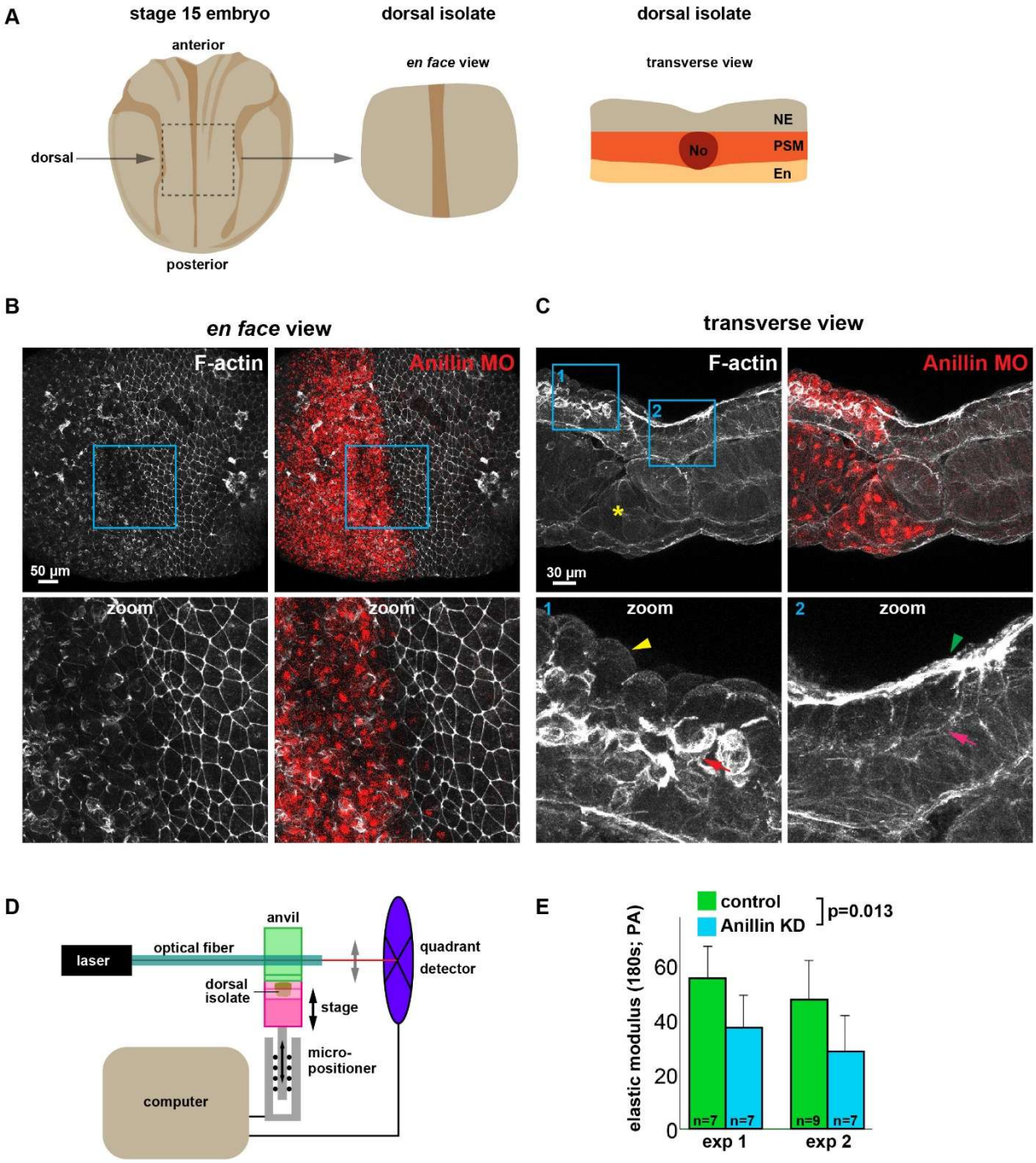

Figure 3.7: Anillin promotes tissue stiffness
A) Cartoons of stage a 15 *Xenopus laevis* embryo and dorsal isolate (reproduced from Nieuwkoop and Faber). Transverse view shows the Neural Ectoderm (NE), Presomitic Mesoderm (PSM), Endoderm (En), and Notochord (No). **B)** *En face* images of fixed dorsal isolates, z-projected (~50 microns deep). F-actin was stained using phallacidin tagged with BODIPY FL. Anillin morpholino was co-injected with Alexa Fluor 647-conjugated Dextran as a lineage tracer. Blue boxes represent zoomed in area below. Notice the reduced junctional and medial-apical F-actin in Anillin-depleted neural ectoderm. **C)** Transverse section views of the dorsal isolates. Blue boxes show zoomed in areas below. Anillin knockdown epithelial cells exhibit an apically domed morphology and loss of F-actin on their apical surface (yellow arrowhead), enhanced basolateral F-actin (red arrow), and disrupted mesoderm organization (yellow asterisk). Control epithelial cells have a flat apical morphology with robust F-actin (green arrowhead) and little basal F-actin (pink arrow). **D)** Diagram of the nanoNewton Force Measurement Device, which measures resistive force generated by the tissue isolate in response to compression using a force-calibrated optical fiber. A computer-controlled stage compresses the tissue isolate against an anvil attached to the optical fiber and the resistive force is measured using the deflection of the optical force probe. **E)** Quantification of the stiffness of dorsal isolates. Tissue stiffness is significantly reduced when Anillin is knocked down. Statistics, 2-way ANOVA, n=number of dorsal isolates.

Discussion

Anillin is a scaffolding protein with diverse binding capabilities, which it uses to organize the cytoskeletal elements including F-actin, Septins, and microtubules (Field and Alberts 1995; Sisson et al. 2000; Silverman-Gavrila, Hales, and Wilde 2008; D'Avino 2009), build actin structures by activating formins (Watanabe et al. 2010), and promote contractility by linking F-actin and Myosin II to the plasma membrane and binding active RhoA and its regulators (Straight, Field, and Mitchison 2005; Piekny and Glotzer 2008; Sun et al. 2015; Manukyan et al. 2015; Descovich et al. 2017). With this diverse set of interactions, it is not surprising that Anillin functions in a range of cellular processes across the tree of life. It is required for cytokinesis in many organisms, from yeast to vertebrates, promotes cellularization in fly embryos, maintains bridges between germ cells in worms, and regulates migration in neurons (Field and Alberts 1995; Piekny and Maddox 2010; Amini et al. 2015; Sun et al. 2015). Furthermore, Anillin has an emerging role in regulating cell-cell junctions and promoting proper tissue barriers through maintaining the contractile actomyosin network connected to cell-cell junctions (Gbadegesin et al. 2014; Reyes et al. 2014; Wang et al. 2015; Budnar et al. 2018).

Here, we have discovered a new role for Anillin in organizing a contractile network of medial-apical actomyosin in frog embryonic epithelia. We demonstrate that perturbing Anillin changes the mechanical properties of both cells and the tissue as a whole.

Multiple factors contribute to junction recoil after laser ablation

Laser ablation has been a useful tool for inferring the relative amount of tension on cell-cell junctions, leading to many insights about the proteins involved in generating tension on junctions (Farhadifar et al. 2007; Fernandez-Gonzalez et al. 2009; Ratheesh et al. 2012; Leerberg et al. 2014; Van Itallie et al. 2015; Choi et al. 2016; Priya et al. 2016; Bertocchi et al. 2017). Generally, laser ablation is thought to measure the amount of line tension or tension in the direction parallel to the edge of a cell (Rauzi and Lenne 2015). However, there is evidence that the medial-apical actin network can also contribute significantly to load bearing within the cell (Ma et al. 2009). Here, our laser ablation experiments produced unexpected results with respect to the prevalent line tension paradigm **(Fig. 3.8 A)** and led us to characterize a new function for Anillin in organizing contractile medial-apical actomyosin structures.

Taken together, our results indicate that Anillin is important for establishing medial-apical actomyosin, which acts as a load-bearing structural network in epithelia. By stabilizing and organizing medial-apical F-actin and Myosin II, Anillin promotes a contractile network that produces tensile forces that act perpendicular to cell-cell junctions **(Fig. 3.8 B)**. These perpendicular forces can reorient the direction of junction separation after laser ablation, causing the cells to separate in the direction perpendicular to the junction. If we had performed either the Vinculin recruitment or laser ablation experiments in isolation, opposite conclusions would have been drawn about how the Anillin expression level affects junctional tension. A

weakness of these tension probing techniques is that they do not easily reveal the direction of forces acting on the junction. For example, if a junction recoils slowly parallel to the junction after laser ablation, is this because there is less parallel tension, more perpendicular tension, or other mechanical changes? Additionally, we found that Anillin stabilizes medial-apical F-actin helping to generate a load-bearing structural network in epithelia **(Fig. 3.8 C)**. When we stabilized F-actin with jasplakinolide, junction recoil was dramatically decreased, similar to the effect with Anillin overexpression, indicating that cellular mechanics are regulated by the physical properties of the F-actin network **(Fig. 3.8 C)** in addition to the contractile forces generated by the network. Finally, we showed that Anillin promotes tissue-wide stiffness, and this likely contributes to the changes we observe in cellular mechanics **(Fig. 3.8 D)**.

While there is little direct evidence about how tissue compliance affects laser ablation results, it is easy to conceive how two junctions under the same tension - one in a compliant tissue vs. one in a non-compliant tissue - would recoil at different velocities. A recent study found that cell boundary stiffness was locally increased by unidirectional actomyosin-generated tension, and when ablated parallel to this axis, the tissue displayed high recoil (Chanet et al. 2017). In contrast, when actomyosin-generated contractility was omnidirectional cell boundary stiffness increased evenly around the cell boundary, and when ablated, the tissue displayed reduced recoil (Chanet et al. 2017). While changes in the direction of actomyosin contractility certainly contribute to the changes in junction recoil, the changes in boundary stiffness may also play an essential role. Future studies using laser ablation or other methods of measuring junctional tension should consider potential contributions of perpendicular tensile forces

generated by the medial-apical actomyosin network, the stability of F-actin filaments, and the compliance of the junction and surrounding tissue.

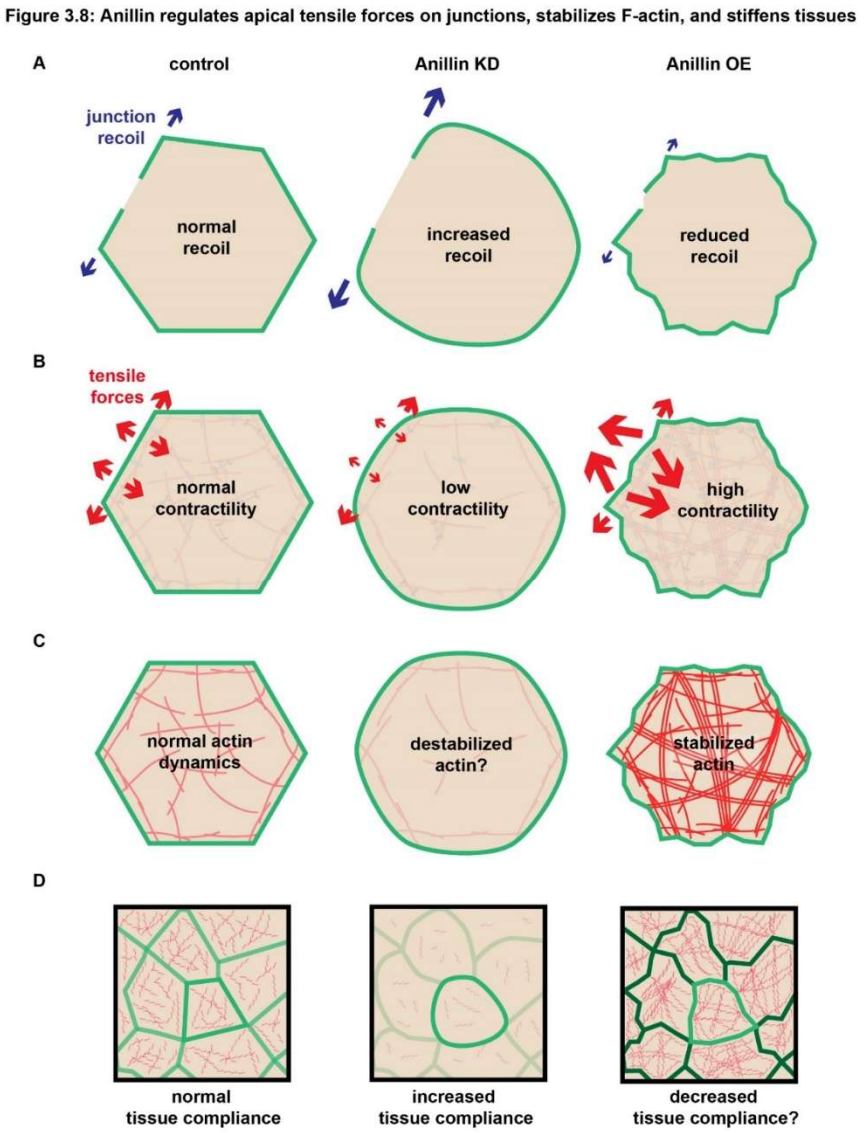

Figure 3.8: Anillin regulates apical tensile forces, stabilizes F-actin, and stiffens tissues.
A) Schematic of our results showing that increased Anillin expression slows junction recoil. **B)** Model of how Anillin slows junction recoil by reorienting tensile forces across the apical surface of cells, transitioning the dominant tensile force from being in line with the junction to being perpendicular to the junction, which may contribute to the observed changes in junction recoil. **C)** Model of how Anillin stabilizes F-actin, which may contribute to the observed changes in junction recoil. **D)** Model of how Anillin modulates tissue compliance, which may contribute to the observed changes in junction recoil.

Anillin regulates apical contractility in epithelia

Combining our previous study, which showed that Anillin maintains F-actin, Myosin II, and proper RhoA activity at cell-cell junctions (Reyes et al. 2014), with this study, which shows that Anillin promotes a contractile medial-apical network, positions Anillin as a key regulator of contractility at the apical surface of epithelial cells. Our results also suggest that the level of Anillin expression may modulate redistribution of cellular load-bearing structures from junctional/circumferential when Anillin is expressed at a low level to cortex-spanning/medial-apical when Anillin is expressed at a high level. This change parallels one seen in *Drosophila* development over the course of germ band elongation. Initially, tissue tension is transmitted primarily through junctional structures, but by the end of germ band elongation, it is carried by cortex-spanning structures (Ma et al. 2009). Additional work will be necessary to distinguish the functions of Anillin-organized contractility at junctional and medial-apical contractile arrays.

Anillin's role in regulating medial-apical contractility may function to prevent junction disassembly by generating forces perpendicular to the junction. Myosin II-generated tension applied on adherens junctions can prevent junction disassembly (Weng and Wieschaus 2016). Here, we showed that Anillin-organized medial-apical contractility produces perpendicular tension on adherens junctions. This raises the possibility that protective tensile forces organized by medial-apical Anillin are lost when Anillin is knocked down, which could lead to the compromised junctions we have previously reported (Reyes et al. 2014).

Our findings establish Anillin as a candidate protein that may be involved in developmental events that require apical constriction including gastrulation and neurulation.

Anillin's potential role in development is supported by the fact that many of Anillin's interacting proteins - including active RhoA, the formin Diaphanous, F-actin, and Myosin II - also localize to the medial-apical actomyosin network and are required for apical constriction events during development (Mason, Tworoger, and Martin 2013; Martin and Goldstein 2014). Of note, when Shroom3, which is known to induce apical construction during neurulation (Haigo et al. 2003), was overexpressed, Anillin strongly accumulated across the medial-apical surface as apical constriction proceeded **(Fig. S3.2 C)**. In the future, it will be interesting to directly test whether Anillin plays a role in gastrulation and/or neurulation.

Does Anillin regulate tissue stiffness in development and disease?

Our data demonstrating that Anillin promotes tissue stiffness is intriguing because tissue stiffness can affect tissue folding during development (Jackson et al. 2017) as well as cell migration during development and in cancer (Barriga et al. 2018). Although we cannot confirm whether reduction in tissue stiffness after Anillin knock down is directly related to loss of medial-apical Anillin vs. contributions from loss of junctional Anillin, failed cell division events, or the changes in other tissue layers, the idea that Anillin is regulating tissue stiffness by organizing actomyosin contractility at one or more of these sites is supported by previous work. For example, tissue stiffness increases during *Xenopus* development, and this is dependent on F-actin and Myosin II (Zhou, Kim, and Davidson 2009). Indeed, the ~35% reduction in stiffness we observed after Anillin knockdown is in line with the ~50% reduction in stiffness observed after acute drug treatments that disrupt F-actin or Myosin II (Zhou, Kim, and Davidson 2009). Additionally, a recent study directly connected medial-apical contractility with promoting tissue stiffness, and found that the direction of contractility promoted oriented

tissue stiffness, which in turn drove proper tissue invagination (Chanet et al. 2017). Future studies should investigate whether Anillin impacts developmental events that require tissue stiffening.

Our findings may also provide insight into the role Anillin plays in cancer progression. To date, studies examining Anillin's role in tumor progression and survival outcome have produced conflicting evidence. Most studies have found that Anillin is overexpressed in diverse tumors, and its expression correlates with cancer progression and poor survival rates (Hall et al. 2005; Suzuki et al. 2005; Wang et al. 2016; Idichi et al. 2017; Zhang et al. 2017). However, work examining the subcellular localization of Anillin found that *nuclear* localization of Anillin correlates with poor survival rates, whereas *cytoplasmic* localization of Anillin is a marker of favorable prognosis, suggesting that Anillin's localization rather than its expression level is key (Ronkainen et al. 2011; Liang et al. 2015). Our finding that Anillin increases tissue stiffness may help explain Anillin's role in tumor progression. It is well known that tumors increase in stiffness over time due to increased extracellular collagen, and this stiffening promotes tumor progression (Fang et al. 2014); however, measurements of the stiffness of individual cancer cells revealed that cells become less stiff as they become metastatic (Swaminathan et al. 2011; Guo et al. 2014). Considering our results in this context, we speculate that *cytoplasmic* Anillin could help protect against cancer progression, as it stiffens the cells and the tissue by reorganizing actomyosin, preventing cells from entering a migratory metastatic state. Our previous work showing that Anillin is important for maintaining normal cell-cell adhesion could also play a role in preventing cancer cell invasion and metastasis (Reyes et al. 2014).

Conclusions

Our results reveal that by structuring medial-apical actomyosin, Anillin helps orchestrate apical contractility in epithelial cells, affects the direction of tensile forces applied on junctions, and promotes tissue stiffness. Thus, Anillin is potentially a key cytoskeletal organizer in events that require apical constriction, junction maintenance, and/or changes in tissue stiffness. Future work is required to tease apart the contributions and interplay between Anillin's versatile roles in cytokinesis, cell adhesion, and medial-apical actomyosin regulation and how they culminate to promote a functional epithelium.

Materials and methods

Xenopus laevis embryos and microinjections

All studies conducted using *Xenopus laevis* embryos strictly adhered to the compliance standards of the US Department of Health and Human Services Guide for the Care and Use of Laboratory Animals and were approved by the University of Michigan's Institutional Animal Care and Use Committee. *Xenopus* embryos were collected, *in vitro* fertilized, de-jellied, and microinjected with mRNAs for fluorescent probes using methods described previously (Reyes et al. 2014). Embryos were injected at either the two-cell (each cell injected twice) or the four-cell stage (each cell injected once) and allowed to develop to gastrula stage (Nieuwkoop and Faber stages 10 to 11) or neurula stage (Nieuwkoop and Faber stage 15). For gastrula-stage experiments, embryos were injected at the animal hemisphere at the two cell stage, injecting each cell twice, or the four cell stage, injecting each cell once. For neurula stage experiments, embryos were injected at the equator at the four cell stage, injecting two of the cells to characters defects and all four of the cells for tissue stiffness measurements. Amounts of probes per single injection are as follows: actin-mNeon, 17 pg or 36 pg when Anillin was knocked down; Anillin untagged OE, 70 pg; Anillin-3xmCherry, 70 pg; Anillin-3xGFP or 3xmCherry OE, 300pg; α-catenin, 30pg; E-cadherin-3xGFP, 50pg; Lifeact-GFP or RFP, 16 pg; membrane-TagBFP, 60 pg; SF9-mNeon, 74 pg; Shroom 3 OE, 200 pg; Anillin morpholino 211 pg. Anillin MO was injected similar to (Reyes et al. 2014) except instead of injecting 5 nl of 5mM morpholino, here we injected 10nl of 2.5mM morpholino to make injections easier as the higher dilution made the morpholino less viscous and easier to inject.

Constructs

Xenopus laevis actin was cloned from a cDNA library generated from *Xenopus laevis* tadpoles (Higashi et al. 2016). pCS2+/Shroom 3 was a generous gift from Sergei Sokol. SF9 was a generous gift from Ed

Munro (Hashimoto et al. 2015) and was subcloned into pCS2+mNeon. All other constructs were in pCS2+ plasmid and mRNA was synthesized as previously reported in (Reyes et al. 2014; Higashi et al. 2016).

Experiment replicates

Multiple embryos were used for all experimental replicates. Each experiment was conducted in three separate replicates except the following: Laser ablation with jasplakinolide treatment, two replicates. Laser ablation with Anillin knockdown and jasplakinolide treatment, two replicates. FRAP of medial apical F-actin with Anillin knockdown, two replicates. Shroom 3 overexpression in animal cap epithelium observing Anillin localization, two replicates. Dorsal isolate characterization when Anillin was knocked down, two replicates. Dorsal isolate tissue stiffness measurements when Anillin was knocked down, two replicates.

Confocal microscopy

Images of gastrula stage embryos were collected on an inverted Olympus Fluoview 1000 microscope equipped with a 60X super corrected PLAPON 60XOSC objective (numerical aperture [NA] = 1.4; working distance = 0.12 mm) and FV10-ASW software as previously described in (Reyes et al. 2014).

Images of dorsal isolates were collected using a confocal laser scan head (SP5 Leica Microsystems) mounted on an inverted compound microscope (DMI6000, Leica Microsystems) equipped with a 25X water immersion objective using acquisition software (LASAF, Leica Microsystems).

Laser ablation

Single plane movies were collected on a Leica Inverted SP5 Confocal Microscope System on a 60X objective with 2-Photon. White-light laser was tuned for emission at 488 nm and or 561 nm to visualize GFP or mCherry, respectively. Junction cuts were made with the 2-Photon laser with a ROI 0.36 x 4 µm. Each embryo was only cut three times and junction cuts were made in distant areas of the embryo.

Fixed staining and immunofluorescence

Gastrula-stage embryos were immunostained by methods described previously (Reyes et al. 2014) with the following changes: embryos were fixed with 1.5% formaldehyde, 0.25% glutaraldehyde, 0.2% Triton X-100, and 0.88X MT fix buffer (1X MT buffer: 80 mM K-PIPES, 5 mM EGTA, 1 mM $MgCl_2$ [pH 6.8]) and blocked in Tris-buffered saline (50 mM Tris and 150 mM NaCl [pH 7.4]) containing 10% fetal bovine serum (10082-139; Invitrogen), 5% DMSO and 0.1% NP-40 overnight at room temperature. Embryos were stained with anti-Anillin antibody (generously provided by Aaron Straight, Stanford University (Straight, Field, and Mitchison 2005)) and detected with goat anti-rabbit-Alexa Fluor 488 (Life technologies A11008 Lot:1583138),1:500 and phalloidin Alexa Fluor 568 (Life Technologies A12380 Lot:1154065), 1:100.

ATP experiments

Whole gastrula-stage embryos (NF stage 10.5) were imaged on an Olympus SZX16 Fluorescent Stereoscope, and 320 nl of 50 mM ATP (Sigma A2383-5G Lot: SLBD2725V) diluted in 0.1X MMR was added to one side of the embryo with a microinjector needle. For cell view experiments, gastrula-stage embryos were mounted in 0.1X MMR for confocal imaging in an imaging slide with an opening in the top of the chamber. During live imaging, 100 ul of 500 µM ATP diluted in 0.1X MMR was added to the chamber.

Jasplakinolide experiments

For confocal timelapse gastrula-stage embryos were mounted in 0.1X MMR for confocal imaging in an imaging slide with an opening in the top of the chamber. During live imaging, 100 ul of 20µM Jasplakinolide diluted in 0.1X MMR was added to the chamber. For laser ablation experiments embryos were added to microcentrifuge tube with 20 µM Jasplakinolide diluted in 0.1X MMR. After 1 hr of incubation embryos were mounted on a slide and imaged.

Actin localization in dorsal isolates

Anillin morpholino was co-injected with Alexa Fluor 647-conjugated dextran into one dorsal blastomere at the 4-cell stage. At NF stage 15, dorsal isolates were microsurgically isolated, fixed in 4% paraformaldehyde for 4 hours, bisected, and stained for F-actin (BODIPY FL phallacidin ThermoFischer Scientific B607). Some explants were not bisected, but instead the neural ectoderm was imaged *en face*.

Dorsal isolate stiffness

Anillin morpholino or water (control) was injected into each dorsal blastomere at the 4-cell stage. Dorsal isolates were isolated from embryos at NF stage 15 and loaded into the nanoNewton Force Measurement Device to measure time-varying elastic modulus using a stress-relaxtion protocol (Davidson and Keller 2007). In brief, the tissue sample is compressed along its anterior-posterior axis while the resistive force is measured by the deflection of an optical fiber force transducer. Young's modulus after 180 seconds of compression is then calculated using measured resistive force, explant cross-sectional area and strain measurements.

Image analysis

Vinculin and α-catenin intensities: A bicellular junction was traced from tricellular junction to tricellular junction with a segmented line 5 pixels wide in Fiji (Schindelin et al. 2012). Vinculin and α-catenin intensities were normalized by dividing by the membrane probe intensity.

Vertex recoil after laser ablation: In Fiji, a straight line was drawn between the vertices to measure the amount of separation over time.

F-actin and Myosin II intensity: In Fiji, a circular ROI with a diameter of 10 μm placed in the center of the cell was used to measure medial-apical intensity. For fixed phalloidin staining of F-actin, the raw intensity values were used. For live imaging of Myosin II with SF9-mNeon, the intensity was normalized by dividing by the membrane probe intensity.

ATP contraction index: Kymographs were generated in Fiji, and shift of the pigment in the kymograph was measured three times as length by tracing a line across the image: near the top, center, and bottom of the kymograph. These values were averaged, and movement of the whole embryo in the field of view was subtracted from the contraction by tracing the bottom edge of the embryo in the kymograph to obtain the contraction index.

F-actin intensity after ATP: In Fiji, a circular ROI with a diameter of 10 μm placed in the center of the cell was used to measure medial-apical intensity over time. Change in F-actin intensity was measured by subtracting baseline intensity from peak intensity. Baseline was the average of the 10 time points before ATP, and peak was the average of the 10 time points starting at 45 s after ATP. For near junction vs.

center of cell F-actin intensity comparisons, a smaller ROI with a diameter of 3 µm was used to measure F-actin intensity in the center of the cell or near the cell periphery.

Blinded catagorization of medial-apical F-actin organization: Confocal images of the F-actin channel (Lifeact-RFP) when full length Anillin or Anillin mutants were overexpressed were exported as JPEGs using ImageJ. File names were then randomly generated using the Random Names program created by Jason Faulkner from How-To-Geek https://goo.gl/1EcGCa. Cells that were ~80% or more visible in the field of view were then categorized as: 1) no F-actin fibers, 2) short F-actin fibers that do not span the apical surface, or 3) long F-actin fibers that do span the surface. Each cell could only be palced into one category, so if for example a cell contained both short and long fibers it would go into the long fiber category. Categorization was done by three different blinded individuals, and their categorizations were averaged to produce the final graph.

Anillin medial-apical intensity: A circular ROI with a diameter of 10 µm was placed in the center of the cell, and average intensity was collected for full length Anillin or Anillin mutant constructs tagged with 3xGFP. These values were not normalized but the same excitation laser intensity was used for acquisition across experiments.

FRAP: FRAP data was collected and analyzed as described in (Higashi et al. 2016) with the following modifications: only a single plane was captured instead of Z-stacks. Medial-apical actin-mNeon was bleached instead of junction proteins. Curves were fit with a double association curve in Prism6.

Statistical analysis

Unpaired t-tests were performed using GraphPad Prism version 6.01 for Windows, GraphPad Software, La Jolla California USA, www.graphpad.com. Double exponential curves with the following contraints,

Y=0 and plateau must be <1, were fit to FRAP data in GraphPad Prism version 6.01 for Windows. 2-way ANOVA was performed using IBM SPSS Statistics for Windows, Armonk, NY: IBM Corp.

Supplemental figures

Figure S3.1: Anillin increases junctional Vinculin recruitment but reduces recoil of junction vertices after laser ablation

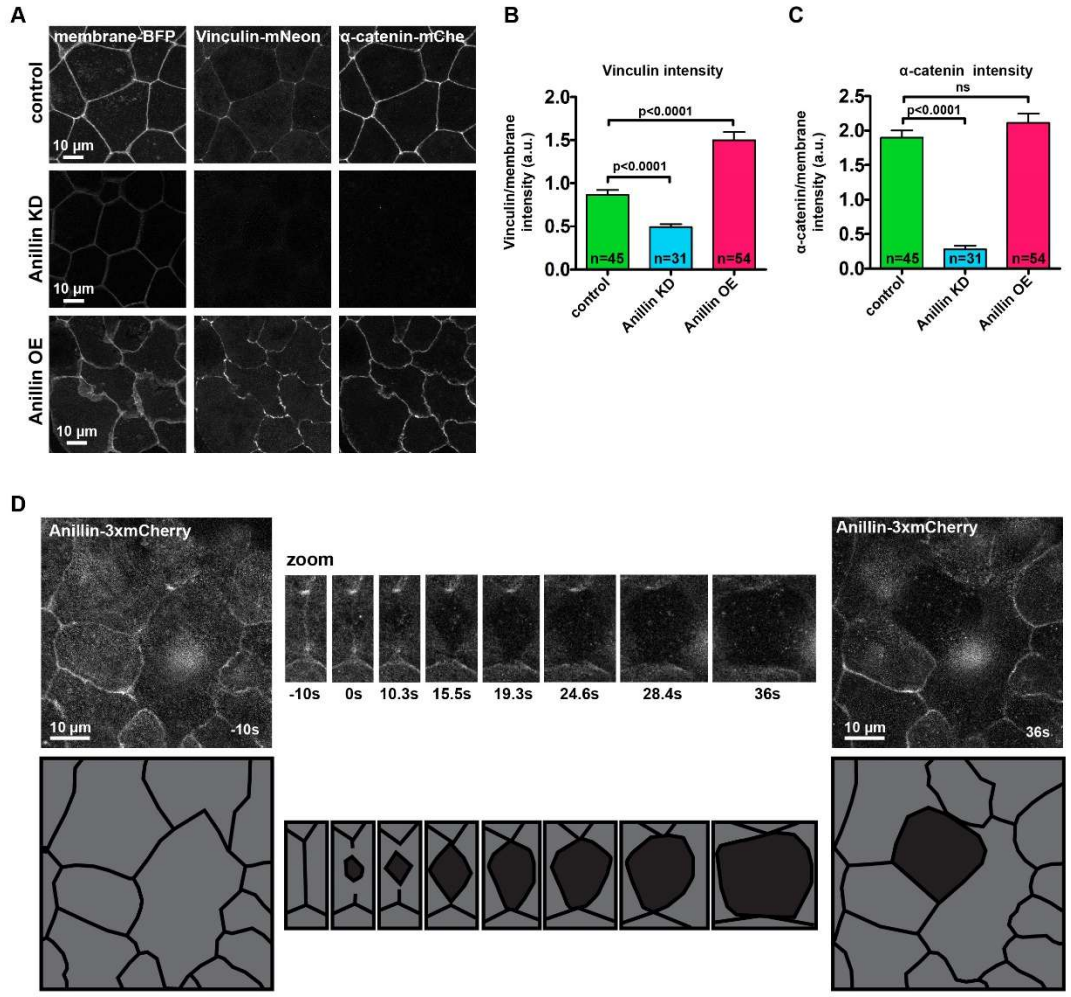

A) Confocal images of live epithelial cells in gastrula-stage *Xenopus laevis* embryos expressing a probe for the plasma membrane (2x membrane localization signal of Src family tyrosine kinase Lyn tagged with TagBFP at its C-terminus), α-catenin-mCherry, and Vinculin-mNeon as a tension sensor when Anillin is knocked down (KD) or overexpressed (OE). **B)** Quantification of Vinculin intensity as a ratio to membrane intensity. Measurements were taken by tracing a bicelllular junction from vertex to vertex. Error bars, S.E.M. Statistics, unpaired t-test, n=number of junctions. **C)** Quantification of α-catenin intensity as a ratio to membrane intensity. Measurements were taken by tracing a bicelllular junction from vertex to vertex. Error bars, S.E.M. Statistics, unpaired t-test, n=number of junctions. **D)** Unannotated version of Fig. 3.1 F: cell view of embryo overexpressing Anillin tagged with 3xmCherry. Cartoon traces of ablation data depicting the events during ablation.

Figure S3.2: In apically constricting cells, F-actin and Anillin emanate from junctions and spread medial-apically

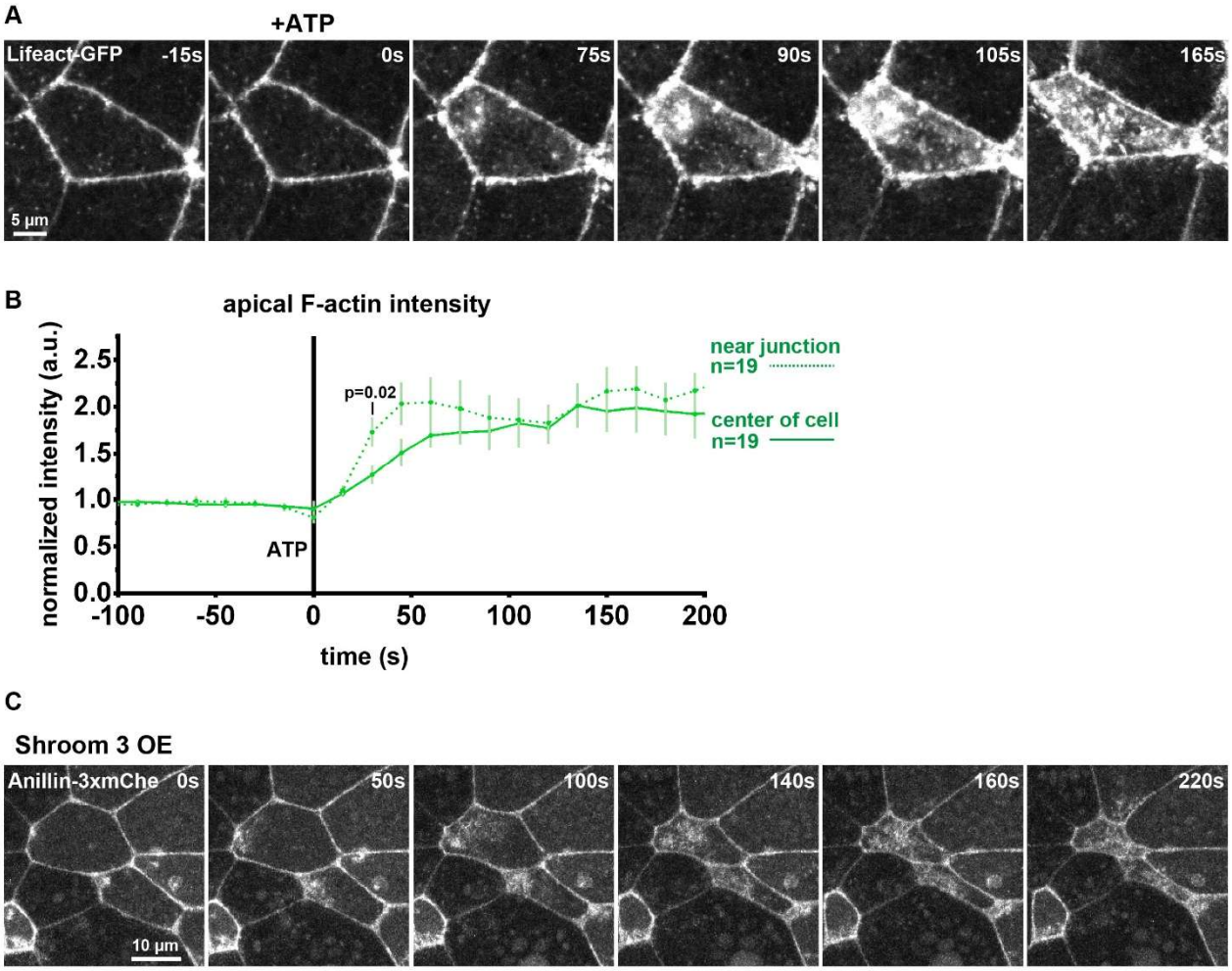

Figure S3.2: In apically constricting cells, F-actin and Anillin emanate from junctions and spread medial-apically
A) Confocal images of live epithelial cells from gastrula-stage *Xenopus laevis* embryos expressing a probe for F-actin (LifeAct-GFP). Exogenous ATP is added at time 0 to induce contraction. Notice how F-actin accumulates first near the junctions and then spreads medial apically. **B)** Apical F-actin intensity measured using an ROI with a 5 µm diameter near the junction or in the center of the cell. Error bars, S.E.M. Statistics, unpaired t-test, n=number of cells. **C)** Confocal images of live epithelial cells expressing Anillin-3xmChe at low levels and overexpressing Shroom 3 to induce apical constriction. Notice how Anillin accumulates first near the junctions and then spreads across the center of constricting cells.

Figure S3.3: Stabilizing F-actin rescues junction recoil after laser ablation

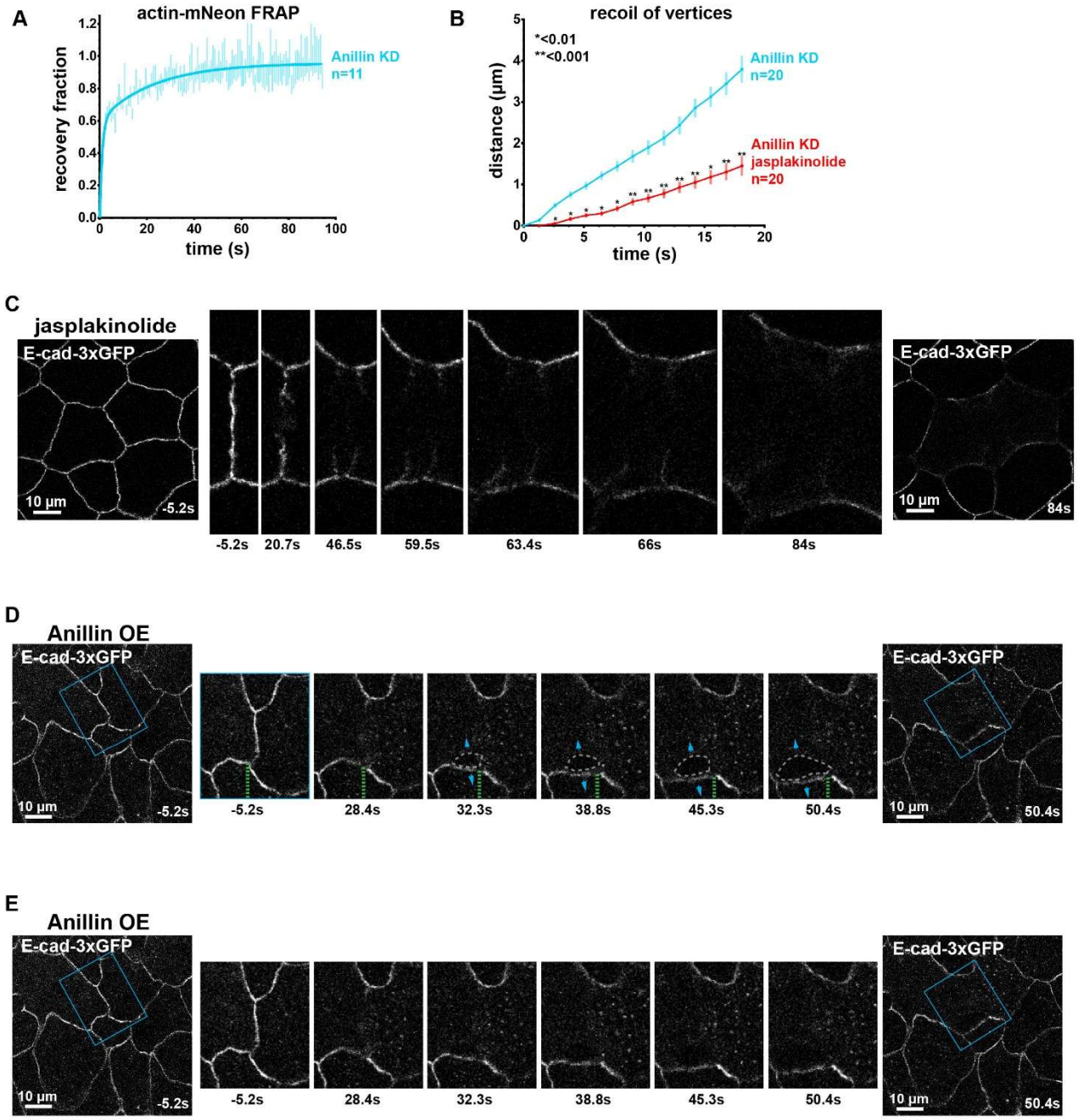

Figure S3.3: Stabilizing F-actin rescues Anillin KD junction recoil defect after laser ablation.
A) Medial-apical FRAP data for actin-mNeon highly expressed in Anillin KD gastrula-stage *Xenopus laevis* embryos. Data fitted with a two phase association curve. n=number of cells. **B)** Quantification of vertex separation over time after ablation. Error bars, S.E.M. Statistics, unpaired t-test, n=number of junctions. **C)** Unannotated version of laser ablation results in Fig. 3.6 G. Cell view of gastrula-stage *Xenopus laevis* embryos expressing E-cad-3xGFP and treated with 20 µm jasplakinolide. **D)** Confocal images of an embryo expressing E-cad-3xGFP and overexpressing Anillin-3xmCherry (not shown) before and after laser ablation. Blue boxes show the zoomed area for the ablation montage. Green dashed line indicates the position of the vertices relative to the edge of the image, the grey dashed line indicates the space forming between the two cells, and blue arrows represent forces between junctions adjacent to the measured vertex. Notice how the lower vertex only begins to separate, detected by a reduction in the length of the green dashed line, after the forces perpendicular (blue arrows) to the adjacent junction cause loss of adhesion between the two cells. **E)** Unannotated version of laser ablation results in D.

Figure S3.4: Anillin maintains apical F-actin in dorsal epithelium

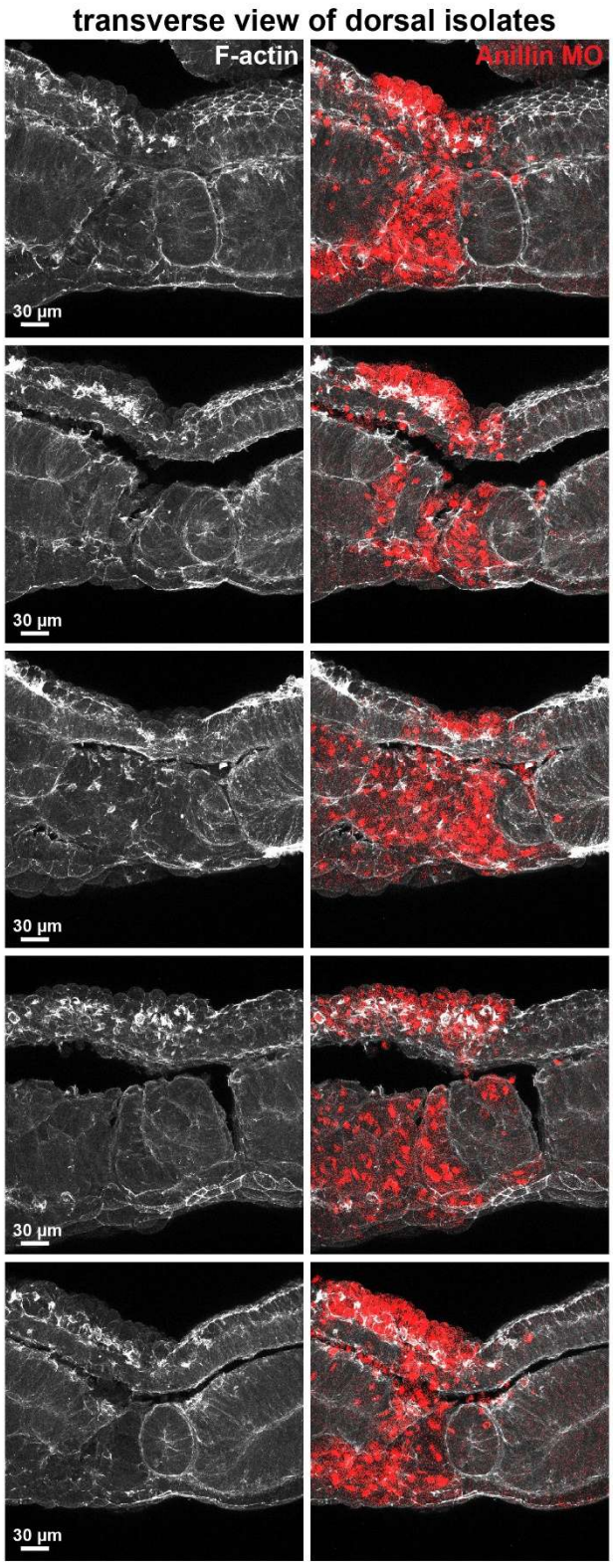

Figure S3.4: Anillin maintains apical F-actin in dorsal epithelium
Transverse sections of dorsal isolates explanted from *Xenopus laevis* embryos injected with Anillin morpholino. Anillin morpholino was co-injected with Alexa Fluor 647-conjugated Dextran as a lineage tracer. Anillin knockdown dorsal epithelial cells (red) exhibit a rounded apical morphology, loss of F-actin on their apical surface, enhanced basal F-actin, and disrupted mesodermal organization. Control epithelial cells have a flat apical morphology, robust apical F-actin, and weak basal F-actin.

Contributions and acknowledgements

Conceptualization, T.R.A. and A.L.M.; Methodology, T.R.A., T.H., L.A.D., and A.L.M.; Investigation, T.R.A., J.H.S., R.E.S.; Plasmid cloning, T.R.A., K.M.D., F.H.; Writing original draft T.R.A.; Writing reviewing and editing, T.R.A., R.E.S., T.H., J.H.S., L.A.D., A.L.M. Funding acquisition, A.L.M.; Additional funding resources, T.R.A., J.H.S., R.E.S., K.M.D., T.H., L.A.D.; Supervision, A.L.M.

We thank E.M. Munro for SF9 Myosin II intrabody construct and S. Sokol for the Shroom 3 construct. Members of the A.L.M. and L.A. Davidson lab and for reviewing the manuscript and providing useful discussion and critical feedback. A.C. Martin for useful discussion and critical feedback on experiments. Saranyaraajan Varadarajan, Shahana Chumki, and Lauren Smith for blinded characterization of data. Biomedical Research Core Facilities at U.M. for technical support and access to the Leica Inverted SP5 Confocal Microscope System with 2-Photon. This work was supported by National Institutes of Health (NIH) (R01 GM112794) to A.L.M (R01 HD04475 and R56 HL134195) to L.A.D., NSF Graduate Research Fellowships to T.R.A. and R.E.S., Rackham Merit Fellowship to T.R.A., NIH Biomechanics in Regenerative Medicine Training Grant to J.H.S., a Beckman Scholars Fellowship to K.M.D., and a Japanese Society for the Promotion of Science Postdoctoral Fellowship to T.H.

References

Amini, R, E Goupil, S Labella, M Zetka, AS Maddox, JC Labbé, and NT Chartier. 2015. “C. Elegans Anillin Proteins Regulate Intercellular Bridge Stability and Germline Syncytial Organization”. *J Cell Biol* 209: 467.

Barriga, EH, K Franze, G Charras, and R Mayor. 2018. “Tissue Stiffening Coordinates Morphogenesis by Triggering Collective Cell Migration in Vivo”. *Nature* 554: 523–27.

Bement, WM, M Leda, AM Moe, AM Kita, ME Larson, AE Golding, C Pfeuti, et al. 2015. “Activator-Inhibitor Coupling between Rho Signalling and Actin Assembly Makes the Cell Cortex an Excitable Medium”. *Nat Cell Biol* 17: 1471–83.

Bertocchi, C, Y Wang, A Ravasio, Y Hara, Y Wu, T Sailov, MA Baird, et al. 2017. “Nanoscale Architecture of Cadherin-Based Cell Adhesions”. *Nat Cell Biol* 19: 28–37.

Budnar, Srikanth, Kabir B. Husain, Guillermo A. Gomez, Maedeh Naghibosidat, Suzie Verma, Nicholas A. Hamilton, Richard G. Morris, and Alpha S. Yap. 2018. “Scaffolding of RhoA Contractile Signaling by Anillin: a Regulatory Analogue of Kinetic Proofreading”, March. Cold Spring Harbor Laboratory. doi:10.1101/282756.

Butcher, DT, T Alliston, and VM Weaver. 2009. “A Tense Situation: Forcing Tumour Progression”. *Nat Rev Cancer* 9: 108–22.

Chanet, S, CJ Miller, ED Vaishnav, B Ermentrout, LA Davidson, and AC Martin. 2017. “Actomyosin Meshwork Mechanosensing Enables Tissue Shape to Orient Cell Force”. *Nat Commun* 8: 15014.

Choi, W, BR Acharya, G Peyret, MA Fardin, RM Mège, B Ladoux, AS Yap, AS Fanning, and M Peifer. 2016. “Remodeling the Zonula Adherens in Response to Tension and the Role of Afadin in This Response”. *J Cell Biol* 213: 243–60.

D’Avino, P. Paolo. 2009. “How to Scaffold the Contractile Ring for a Safe Cytokinesis - Lessons from Anillin-Related Proteins”. *Journal of Cell Science* 122 (8). The Company of Biologists: 1071–79. doi:10.1242/jcs.034785.

Davidson, LA, and R Keller. 2007. “Measuring Mechanical Properties of Embryos and Embryonic Tissues”. *Methods Cell Biol* 83: 425–39.

Davidson, LA. 2012. “Epithelial Machines That Shape the Embryo”. *Trends in Cell Biology* 22 (2). Elsevier BV: 82–87. doi:10.1016/j.tcb.2011.10.005.

Dawes-Hoang, RE, KM Parmar, AE Christiansen, CB Phelps, AH Brand, and EF Wieschaus. 2005. “Folded Gastrulation, Cell Shape Change and the Control of Myosin Localization”. *Development* 132: 4165–78.

Descovich, CP, DB Cortes, S Ryan, J Nash, L Zhang, PS Maddox, F Nedelec, and AS Maddox. 2017. “Crosslinkers Both Drive and Brake Cytoskeletal Remodeling and Furrowing in Cytokinesis”. *Mol Biol Cell*.

Fang, M, J YC Peng, and Y Li. 2014. “Collagen as a Double-Edged Sword in Tumor Progression”. *Tumour Biol* 35: 2871–82.

Farhadifar, R, JC Röper, B Aigouy, S Eaton, and F Jülicher. 2007. “The Influence of Cell Mechanics Cell-Cell Interactions, and Proliferation on Epithelial Packing”. *Current Biology* 17 (24). Elsevier BV: 2095–2104. doi:10.1016/j.cub.2007.11.049.

Fernandez-Gonzalez, R, SSM Simoes, JC Röper, S Eaton, and JA Zallen. 2009. “Myosin II Dynamics Are Regulated by Tension in Intercalating Cells”. *Developmental Cell* 17 (5). Elsevier BV: 736–43. doi:10.1016/j.devcel.2009.09.003.

Field, CM, and BM Alberts. 1995. “Anillin, a Contractile Ring Protein That Cycles from the Nucleus to the Cell Cortex”. *J Cell Biol* 131: 165–78.

Frenette, P, E Haines, M Loloyan, M Kinal, P Pakarian, and A Piekny. 2012. “An Anillin-Ect2 Complex Stabilizes Central Spindle Microtubules at the Cortex during Cytokinesis”. *PLoS One* 7: e34888.

Gbadegesin, RA, G Hall, A Adeyemo, N Hanke, I Tossidou, J Burchette, G Wu, et al. 2014. “Mutations in the Gene That Encodes the F-Actin Binding Protein Anillin Cause FSGS”. *J Am Soc Nephrol* 25: 1991–2002.

Guo, X, K Bonin, K Scarpinato, and M Guthold. 2014. “The Effect of Neighboring Cells on the Stiffness of Cancerous and Non-Cancerous Human Mammary Epithelial Cells”. *New Journal of Physics* 16 (10). IOP Publishing: 105002. doi:10.1088/1367-2630/16/10/105002.

Guo, Z, LJ Neilson, H Zhong, PS Murray, S Zanivan, and R Zaidel-Bar. 2014. “E-Cadherin Interactome Complexity and Robustness Resolved by Quantitative Proteomics”. *Sci Signal* 7: rs7.

Haigo, SL, JD Hildebrand, RM Harland, and JB Wallingford. 2003. “Shroom Induces Apical Constriction and Is Required for Hingepoint Formation during Neural Tube Closure”. *Curr Biol* 13: 2125–37.

Hall, PA, CB Todd, PL Hyland, SS McDade, H Grabsch, M Dattani, KJ Hillan, and SE Russell. 2005. “The Septin-Binding Protein Anillin Is Overexpressed in Diverse Human Tumors”. *Clin Cancer Res* 11: 6780–86.

Hashimoto, H, FB Robin, KM Sherrard, and EM Munro. 2015. “Sequential Contraction and Exchange of Apical Junctions Drives Zippering and Neural Tube Closure in a Simple Chordate”. *Dev Cell* 32: 241–55.

Higashi, T, and AL Miller. 2017. “Tricellular Junctions: How to Build Junctions at the TRICkiest Points of Epithelial Cells”. *Mol Biol Cell* 28: 2023–34.

Higashi, T, TR Arnold, RE Stephenson, KM Dinshaw, and AL Miller. 2016. “Maintenance of the Epithelial Barrier and Remodeling of Cell-Cell Junctions during Cytokinesis”. *Curr Biol* 26: 1829–42.

Holzinger, A. 2001. “Jasplakinolide. An Actin-Specific Reagent That Promotes Actin Polymerization”. *Methods Mol Biol* 161: 109–20.

Idichi, T, N Seki, H Kurahara, K Yonemori, Y Osako, T Arai, A Okato, et al. 2017. “Regulation of Actin-Binding Protein ANLN by Antitumor MiR-217 Inhibits Cancer Cell Aggressiveness in Pancreatic Ductal Adenocarcinoma”. *Oncotarget* 8: 53180–93.

Itoh, K, O Ossipova, and SY Sokol. 2014. “GEF-H1 Functions in Apical Constriction and Cell Intercalations and Is Essential for Vertebrate Neural Tube Closure”. *J Cell Sci* 127: 2542–53.

Jackson, TR., HY Kim, UL Balakrishnan, C Stuckenholz, and LA Davidson. 2017. “Spatiotemporally Controlled Mechanical Cues Drive Progenitor Mesenchymal-to-Epithelial Transition Enabling Proper Heart Formation and Function”. *Current Biology* 27 (9). Elsevier BV: 1326–35. doi:10.1016/j.cub.2017.03.065.

Joshi, SD, Dassow M von, and LA Davidson. 2010. “Experimental Control of Excitable Embryonic Tissues: Three Stimuli Induce Rapid Epithelial Contraction”. *Exp Cell Res* 316: 103–14.

Kim, Y, M Hazar, DS Vijayraghavan, J Song, TR Jackson, SD Joshi, WC Messner, LA Davidson, and PR LeDuc. 2014. “Mechanochemical Actuators of Embryonic Epithelial Contractility”. *Proc Natl Acad Sci USA* 111: 14366–71.

Kumar, S, and VM Weaver. 2009. “Mechanics, Malignancy, and Metastasis: the Force Journey of a Tumor Cell”. *Cancer Metastasis Rev* 28: 113–27.

Leerberg, JM, GA Gomez, S Verma, EJ Moussa, SK Wu, R Priya, BD Hoffman, C Grashoff, MA Schwartz, and AS Yap. 2014. “Tension-Sensitive Actin Assembly Supports Contractility at the Epithelial Zonula Adherens”. *Curr Biol* 24: 1689–99.

Liang, PI, WT Chen, CF Li, CC Li, WM Li, CN Huang, HC Yeh, HL Ke, WJ Wu, and CY Chai. 2015. “Subcellular Localisation of Anillin Is Associated with Different Survival Outcomes in Upper Urinary Tract Urothelial Carcinoma”. *J Clin Pathol* 68: 1026–32.

Liu, J, GD Fairn, DF Ceccarelli, F Sicheri, and A Wilde. 2012. “Cleavage Furrow Organization Requires PIP(2)-Mediated Recruitment of Anillin”. *Curr Biol* 22: 64–69.

Ma, X, HE Lynch, PC Scully, and MS Hutson. 2009. “Probing Embryonic Tissue Mechanics with Laser Hole Drilling”. *Phys Biol* 6: 036004.

Magnusson, K, G Gremel, L Rydén, V Pontén, M Uhlén, A Dimberg, K Jirström, and F Pontén. 2016. “ANLN Is a Prognostic Biomarker Independent of Ki-67 and Essential for Cell Cycle Progression in Primary Breast Cancer”. *BMC Cancer* 16: 904.

Manukyan, A, K Ludwig, S Sanchez-Manchinelly, SJ Parsons, and PT Stukenberg. 2015. “A Complex of p190RhoGAP-A and Anillin Modulates RhoA-GTP and the Cytokinetic Furrow in Human Cells”. *J Cell Sci* 128: 50–60.

Martin, AC, and B Goldstein. 2014. “Apical Constriction: Themes and Variations on a Cellular Mechanism Driving Morphogenesis”. *Development* 141: 1987–98.

Martin, AC, M Kaschube, and EF Wieschaus. 2009. “Pulsed Contractions of an Actin-Myosin Network Drive Apical Constriction”. *Nature* 457: 495–99.

Mason, FM, M Tworoger, and AC Martin. 2013. “Apical Domain Polarization Localizes Actin-Myosin Activity to Drive Ratchet-like Apical Constriction”. *Nat Cell Biol* 15: 926–36.

Nizak, C, S Martin-Lluesma, S Moutel, A Roux, TE Kreis, B Goud, and F Perez. 2003. “Recombinant Antibodies against Subcellular Fractions Used to Track Endogenous Golgi Protein Dynamics in Vivo”. *Traffic* 4: 739–53.

Nowotarski, SH, and M Peifer. 2014. “Cell Biology: a Tense but Good Day for Actin at Cell-Cell Junctions”. *Curr Biol* 24: R688–90.

Oegema, K, MS Savoian, TJ Mitchison, and CM Field. 2000. “Functional Analysis of a Human Homologue of the Drosophila Actin Binding Protein Anillin Suggests a Role in Cytokinesis”. *J Cell Biol* 150: 539–52.

Piekny, AJ, and AS Maddox. 2010. “The Myriad Roles of Anillin during Cytokinesis”. *Semin Cell Dev Biol* 21: 881–91.

Piekny, AJ, and M Glotzer. 2008. “Anillin Is a Scaffold Protein That Links RhoA, Actin, and Myosin during Cytokinesis”. *Curr Biol* 18: 30–36.

Plageman, T. F., B. K. Chauhan, C. Yang, F. Jaudon, X. Shang, Y. Zheng, M. Lou, A. Debant, J. D. Hildebrand, and R. A. Lang. 2011. “A Trio-RhoA-Shroom3 Pathway Is Required for Apical Constriction and Epithelial Invagination”. *Development* 138 (23). The Company of Biologists: 5177–88. doi:10.1242/dev.067868.

Priya, R, X Liang, JL Teo, K Duszyc, AS Yap, and GA Gomez. 2016. “ROCK1 but Not ROCK2 Contributes to RhoA Signaling and NMIIA-Mediated Contractility at the Epithelial Zonula Adherens”. Edited by Jeffrey D. Hardin. *Molecular Biology of the Cell* 28 (1). American Society for Cell Biology (ASCB): 12–20. doi:10.1091/mbc.e16-04-0262.

Ratheesh, A, GA Gomez, R Priya, S Verma, EM Kovacs, K Jiang, NH Brown, A Akhmanova, SJ Stehbens, and AS Yap. 2012. “Centralspindlin and α-Catenin Regulate Rho Signalling at the Epithelial Zonula Adherens”. *Nat Cell Biol* 14: 818–28.

Rauzi, M, and PF Lenne. 2015. “Probing Cell Mechanics with Subcellular Laser Dissection of Actomyosin Networks in the Early Developing Drosophila Embryo”. *Methods Mol Biol* 1189: 209–18.

Reyes, CC, M Jin, EB Breznau, R Espino, R Delgado-Gonzalo, AB Goryachev, and AL Miller. 2014. “Anillin Regulates Cell-Cell Junction Integrity by Organizing Junctional Accumulation of Rho-GTP and Actomyosin”. *Curr Biol* 24: 1263–70.

Ronkainen, H, P Hirvikoski, S Kauppila, and MH Vaarala. 2011. “Anillin Expression Is a Marker of Favourable Prognosis in Patients with Renal Cell Carcinoma”. *Oncol Rep* 25: 129–33.

Schindelin, J, I Arganda-Carreras, E Frise, V Kaynig, M Longair, T Pietzsch, S Preibisch, C Rueden, S Saalfeld, B Schmid, DJ White, V Hartenstein, K Eliceiri, P Tomancak, A Cardona. 2012. “Fiji: an Open-Source Platform for Biological-Image Analysis”. *Nature Methods* 9 (7). Springer Nature: 676–82. doi:10.1038/nmeth.2019.

Silverman-Gavrila, RV, KG Hales, and A Wilde. 2008. “Anillin-Mediated Targeting of Peanut to Pseudocleavage Furrows Is Regulated by the GTPase Ran”. *Mol Biol Cell* 19: 3735–44.

Sisson, JC, C Field, R Ventura, A Royou, and W Sullivan. 2000. “Lava Lamp, a Novel Peripheral Golgi Protein, Is Required for Drosophila Melanogaster Cellularization”. *J Cell Biol* 151: 905–18.

Straight, AF, CM Field, and TJ Mitchison. 2005. “Anillin Binds Nonmuscle Myosin II and Regulates the Contractile Ring”. *Mol Biol Cell* 16: 193–201.

Sun, L, R Guan, IJ Lee, Y Liu, M Chen, J Wang, JQ Wu, and Z Chen. 2015. “Mechanistic Insights into the Anchorage of the Contractile Ring by Anillin and Mid1”. *Dev Cell* 33: 413–26.

Suzuki, C, Y Daigo, N Ishikawa, T Kato, S Hayama, T Ito, E Tsuchiya, and Y Nakamura. 2005. “ANLN Plays a Critical Role in Human Lung Carcinogenesis through the Activation of RHOA and by Involvement in the Phosphoinositide 3-Kinase/AKT Pathway”. *Cancer Res* 65: 11314–25.

Swaminathan, V, K Mythreye, ET O’Brien, A Berchuck, GC Blobe, and R Superfine. 2011. “Mechanical Stiffness Grades Metastatic Potential in Patient Tumor Cells and in Cancer Cell Lines”. *Cancer Res* 71: 5075–80.

Tian, D, M Diao, Y Jiang, L Sun, Y Zhang, Z Chen, S Huang, and G Ou. 2015. “Anillin Regulates Neuronal Migration and Neurite Growth by Linking RhoG to the Actin Cytoskeleton”. *Curr Biol* 25: 1135–45.

Tokuda, S, T Higashi, and M Furuse. 2014. “ZO-1 Knockout by TALEN-Mediated Gene Targeting in MDCK Cells: Involvement of ZO-1 in the Regulation of Cytoskeleton and Cell Shape”. *PLoS One* 9: e104994.

Toret, CP, MV D’Ambrosio, RD Vale, MA Simon, and WJ Nelson. 2014. “A Genome-Wide Screen Identifies Conserved Protein Hubs Required for Cadherin-Mediated Cell-Cell Adhesion”. *J Cell Biol* 204: 265–79.

Van Itallie, CM, AJ Tietgens, E Krystofiak, B Kachar, and JM Anderson. 2015. “A Complex of ZO-1 and the BAR-Domain Protein TOCA-1 Regulates Actin Assembly at the Tight Junction”. *Mol Biol Cell* 26: 2769–87.

Vielemeyer, O, C Nizak, AJ Jimenez, A Echard, B Goud, J Camonis, JC Rain, and F Perez. 2010. “Characterization of Single Chain Antibody Targets through Yeast Two Hybrid”. *BMC Biotechnol* 10: 59.

Wang, D, GK Chadha, A Feygin, and AI Ivanov. 2015. “F-Actin Binding Protein, Anillin, Regulates Integrity of Intercellular Junctions in Human Epithelial Cells”. *Cell Mol Life Sci* 72: 3185–3200.

Wang, G, W Shen, L Cui, W Chen, X Hu, and J Fu. 2016. “Overexpression of Anillin (ANLN) Is Correlated with Colorectal Cancer Progression and Poor Prognosis”. *Cancer Biomark* 16: 459–65.

Watanabe, S, K Okawa, T Miki, S Sakamoto, T Morinaga, K Segawa, T Arakawa, M Kinoshita, T Ishizaki, and S Narumiya. 2010. “Rho and Anillin-Dependent Control of mDia2 Localization and Function in Cytokinesis”. *Mol Biol Cell* 21: 3193–3204.

Weng, M, and E Wieschaus. 2016. “Myosin-Dependent Remodeling of Adherens Junctions Protects Junctions from Snail-Dependent Disassembly”. *J Cell Biol* 212: 219–29.

Yonemura, S, Y Wada, T Watanabe, A Nagafuchi, and M Shibata. 2010. “Alpha-Catenin as a Tension Transducer That Induces Adherens Junction Development”. *Nat Cell Biol* 12: 533–42.

Zhang, S, LH Nguyen, K Zhou, HC Tu, A Sehgal, I Nassour, L Li, et al. 2017. “Knockdown of Anillin Actin Binding Protein Blocks Cytokinesis in Hepatocytes and Reduces Liver Tumor Development in Mice without Affecting Regeneration”. *Gastroenterology*.

Zhou, J, HY Kim, and LA Davidson. 2009. “Actomyosin Stiffens the Vertebrate Embryo during Crucial Stages of Elongation and Neural Tube Closure”. *Development* 136: 677–88.

Chapter 4

Discussion

In this dissertation, I have demonstrated that during cytokinesis, epithelial cells remain connected to one another, maintain the barrier function of the tissue, and reinforce their adherens junctions in response to tension generated by the contractile ring. I have also shown that Anillin regulates cell mechanics by organizing the medial-apical contractile network. Together, these data support the notion that epithelia act as mechanical sensors and that an individual protein can have dramatic mechanical impacts at the cellular level that propagate to the tissue level. While the work presented here has answered several questions about how epithelial cells regulate and respond to mechanical inputs in order to build and maintain a functional tissue, there are many unanswered questions that stem from this work. In the following sections, I explore these questions, put them in the context of the field, and propose experiments to address them

Epithelial cytokinesis

Why don't tight junctions feel the force from cytokinesis?

Are the forces from cytokinesis transmitted to tight junctions? If so, how do those forces impact barrier function? These are especially pressing questions in epithelial tissues that undergo rapid cell division, such as the intestinal epithelium. Previous work has shown that tight junction dynamics are globally stabilized in a tension-sensitive manner (Higashi et al. 2016; Yu et al. 2010). Here, I showed that tight junction components are not locally stabilized by forces from the contractile ring **(Fig. 2.3, 2.4)**. This indicates that adherens junctions are the major load-bearing junction during cell division, while tight junctions appear to simply be along for the ride. However, tight junctions are connected to junctional F-actin, are mechanically sensitive, and regulate epithelial mechanics (Fanning, Van, and Anderson 2012; Choi et al. 2016; Hatte, Prigent, and Tassan 2018; Spadaro et al. 2017). Why, then, are tight junctions uncoupled from the forces driving cytokinesis? One possibility is that forces from cytokinesis directly coupled to tight junctions could disrupt barrier function. If this is true, one might expect to see uncoupling of tight junctions during other events that increase apical tension, such as apical constriction and convergent extension.

Experimental manipulation of Myosin II-driven contractility has revealed it to be an important regulator of barrier function (Arnold, Stephenson, and Miller 2017). However, in some cases inhibiting Myosin II activity increases the permeability of tight junctions (Ivanov et al. 2007; Ivanov et al. 2004), while in other cases loss of Myosin II activity decreases permeability (Yu et al. 2010). Similar contradicting evidence can be found for increased apical tension, where activation of Myosin II has no effect on barrier function in human epithelial

colorectal adenocarcinoma cells (Acharya et al. 2018), but in endothelial cells, Myosin II activation strengthens barrier function (Dudek et al. 2004). It is clear that Myosin II activity is a regulator of barrier function; however, it is unclear how elevated levels of acute tension affect barrier function.

To test how actomyosin forces affect barrier function, manipulations such as treatment with the phosphatase inhibitor Calyculin A to increase active Myosin II or mosaic Anillin overexpression to increase tension, or drugs such as the ROCK inhibitor Y-27632, or Myosin II inhibitor blebbistatin to decrease tension, could be used in conjunction with a barrier assay more sensitive than the tracer dye experiment in **(Fig. 2.1).** A former postdoc in the lab developed a Zinc-based Ultrasensitive Microscopic Barrier Assay (ZnUMBA) that would perfectly serve this role (Tomohito Higashi, unpublished). After determining how actomyosin forces affect barrier breaches on the cellular scale using ZnUMBA, it would be informative to look more closely at the epithelial barrier during cell division**.** It is possible that there are small barrier breaches around the dividing cells that are undetected via the tracer dye method used in Chapter 2 **(Fig. 2.1)**. Indeed, flares of RhoA activity, which are sites of barrier leaks, are increased around dividing cells (Rachel Stephenson, Torey Arnold, & Farah Huq, unpublished). Specifically, there may be an increased number of breaches at the cleavage furrow where the forces are acutely increased, and where the shapes of the junction and the membrane are drastically changing. Additionally, using chimeric proteins, such as a ZO-1/α-catenin or ZO-1/Anillin fusion protein, to artificially connect tight junctions to adherens junctions or connect tight junctions to the contractile ring would allow us to test how directly connecting tight junctions to the forces from the contractile ring affects barrier function. To summarize, there is

little consensus on how global tensile forces affect tight junction barrier function, and even less known about how large, acute tensile forces such as those generated during cytokinesis affect barrier function, making this an interesting question to pursue

Why are adherens junctions reinforced during cytokinesis?

Adherens junctions maintain epithelial integrity by mechanically linking cells together, which is required for tight junction formation and barrier establishment (Hartsock and Nelson 2008). Through my research, I showed that adherens junctions are reinforced via Vinculin recruitment during cytokinesis **(Fig. 2.5)**. Vinculin reinforcement at the cleavage furrow was simultaneously expected and surprising. It was expected because adherens junction are well known to be mechanically sensitive and recruit Vinculin to their junctions under mechanical stress (Yonemura et al. 2010; Yao et al. 2014; Kim et al. 2015). However, it was surprising because recent studies investigating cytokinesis in *Drosophila* showed a weakening or break in adherens junctions at the cleavage furrow (Herszterg et al. 2013; Guillot and Lecuit 2013; Founounou, Loyer, and Le 2013).

Why do vertebrates reinforce their junctions at the cleavage furrow while invertebrates allow theirs to be disrupted? One possibility is the requirement for and maintenance of barrier function in the embryos. The studies in *Drosophila* were carried out in stage 8-10 embryos which do not form an epithelial barrier (Tepass and Hartenstein 1994). In contrast, the experiments we conducted were in stage 10.5 *Xenopus* embryos, which form a complete tight junction seal. *Xenopus* may require a strong barrier at stage 10.5 in order to develop properly; however, this has not been directly tested. In *Drosophila* stage 8-10 embryos, there is no requirement to maintain adhesion to preserve barrier function, so adherens junctions can

decouple in *Drosophila* without much consequence. In support of this hypothesis, recent work in *Drosophila* examining cytokinesis in epithelia that do develop barriers showed that both the adherens junctions and the barrier forming septate junction remain intact at the cleavage furrow (Wang, Bosveld, and Bellaiche 2018; Daniel et al. 2018).

The work I presented in Chapter 2 shows that forces from cytokinesis recruit Vinculin to adherens junctions, and this in turn stabilizes junction components and reinforces the connection between the actin cytoskeleton and the junction. However, we have less evidence about why this is happening and if it is required for successful cytokinesis or maintaining the barrier functions during cell division. We had difficulty depleting Vinculin in *Xenopus*; however, I think Vinculin depletion will be a critical step towards understanding Vinculin's role in cytokinesis. Dominant negative Vinculin-D1 increased the speed of contractile ring closure; however, we saw no dramatic defects in cytokinesis using this perturbation **(Fig. 2.6)**. Additionally, dominant negative Vinculin decreased E-cadherin and ZO-1 intensity at the cleavage furrow, which may indicate increased barrier permeability that we could test with the ZnUMBA barrier assay. Complementing this work with studies in cultured epithelia, where we could more readily deplete Vinculin, could reveal more about the role of Vinculin reinforcement in cytokinesis. Alternatively, in *Xenopus* we could use try different morpholinos, or use a combination approach by expressing Vinculin-D1 along with Vinculin morpholinos. Another possibility would be knocking down α-catenin and replacing it with mutant α-catenin that cannot bind to Vinculin. Together, these experiments will be informative about the function of adherens junction reinforcement during cell division.

What is the role of Vinculin in dividing and neighboring cells?

In order to understand cell division in a tissue, it is equally important to consider the mechanics of both the dividing cell and the neighboring cells. Based on work presented in Chapter 2 performed by Tomohito Higashi, it is not clear whether Vinculin accumulates in both the dividing cell and its neighbors in unperturbed cells. Testing this by mosaically expressing Vinculins tagged with different fluorophores could address this question. For example, expressing red tagged Vinculin in neighboring cells and green tagged Vinculin in division cells and measuring their accumulation at the cleavage furrow. If Vinculin does accumulate in both cells, it would mean that pulling strain is applied to both the diving cell and the neighboring cell. I would expect Vinculin to accumulate in the dividing cell, as its adherens junctions are directly coupled to the contractile ring; however, the situation in the neighboring cell is less clear. Is the circumferential actomyosin network in the neighboring cell providing a *passive* resistance, and is this enough to trigger the strain across α-catenin or is there an *active* contractile response in the network?

I hypothesize that the neighboring cell reinforces the adherens junction to preserve barrier function and epithelial integrity. However, it is possible that reinforcement is simply a consequence of the mechanosensitivity of α-catenin. The resistive force of junctional interfaces in *Drosophila* has been measured to be on the 100 pN scale (Bambardekar et al. 2015), while forces generated from the contractile ring in the first embryonic division of different organisms have been measured to be in the 10 nN range (Rappaport 1967; Miyoshi et al. 2006). The amount of force required to induce the conformational change in α-catenin is only 5 pN (Yao et al. 2014), so it is likely that reinforcement occurs not only in the dividing cell, but also the

neighboring cell as a result of the *passive* resistive force of the junction interface instead of an *active* contractile force in the neighboring cell.

One consequence of Vinculin recruitment is the recruitment of the actin polymerizer Ena/VASP, which binds directly to Vinculin (Leerberg et al. 2014). This raises the possibility that increased actin polymerization at junctions at the cleavage furrow (possibly in both the dividing and neighboring cells) is required for successful cytokinesis, cell adhesion, and barrier function. It would be interesting to perturb this function of Vinculin and observe the effect it has on actin and the barrier at the cleavage furrow. Perhaps Vinculin recruitment is needed to polymerize more F-actin in the contractile ring in order to add more F-actin along the growing junctions during the large shape changes generated during cytokinesis? Understanding how and why Vinculin is being recruited to the cleavage furrow in both the dividing and neighboring cells will be important for understanding how epithelial cells successfully divide and remain adherent to one another.

Understanding the diversity of cytokinesis

Studies in *Xenopus* and *Drosophila* have revealed that cells use dramatically different solutions for cell division in epithelial tissues **(Fig. 2.7)** (Higashi et al. 2016; Herszterg et al. 2013; Guillot and Lecuit 2013; Founounou, Loyer, and Le 2013). In *Drosophila*, researchers have found that cell division in epithelial tissue is a multicellular process. In some *Drosophila* tissues explored, neighboring cells actively contributed to cytokinesis (Herszterg et al. 2013; Guillot and Lecuit 2013; Founounou, Loyer, and Le 2013). As the cleavage furrow ingresses, Myosin II accumulates in the neighboring cell perpendicular to the axis of division, bringing the furrowing interfaces close to one another. Then, the dividing cell uses branched F-actin to push the

neighboring cells' membrane out of the furrow, and adherens junctions are formed between the newly formed daughter cells (Herszterg, Pinheiro, and Bellaïche 2014). This discovery was a paradigm shift for how we think about cytokinesis; what was once thought to be a cell autonomous process actually requires cell cooperation.

Observing cell division in different epithelial tissues, at other stages of development, and in other organisms is likely to lead to other new discoveries. For example, are there instances where cell division is not driven by the dividing cell but by pushing forces from the neighboring cells? Are there tissues where cells divide without actomyosin? Additionally, it is important to understand how cell division changes based on the characteristics of the tissue. For example, how do factors like proliferation rate and cell shape affect cytokinesis? Comparing different tissues types - highly proliferative and less proliferative epithelia, or columnar, cuboidal, and squamous epithelia - could help address these questions.

How does epithelial stiffness affect cytokinesis?

It is well known that stiffness of the extracellular matrix increases proliferation and dedifferentiation of cells, and this has a major impact on the progression of cancers (Handorf et al. 2015). Much less is known about how the stiffness of cells within a tissue affects cell division. Even though tumors as a whole tend to be stiffer than surrounding tissues, the tumorigenic cells themselves tend to be less stiff than surrounding cells (Swaminathan et al. 2011; Guo et al. 2014). This opens interesting questions about where in tumors cells are proliferating: at sites of cell-matrix adhesion, cell-cell adhesion, or both? To test how surrounding cell stiffness affects cytokinesis, we could modulate Anillin expression, which in turn alters tissue stiffness. *Xenopus* is a great model system to study the effects of cancer cell stiffness on cell division because

Xenopus tadpoles are clear, making them amenable to live imaging, and they can be induced to generate tumors (Dahmane et al. 1997; Yang et al. 1998; Wallingford et al. 1997). Alternatively, mammalian tumors can be seeded and grown in tadpoles (Haynes-Gimore et al. 2015). Understanding how cell division is regulated by the mechanical environment imposed by surrounding cells will be useful both for our understanding of disease progression and embryonic development.

Anillin's role in epithelial mechanics

What is Anillin's role in cancer cells and tumor progression?

Tumors are mechanical sensors. As the extracellular matrix of a tumor stiffens, tumor cells become more invasive and metastatic (Reid and Zanivan 2017). In Chapter 3, I showed that Anillin organizes medial-apical actomyosin into a contractile unit and that Anillin overexpression results in structural and mechanical changes that are similar to treatment with the F-actin-stabilizing toxin jasplakinolide **(Fig. 3.1-6)**. Additionally, we found that Anillin depletion reduces tissue stiffness **(Fig. 3.7)**. This result may shed light on how Anillin affects cancer progression. Anillin is overexpressed in many human tumors (Hall et al. 2005), and high levels of Anillin expression in tumors correlates with poor survival rate (Hall et al. 2005; Suzuki et al. 2005; Wang et al. 2016; Idichi et al. 2017; Zhang et al. 2018). However, work examining the subcellular localization of Anillin found that *nuclear* localization of Anillin correlates with poor survival rates, whereas *cytoplasmic* localization of Anillin is a marker of favorable prognosis, suggesting that Anillin's localization is key (Ronkainen et al. 2011; Liang et al. 2015).

What is the mechanism behind this finding? Because cancer cells become less stiff as they become metastatic (Swaminathan et al. 2011; Guo et al. 2014), one possibility is that

Anillin-mediated cell stiffening prevents cells from becoming metastatic. Anillin also promotes normal cell-cell adhesion (Reyes et al. 2014; Wang et al. 2015) and apical actomyosin contractility, which has been shown to protect junctions from disassembly (Weng and Wieschaus 2016), again hinting that Anillin may function to mechanically maintain cells in a non-invasive state. In opposition to this idea, in migratory cells, such as neurons and podocytes, cytoplasmic Anillin *promotes* migration by organizing, protecting, and scaffolding F-actin at the leading edge (Tian et al. 2015; Gbadegesin et al. 2014). One possible reconciliation is that Anillin helps maintain an epithelial cell state by maintaining stiffness and adhesion, but in migratory cells Anillin is relocalized to the leading edge of motile cells to promote migration. It would be interesting to test this by overexpressing Anillin and HIF-1a, which induces metastasis (Yang et al. 2008), and observing if Anillin can prevent epithelial cells from transitioning to motile mesenchymal cells. Likewise, how would cells with increased HIF-1a and decreased Anillin behave? Perhaps they would undergo the epithelial to mesenchymal transition but become less mobile compared to cells with normal levels of Anillin?

Why is *nuclear* Anillin associated with poor cancer prognosis? Little is known about the role of cytoskeletal proteins in the nucleus. Even the nuclear function of actin, which was first confirmed to be in the nucleus in the 1970s (Clark and Merriam 1977), is not fully elucidated. That said, we do know that both globular and filamentous actin has many functions in the nucleus and is more than just a “molecular wanderer” as was first posited (Pederson and Aebi 2002). Actin gives shape to the nucleus and reshapes chromatin after mitotic exit (Baarlink et al. 2017; Moore and Vartiainen 2017). Actin can also regulate transcription, mRNA processing, and genome organization (Visa and Percipalle 2010). Therefore, it is likely that actin-associated

proteins like Anillin perform similar functions, so high levels of Anillin in the nucleus may potentiate metastasis via nuclear functions. Since Anillin is overexpressed in many human tumors (Hall et al. 2005) and can have both negative and positive outcomes for the patient, learning more about the cytoplasmic and nuclear functions of Anillin may allow us to target it to prevent tumors from entering a metastatic state. For example, using a small peptide to inhibit Anillin's interactions with RhoA or other binding partners could be used as a treatment method. This technique has been used successfully on other scaffolds such as the MAP kinase scaffold IQGAP1 and shows promise as a possible treatment option (Jameson et al. 2013).

Is Anillin important for developmental events that require apical constriction?

Developmental process such as gastrulation, neurulation, and eye and gland formation require apical constriction (Sawyer et al. 2010). Apical constriction is a well-conserved cell shape change that can induce tissue folding in in urchin, worms, flies, frogs, chicks, and mice (Kimberly and Hardin 1998; Nance and Priess 2002; Young, Pesacreta, and Kiehart 1991; Keller 1981; Schoenwolf and Smith 1990; Sadler et al. 1982). In *Xenopus* gastrulation, a small population of bottle cells on the vegetal (bottom) side of the embryo undergo apical constriction, causing an invagination which initiates the formation of the primary tissue layers (Hardin and Keller 1988). Actomyosin accumulation at the apical surface is required to drive apical constriction in *Xenopus*; however, whether the accumulation of actomyosin is medial-apical or junctional is still unknown (Lee and Harland 2007). Later in *Xenopus* development, the actin-binding protein Shroom3 induces apical constriction to form the neural tube (Haigo et al. 2003; Nishimura and Takeichi 2008). Interestingly, even though there is clear medial-apical accumulation of actomyosin in Shroom3-expressing cells, the authors attributed

apical constriction to the junctional actomyosin (Haigo et al. 2003). *Drosophila* gastrulation was the first place where medial-apical actomyosin accumulation was shown to drive apical constriction (Martin, Kaschube, and Wieschaus 2009). Since then, medial-apical actomyosin has also been found to drive apical constriction during lens pit formation (Plageman et al. 2011), and it is likely to drive apical constriction in mouse neural tube formation, as Shroom3 is required for this process as well (Hildebrand and Soriano 1999).

Because medial-apical actomyosin contraction drives apical constriction during many morphological events, our finding that Anillin affects medial-apical contractility **(Fig. 3.3 & S3.2)** supports a potential role for Anillin in development. Indeed, when Anillin is knocked down in *Xenopus* embryos, gastrulation is delayed and some embryos fail to gastrulate, dying soon after (data not shown). *Xenopus* is a good system for exploring Anillin's role in apical constriction during development, as experiments can be performed in intact embryos or explants of embryonic tissue which still undergo morphogenetic events (Zhou, Kim, and Davidson 2009; Keller, Shih, and Sater 1992; Lee and Harland 2007). Explanting tissues would make direct imaging of bottle cell apical constriction and neural plate apical constriction easier and more consistent than whole embryo experiments, and to my knowledge these would be the first *en face* images of bottles cells to be captured. This would allow the apical constriction to be tracked over time with Anillin perturbations. By imaging probes for F-actin and Myosin II, we would learn if Anillin functions to organize the medial-apical contractile network during apical constriction. One hurdle with studying Anillin in morphogenic events is that Anillin participates in cytokinesis, cell-cell junction structure, and medial-apical contractility. Therefore, regulating the amount of knockdown is critical, but even then, it is difficult to determine if the gastrulation

defects we observe are from defects in cytokinesis, junctional contractility, or medial-apical contractility.

After apical constriction of the bottle cells, cells migrate into the embryo and form several cavities, including the archenteron and the blastocoel. The tissue migration and elongation is driven by actomyosin processes in mesenchymal cells that rearrange to elongate the tissue (Keller et al. 1985; Shindo 2018). When Anillin is knocked down, these cavities are still present; however, when Anillin is overexpressed these cavities appear to be absent and are instead full of cells (data not shown). This could be a result of over-elongation of the tissue, increased migration of mesenchymal cells that break away from the tissue and proliferate in the cavities, loss of cell adhesion between cell in the surround tissues, or a combination of these events. Determining the origin of these cells and a robust characterization of the mechanisms behind this defect could provide insights into the role of Anillin in tumor formation and metastasis. As a whole, Anillin's role in development is uncharacterized and is likely a fruitful area of study given Anillin's role in cellular events that are critical for development.

How does Anillin organize medial-apical F-actin into a contractile unit?

The study that first characterized Anillin determined that a small region near the N-terminus of the protein can bind and bundle F-actin *in vitro* (Field 1995). Using electron microscopy, researchers recently found that Anillin's F-actin binding domain has three separate actin binding regions (Jananji et al. 2017). When they made mutations so that only one F-actin binding site was present, the fragment bound F-actin *in vitro*. When two binding sites were present, the fragment bundled F-actin into two dimension sheets. When all three binding sites were present, the fragment bundled F-actin into three dimensional structures (Jananji et al.

2017). Knowing that the F-actin binding domain alone can bundle F-actin *in vitro* (Field 1995; Kinoshita et al. 2002; Jananji et al. 2017), we hypothesized that the F-actin binding domain of Anillin was required to structure medial-apical F-actin *in vivo*. While this prediction was correct **(Fig. 3.5)**, we were surprised to find that it was not sufficient; all three C-terminal domains were also *required* for Anillin to organize F-actin in bundles **(Fig. 3.5)**.

In vivo, each of the C-terminal deletions localizes to medial apical surface, and they all contain the actin-binding domain **(Fig. 3.5)**. Why, then, don't these mutants bundle F-actin? The Rho binding domain, Calcium2 (C2) domain, and the Pleckstrin Homology (PH) domain all help anchor Anillin to the membrane and impact Anillin's ability to regulate active RhoA. The Rho binding domain directly binds to active RhoA, which helps link Anillin to the membrane. It has been proposed that when Anillin binds to RhoA it resets the timer for RhoA inactivation, allowing it to remain active longer (Budnar et al. 2018; Piekny and Glotzer 2008; Sun et al. 2015). Anillin's C2 domain binds to the membrane and to MgcRacGAP and Ect2, negative and positive regulators of RhoA, respectively (Gregory et al. 2008; Frenette et al. 2012). The PH domain binds to the membrane, septins, and the negative regulator of RhoA, p190RhoGAP-A (Manukyan et al. 2015). While it is possible that membrane binding is important for F-actin bundling *in vivo*, deleting one of three membrane binding domains does not completely disrupt membrane binding. Therefore, it seems more likely that RhoA regulatory activity of these domains is critical for Anillin to bundle and organize F-actin *in vivo*.

The *in vitro* studies that showed Anillin's bundling capabilities used F-actin filaments stabilized by phalloidin or high salt (Field 1995; Sun et al. 2015; Kinoshita et al. 2002). *In vivo*, medial-apical F-actin is very dynamic with a $t_{1/2}$ on the order of 10s **(Fig. 3.6)**. Using FRAP, I

showed that Anillin overexpression stabilizes F-actin **(Fig. 3.6)**, likely through protecting the actin filaments from Cofilin severing (Tian et al. 2015). However, this level of F-actin stabilization does not fully explain the actin bundles caused by full length overexpression, as overexpression of C-terminal mutants did not bundle F-actin. I hypothesize that RhoA-mediated actin polymerization is required for bundling and organizing medial-apical F-actin *in vivo*. To test this idea, we could use actin-intact *Xenopus* egg extracts on a substrate-supported lipid bilayer, a technique that is being optimized in our lab by Jennifer Landino (Field, Pelletier, and Mitchison 2017). With this method, a lipid bilayer is seeded on a cover slip, *Xenopus* egg extracts are added, and a cortex of actin forms on the lipid bilayer (Field, Pelletier, and Mitchison 2017). To perturb the system, purified proteins can be added to the extract for overexpression, antibodies can be used to deplete proteins, and inhibitors can be directly added to the extract. Once established, the actin network can be visualized with Total Internal Reflection Fluorescence (TIRF) microscopy of F-actin probes, such as purified mCherry-Utrophin, which the lab already has, and perturbed through addition of Anillin, inhibition of RhoA, formins, and/or depletion of RhoA regulators such as Ect2. This would provide a more direct and easily perturbable system to determine the mechanism through which Anillin promotes an organized and contractile actin network.

Purifying Anillin would be a hurdle for the experiments described above, but it would be useful here as well as in other *in vitro* experiments. For example, there is evidence that suggests Anillin is a tension-sensitive protein like α-catenin (Manukyan et al. 2015). Having purified Anillin would allow direct *in vitro* laser trap force measurements to test whether Anillin undergoes a mechanically-induced conformational change (Buckley et al. 2014). This would pair

nicely with FRET-based *in vivo* experiments showing a loss of FRET when Anillin is under mechanical stress. In brief, two fluorophores that undergo energy transfer are embedded in the protein on either side of a linker with known mechanics. Tension across the protein deforms the linker leading to a decrease in FRET. This technique has been used for several other junctional proteins as a direct measurement of tension across the protein (Grashoff et al. 2010; Kim et al. 2015; Borghi et al. 2012).

While Anillin has many functions, such as membrane anchoring, RhoA regulation, and F-actin and Myosin II binding, it is not known how all of these functions work together to establish a functional contractile network. A pure *in vitro* system where purified components are added such as F-actin, Anillin, and Myosin II could shed light onto the mechanism(s) through which Anillin builds a contractile network (Gardel et al. 2004; Zimmermann et al. 2017). For example, the binding affinity of Anillin and F-actin is fairly low, with a K_d around 4 µM (Jananji et al. 2017). This weak affinity may be beneficial for several reasons. First, Anillin can bind to Myosin II and formins, both of which are processive: Myosin II walks along actin filaments while formins track growing plus ends. If the formin is anchored in place, the actin filaments will grow from the formin; if the formin is free to move, the formin will have a velocity associated with the growing end of the actin filament (Romero et al. 2004). Anillin binds to both of these processive proteins, so one possibility is that Anillin has multiple weak interactions with F-actin to allow the filaments to "slide" through Anillin. This would allow Anillin to ride along with a formin at the growing end of polymerizing actin filament or allow the filaments to slide through Anillin as Myosin II motors translocate filaments. To test this hypothesis, purified tagged versions of Anillin, Myosin II, and mDia2 (formin) could be added to stabilized, coverslip-

anchored actin filaments and observed with TIRF microscopy (Zimmermann et al. 2017). If Anillin becomes processive when untethered formins or Myosin II are added, this would support my hypothesis. Instead of actin filaments, formins or Myosin II could also be tethered to beads or the coverslip (Zimmermann et al. 2017). If Anillin does not allow sliding of actin filaments, then high levels of Anillin should inhibit formin polymerization of F-actin or Myosin II induced sliding of actin filaments.

Finally, many of Anillin's interactions and functions have been mapped, so mathematical modeling of Anillin's role in organizing a contractile actomyosin network could be done in conjunction with *in vitro* experiments. This would allow confirmation of *in vitro* results and may provide unexpected insights for future experiments as variables and parameters can be adjusted more readily. This could be particularly useful for guiding experiments to tease apart Anillin's role in regulating junctional vs. medial-apical F-actin. While there is a great deal known about *what* Anillin does in a contractile network, there is very little known about *how* Anillin actually does it. This multi-pronged approach of *in vitro*, *in silico,* and *in vivo* experiments will help to tease apart the molecular mechanisms of *how* Anillin organizes and orchestrates F-actin, Myosin II, formins, and RhoA activity flux into a contractile network.

What is the interplay between junctional and medial-apical actomyosin?

The apical surface of cells is organized into two types of contractile units, junctional and medial-apical. These distinct yet similar contractile networks can function to perform the same task, such as embryonic wound healing, or distinct functions, like junctional actomyosin-mediated mechanical coupling of cells during cytokinesis, or medial-apical actomyosin-mediated apical constriction during ventral furrow formation in *Drosophila*. While it is clear that

forces from medial-apical actomyosin contractility are directed upon junctional actomyosin and transmitted to neighboring cells, how junctional actomyosin impacts medial-apical actomyosin is less well understood.

It is specifically difficult to attribute Anillin's role in regulating cellular mechanics at the apical surface of cells to one of the populations of actomyosin because Anillin localizes to both. For example, when Anillin is knocked down, we see reduced levels of junction proteins, indicating possible junction disassembly (Reyes et al. 2014). It is known that Myosin II-dependent contractility prevents junction disassembly (Weng and Wieschaus 2016), but in the case of Anillin knockdown, is disassembly caused by lack of forces generated by junctional actomyosin, the loss of medial-apical forces applied to junctions, or something else? This is a difficult question to tease apart, and would require knockdown of Anillin and rescue with Anillin constructs that could distinctly localize to junctions or the medial-apical surface. This could be accomplished by fusing Anillin to a junctional protein or a protein that only localizes to the medial-apical surface such as Endolyn (Ihrke et al. 2001; Hildebrand 2005). Possible issues might arise from this, as Anillin might still target the chimeric proteins to both locations. A method (independent of Anillin) to help tease apart how medial-apical forces affect junction maintenance would be to laser ablate medial-apical actomyosin and observe the effects on cell-cell junctions. Low levels of the actin depolymerizing drug latrunculin B could also be used, as I have observed actin depolymerization seems to occur first across the medial-apical surface, then junctionally at fairly high concentrations (25 µM) of latrunculin B (data not shown). A lower concentration of latrunculin B in the nanomolar range might disrupt medal-apical F-actin while preserving the junctional network.

In addition to the force interplay, another area of interest is to explore the interplay of signaling and protein components between junctional and medial-apical actomyosin. For example, my data exploring apical contractility after the addition of ATP demonstrated that medial-apical accumulation of F-actin occurs first near cell-cell junctions and then sweeps across the apical surface of the cell **(Fig. 3.3)**. Additionally, when Shroom3 was overexpressed to induce apical constriction, Anillin accumulated first near cell-cell junctions and then propagated across the apical surface of the cell **(Fig. S3.2)**. These data position junctions as potential signaling centers or protein stores for medial-apical contractility. In the case of ATP addition, it is possible that the P2Y receptors that bind ATP and induce the signaling cascade are accumulated near junctions. Immunostaining or live imaging of tagged P2Y receptors could determine if this is true. Relocalization of the receptor across the apical surface instead of at junctions would test whether junctional localization is the mechanism for propagation from junctional to medial-apical. Another possibility is that the large accumulation of active RhoA at cell-cell junctions is what initiates this propagation, so even if the P2Y receptor is mislocalized, the accumulation of F-actin will still sweep out from junctions to the medial-apical surface.

To test if protein populations are shared between junctional and medial-apical, photoactivatable or photo switchable tagged proteins could be used. For example, Anillin tagged with a photo-switchable fluorophore could be switched from green to red at junctions, and the medial-apical intensity of red to green florescence could be measured at the medial-apical surface. This would provide evidence as to the origin of the newly accumulating proteins across the apical surface. If, for example, the junctional pool was switched to red while the cytoplasmic population remained green, and the Anillin accumulating on the medial-apical

surface was predominantly green, this would support the idea that the newly accumulated medial-apical Anillin is mostly from the cytoplasm. This would demonstrate that the observed propagation of Anillin from junctions to the medial-apical surface is not a result of diffusion, but likely occurs through the propagation of a signal that spreads from junctions across the medial-apical surface. To my knowledge, there is little evidence about how junctional and medial-apical networks communicate with one another to build a functional apical contractile network, even though the two structures are closely related and mechanically integrated, and these experiments could begin to illuminate this question.

Closing thoughts

Being a part of the Miller lab for the past 5 years has given me the opportunity to expand our knowledge about how epithelial cells respond to and organize mechanical forces. With my work and the work of others in the lab, we have shown that epithelial cells reinforce their junctions in response to the forces generated by the contractile ring. I think the most important questions to pursue next are: Why are these force only transmitted to adherens junction and not the barrier-producing tight junctions? And what are the consequences for development and barrier function if adherens junctions are not reinforced during cell division?

My main project on Anillin regulating forces across the apical surface of cells only started to come together in the last two years of my graduate career, and the driving force behind it was the surprising and peculiar results of the laser ablation data. I feel extremely lucky to have had a “well that’s funny” moment fall into my path during graduate school. This motivated me to keep an open mind and explore what Anillin was doing across the apical

surface. This open mindset and curiosity allowed me to characterize a new role for Anillin in regulating medial-apical contractility.

Anillin is a Swiss Army Knife of a protein. With many protein-protein interactions and cellular functions, it is difficult to tease apart Anillin's functions and mechanism with accuracy. There are many future paths I would take in exploring Anillin's function in regulating epithelial mechanics. However, the one I am most curious about is how my findings can tie into and explain the mechanisms for Anillin's role in cancer progression. Uncovering the conundrum of why Anillin overexpression can be favorable or unfavorable for cancer prognoses would be a useful path of research, as Anillin could be a potential target for cancer treatment. There is still so much to be learned about how cells respond to and generate mechanical cues to establish a functional epithelial sheet. I hope the data presented here have added useful pieces to the puzzle for future researchers to build upon, so that eventually we can unlock the mysteries of the mechanical information stored within these cells.

References

Acharya, BR, A Nestor-Bergmann, X Liang, S Budnar, OE Jensen, Z Bryant, and AS Yap. 2018. “A Mechanosensitive RhoA Pathway That Protects Epithelia against Acute Tensile Stress”, March. Cold Spring Harbor Laboratory. doi:10.1101/281154.

Arnold, Torey R., RE Stephenson, and AL Miller. 2017. “Rho GTPases and Actomyosin: Partners in Regulating Epithelial Cell-Cell Junction Structure and Function”. *Experimental Cell Research* 358 (1). Elsevier BV: 20–30. doi:10.1016/j.yexcr.2017.03.053.

Baarlink, C, M Plessner, A Sherrard, K Morita, S Misu, D Virant, EM Kleinschnitz, R Harniman, D Alibhai, S Baumeister, K Miyamoto, U Edesfelder, A Kaidi, R Grosse. 2017. “A Transient Pool of Nuclear F-Actin at Mitotic Exit Controls Chromatin Organization”. *Nat Cell Biol* 19: 1389–99.

Bambardekar, K, R Clément, O Blanc, C Chardès, and PF Lenne. 2015. “Direct Laser Manipulation Reveals the Mechanics of Cell Contacts in Vivo”. *Proc Natl Acad Sci U S A* 112: 1416–21.

Borghi, N, M Sorokina, OG Shcherbakova, WI Weis, BL Pruitt, WJ Nelson, and AR Dunn. 2012. “E-Cadherin Is under Constitutive Actomyosin-Generated Tension That Is Increased at Cell-Cell Contacts upon Externally Applied Stretch.”. *Proc Natl Acad Sci U S A* 109: 12568–73.

Buckley, CD, J Tan, KL Anderson, D Hanein, N Volkmann, WI Weis, WJ Nelson, and AR Dunn. 2014. “Cell Adhesion. The Minimal Cadherin-Catenin Complex Binds to Actin Filaments under Force”. *Science* 346: 1254211.

Budnar, S, KB Husain, GA Gomez, M Naghibosidat, S Verma, NA Hamilton, RG Morris, and AS Yap. 2018. “Scaffolding of RhoA Contractile Signaling by Anillin: a Regulatory Analogue of Kinetic Proofreading”, March. Cold Spring Harbor Laboratory. doi:10.1101/282756.

Choi, W, BR Acharya, G Peyret, MA Fardin, RM Mège, B Ladoux, AS Yap, AS Fanning, and M Peifer. 2016. “Remodeling the Zonula Adherens in Response to Tension and the Role of Afadin in This Response”. *J Cell Biol* 213: 243–60.

Clark, TG, and RW Merriam. 1977. “Diffusible and Bound Actin in Nuclei of Xenopus Laevis Oocytes”. *Cell* 12 (4). Elsevier BV: 883–91. doi:10.1016/0092-8674(77)90152-0.

Dahmane, N, J Lee, P Robins, P Heller, and A Ruiz i Altaba. 1997. “Activation of the Transcription Factor Gli1 and the Sonic Hedgehog Signalling Pathway in Skin Tumours”. *Nature* 389: 876–81.

Dudek, SM, JR Jacobson, ET Chiang, KG Birukov, P Wang, X Zhan, and JGN Garcia. 2004. “Pulmonary Endothelial Cell Barrier Enhancement by Sphingosine 1-Phosphate”. *Journal of Biological Chemistry* 279 (23). American Society for Biochemistry & Molecular Biology (ASBMB): 24692–700. doi:10.1074/jbc.m313969200.

Fanning, AS, CM Van Itallie , and JM Anderson. 2012. “Zonula Occludens-1 and -2 Regulate Apical Cell Structure and the Zonula Adherens Cytoskeleton in Polarized Epithelia”. *Mol Biol Cell* 23: 577–90.

Field, CM, BM Alberts. 1995. “Anillin a Contractile Ring Protein That Cycles from the Nucleus to the Cell Cortex”. *The Journal of Cell Biology* 131 (1). Rockefeller University Press: 165–78. doi:10.1083/jcb.131.1.165.

Field, CM, JF Pelletier, and TJ Mitchison. 2017. “Xenopus Extract Approaches to Studying Microtubule Organization and Signaling in Cytokinesis”. *Methods Cell Biol* 137: 395–435.

Founounou, N, N Loyer, and R Le Borgne. 2013. “Septins Regulate the Contractility of the Actomyosin Ring to Enable Adherens Junction Remodeling during Cytokinesis of Epithelial Cells”. *Dev Cell* 24: 242–55.

Frenette, P, E Haines, M Loloyan, M Kinal, P Pakarian, and A Piekny. 2012. “An Anillin-Ect2 Complex Stabilizes Central Spindle Microtubules at the Cortex during Cytokinesis”. *PLoS One* 7: e34888.

Gardel, ML, JH Shin, FC MacKintosh, L Mahadevan, P Matsudaira, DA Weitz. 2004. “Elastic Behavior of Cross-Linked and Bundled Actin Networks”. *Science* 304 (5675). American Association for the Advancement of Science (AAAS): 1301–5. doi:10.1126/science.1095087.

Gbadegesin, RA, G Hall, A Adeyemo, N Hanke, I Tossidou, J Burchette, G Wu, et al. 2014. “Mutations in the Gene That Encodes the F-Actin Binding Protein Anillin Cause FSGS”. *J Am Soc Nephrol* 25: 1991–2002.

Grashoff, C, BD Hoffman, MD Brenner, R Zhou, M Parsons, MT Yang, MA McLean, SG Sligar, CS Chen, T Ha, MA Schwartz. 2010. “Measuring Mechanical Tension across Vinculin Reveals Regulation of Focal Adhesion Dynamics”. *Nature* 466: 263–66.

Gregory, SL, S Ebrahimi, J Milverton, WM Jones, A Bejsovec, and R Saint. 2008. “Cell Division Requires a Direct Link between Microtubule-Bound RacGAP and Anillin in the Contractile Ring”. *Current Biology* 18 (1). Elsevier BV: 25–29. doi:10.1016/j.cub.2007.11.050.

Guillot, C, and T Lecuit. 2013. “Adhesion Disengagement Uncouples Intrinsic and Extrinsic Forces to Drive Cytokinesis in Epithelial Tissues”. *Dev Cell* 24: 227–41.

Guo, X, K Bonin, K Scarpinato, and M Guthold. 2014. “The Effect of Neighboring Cells on the Stiffness of Cancerous and Non-Cancerous Human Mammary Epithelial Cells”. *New Journal of Physics* 16 (10). IOP Publishing: 105002. doi:10.1088/1367-2630/16/10/105002.

Guo, X, K Bonin, K Scarpinato, and M Guthold. 2014. “The Effect of Neighboring Cells on the Stiffness of Cancerous and Non-Cancerous Human Mammary Epithelial Cells”. *New Journal of Physics* 16 (10). IOP Publishing: 105002. doi:10.1088/1367-2630/16/10/105002.

Haigo, SL, JD Hildebrand, RM Harland, and JB Wallingford. 2003. “Shroom Induces Apical Constriction and Is Required for Hingepoint Formation during Neural Tube Closure”. *Curr Biol* 13: 2125–37.

Hall, PA, CB Todd, PL Hyland, SS McDade, H Grabsch, M Dattani, KJ Hillan, and SE Russell. 2005. “The Septin-Binding Protein Anillin Is Overexpressed in Diverse Human Tumors”. *Clin Cancer Res* 11: 6780–86.

Handorf, AM, Y Zhou, MA Halanski, and WJ Li. 2015. “Tissue Stiffness Dictates Development, Homeostasis, and Disease Progression”. *Organogenesis* 11: 1–15.

Hardin, J, and R Keller. 1988. “The Behaviour and Function of Bottle Cells during Gastrulation of Xenopus Laevis”. *Development* 103: 211–30.

Hatte, G, C Prigent, and JP Tassan. 2018. “Tight Junctions Negatively Regulate Mechanical Forces Applied to Adherens Junctions in Vertebrate Epithelial Tissue”. *J Cell Sci* 131.

Haynes-Gimore, N, M Banach, E Brown, R Dawes, ES Edholm, M Kim, and J Robert. 2015. “Semi-Solid Tumor Model in Xenopus Laevis/Gilli Cloned Tadpoles for Intravital Study of Neovascularization, Immune Cells and Melanophore Infiltration”. *Dev Biol* 408: 205–12.

Herszterg, S, A Leibfried, F Bosveld, C Martin, and Y Bellaiche. 2013. “Interplay between the Dividing Cell and Its Neighbors Regulates Adherens Junction Formation during Cytokinesis in Epithelial Tissue”. *Dev Cell* 24: 256–70.

Herszterg, S, D Pinheiro, and Y Bellaïche. 2014. “A Multicellular View of Cytokinesis in Epithelial Tissue”. *Trends Cell Biol* 24: 285–93.

Higashi, T, TR Arnold, RE Stephenson, KM Dinshaw, and Ann L. Miller. 2016. “Maintenance of the Epithelial Barrier and Remodeling of Cell-Cell Junctions during Cytokinesis”. *Current Biology* 26 (14). Elsevier BV: 1829–42. doi:10.1016/j.cub.2016.05.036.

Hildebrand, JD, and P Soriano. 1999. “Shroom, a PDZ Domain-Containing Actin-Binding Protein, Is Required for Neural Tube Morphogenesis in Mice”. *Cell* 99: 485–97.

Hildebrand, JD. 2005. “Shroom Regulates Epithelial Cell Shape via the Apical Positioning of an Actomyosin Network”. *J Cell Sci* 118: 5191–5203.

Idichi, T, N Seki, H Kurahara, K Yonemori, Y Osako, T Arai, A Okato, et al. 2017. “Regulation of Actin-Binding Protein ANLN by Antitumor *miR-217* Inhibits Cancer Cell Aggressiveness in Pancreatic Ductal Adenocarcinoma”. *Oncotarget* 8: 53180–93.

Ihrke, G, JR Bruns, JP Luzio, and OA Weisz. 2001. “Competing Sorting Signals Guide Endolyn along a Novel Route to Lysosomes in MDCK Cells”. *EMBO J* 20: 6256–64.

Ivanov, AI, IC McCall, CA Parkos, and A Nusrat. 2004. “Role for Actin Filament Turnover and a Myosin II Motor in Cytoskeleton-Driven Disassembly of the Epithelial Apical Junctional Complex”. *Molecular Biology of the Cell* 15 (6). American Society for Cell Biology (ASCB): 2639–51. doi:10.1091/mbc.e04-02-0163.

Ivanov, AI, M Bachar, BA Babbin, RS Adelstein, A Nusrat, and CA Parkos. 2007. “A Unique Role for Nonmuscle Myosin Heavy Chain IIA in Regulation of Epithelial Apical Junctions”. *PLoS ONE* 2 (8). Public Library of Science (PLoS): e658. doi:10.1371/journal.pone.0000658.

Jameson, KL, PK Mazur, AM Zehnder, J Zhang, B Zarnegar, J Sage, and PA Khavari. 2013. “IQGAP1 Scaffold-Kinase Interaction Blockade Selectively Targets RAS-MAP KinaseDriven Tumors”. *Nature Medicine* 19 (5). Springer Nature: 626–30. doi:10.1038/nm.3165.

Jananji, S, C Risi, IKS Lindamulage, LP Picard, SR Van, G Laflamme, A Albaghjati, GRX Hickson, BH Kwok, and VE Galkin. 2017. “Multimodal and Polymorphic Interactions between Anillin and Actin: Their Implications for Cytokinesis”. *J Mol Biol* 429: 715–31.

Keller, R, J Shih, and A Sater. 1992. “The Cellular Basis of the Convergence and Extension of the Xenopus Neural Plate”. *Dev Dyn* 193: 199–217.

Keller, RE, M Danilchik, R Gimlich, and J Shih. 1985. “The Function and Mechanism of Convergent Extension during Gastrulation of Xenopus Laevis”. *J Embryol Exp Morphol* 89 Suppl: 185–209.

Keller, RE. 1981. “An Experimental Analysis of the Role of Bottle Cells and the Deep Marginal Zone in Gastrulation of Xenopus Laevis”. *J Exp Zool* 216: 81–101.

Kim, TJ, S Zheng, J Sun, I Muhamed, J Wu, L Lei, X Kong, DE Leckband, and Y Wang. 2015. “Dynamic Visualization of α-Catenin Reveals Rapid, Reversible Conformation Switching between Tension States”. *Curr Biol* 25: 218–24.

Kimberly, EL, and J Hardin. 1998. “Bottle Cells Are Required for the Initiation of Primary Invagination in the Sea Urchin Embryo”. *Dev Biol* 204: 235–50.

Kinoshita, M, CM Field, ML Coughlin, AF Straight, and TJ Mitchison. 2002. “Self- and Actin-Templated Assembly of Mammalian Septins”. *Developmental Cell* 3 (6). Elsevier BV: 791–802. doi:10.1016/s1534-5807(02)00366-0.

Kinoshita, Makoto, Christine M. Field, Margaret L. Coughlin, Aaron F. Straight, and Timothy J. Mitchison. 2002. “Self- and Actin-Templated Assembly of Mammalian Septins”. *Developmental Cell* 3 (6). Elsevier BV: 791–802. doi:10.1016/s1534-5807(02)00366-0.

Lee, JY, and RM Harland. 2007. “Actomyosin Contractility and Microtubules Drive Apical Constriction in Xenopus Bottle Cells”. *Dev Biol* 311: 40–52.

Leerberg, JM, GA Gomez, S Verma, EJ Moussa, SK Wu, R Priya, BD Hoffman, C Grashoff, MA Schwartz, and AS Yap. 2014. “Tension-Sensitive Actin Assembly Supports Contractility at the Epithelial Zonula Adherens”. *Curr Biol* 24: 1689–99.

Liang, PI, WT Chen, CF Li, CC Li, WM Li, CN Huang, HC Yeh, HL Ke, WJ Wu, and CY Chai. 2015. “Subcellular Localisation of Anillin Is Associated with Different Survival Outcomes in Upper Urinary Tract Urothelial Carcinoma”. *J Clin Pathol* 68: 1026–32.

Manukyan, A, K Ludwig, S Sanchez-Manchinelly, SJ Parsons, and PT Stukenberg. 2015. “A Complex of p190RhoGAP-A and Anillin Modulates RhoA-GTP and the Cytokinetic Furrow in Human Cells”. *J Cell Sci* 128: 50–60.

Martin, AC, M Kaschube, and EF Wieschaus. 2009. “Pulsed Contractions of an Actin-Myosin Network Drive Apical Constriction”. *Nature* 457: 495–99.

Miyoshi, H, SK Satoh, E Yamada, and Y Hamaguchi. 2006. “Temporal Change in Local Forces and Total Force All over the Surface of the Sea Urchin Egg during Cytokinesis”. *Cell Motil Cytoskeleton* 63: 208–21.

Moore, HM, and MK Vartiainen. 2017. “F-Actin Organizes the Nucleus”. *Nat Cell Biol* 19: 1386–88.

Nance, J, and JR Priess. 2002. “Cell Polarity and Gastrulation in C. Elegans”. *Development* 129: 387–97.

Nishimura, T, and M Takeichi. 2008. “Shroom3-Mediated Recruitment of Rho Kinases to the Apical Cell Junctions Regulates Epithelial and Neuroepithelial Planar Remodeling”. *Development* 135: 1493–1502.

Pederson, T, and U Aebi. 2002. “Actin in the Nucleus: What Form and What for?”. *Journal of Structural Biology* 140 (1-3). Elsevier BV: 3–9. doi:10.1016/s1047-8477(02)00528-2.

Piekny, AJ, and M Glotzer. 2008. “Anillin Is a Scaffold Protein That Links RhoA Actin and Myosin during Cytokinesis”. *Current Biology* 18 (1). Elsevier BV: 30–36. doi:10.1016/j.cub.2007.11.068.

Plageman, TF Jr, BK Chauhan, C Yang, F Jaudon, X Shang, Y Zheng, M Lou, A Debant, JD Hildebrand, and RA Lang. 2011. “A Trio-RhoA-Shroom3 Pathway Is Required for Apical Constriction and Epithelial Invagination”. *Development* 138: 5177–88.

Rappaport, R. 1967. “Cell Division: Direct Measurement of Maximum Tension Exerted by Furrow of Echinoderm Eggs”. *Science* 156: 1241–43.

Reid, SE, and S Zanivan. 2017. “Tumor Stiffness Extends Its Grip on the Metastatic Microenvironment”. *Mol Cell Oncol* 4: e1372866.

Reyes, CC, M Jin, EB Breznau, R Espino, R Delgado-Gonzalo, AB Goryachev, and AL Miller. 2014. “Anillin Regulates Cell-Cell Junction Integrity by Organizing Junctional Accumulation of Rho-GTP and Actomyosin”. *Curr Biol* 24: 1263–70.

Romero, S, C Le Clainche, D Didry, C Egile, D Pantaloni, and MF Carlier. 2004. “Formin Is a Processive Motor That Requires Profilin to Accelerate Actin Assembly and Associated ATP Hydrolysis”. *Cell* 119: 419–29.

Ronkainen, H, P Hirvikoski, S Kauppila, and MH Vaarala. 2011. “Anillin Expression Is a Marker of Favourable Prognosis in Patients with Renal Cell Carcinoma”. *Oncol Rep* 25: 129–33.

Sadler, TW, D Greenberg, P Coughlin, and JL Lessard. 1982. “Actin Distribution Patterns in the Mouse Neural Tube during Neurulation”. *Science* 215: 172–74.

Sawyer, JM, JR Harrell, G Shemer, J Sullivan-Brown, M Roh-Johnson, and B Goldstein. 2010. “Apical Constriction: A Cell Shape Change That Can Drive Morphogenesis”. *Developmental Biology* 341 (1). Elsevier BV: 5–19. doi:10.1016/j.ydbio.2009.09.009.

Schoenwolf, GC, and JL Smith. 1990. “Mechanisms of Neurulation: Traditional Viewpoint and Recent Advances”. *Development* 109: 243–70.

Shindo, A. 2018. “Models of Convergent Extension during Morphogenesis”. *Wiley Interdiscip Rev Dev Biol* 7.

Spadaro, D, S Le, T Laroche, I Mean, L Jond, J Yan, and S Citi. 2017. “Tension-Dependent Stretching Activates ZO-1 to Control the Junctional Localization of Its Interactors”. *Curr Biol* 27: 3783–95.e8.

Sun, L, R Guan, IJ Lee, Y Liu, M Chen, J Wang, JQ Wu, and Z Chen. 2015. “Mechanistic Insights into the Anchorage of the Contractile Ring by Anillin and Mid1”. *Developmental Cell* 33 (4). Elsevier BV: 413–26. doi:10.1016/j.devcel.2015.03.003.

Suzuki, C, Y Daigo, N Ishikawa, T Kato, S Hayama, T Ito, E Tsuchiya, and Y Nakamura. 2005. “ANLN Plays a Critical Role in Human Lung Carcinogenesis through the Activation of RHOA and by Involvement in the Phosphoinositide 3-Kinase/AKT Pathway”. *Cancer Res* 65: 11314–25.

Swaminathan, V, K Mythreye, ET O'Brien, A Berchuck, GC Blobe, and R Superfine. 2011. "Mechanical Stiffness Grades Metastatic Potential in Patient Tumor Cells and in Cancer Cell Lines". *Cancer Res* 71: 5075–80.

Swaminathan, V, K Mythreye, ET O'Brien, A Berchuck, GC Blobe, and R Superfine. 2011. "Mechanical Stiffness Grades Metastatic Potential in Patient Tumor Cells and in Cancer Cell Lines". *Cancer Res* 71: 5075–80.

Tepass, U, and V Hartenstein. 1994. "The Development of Cellular Junctions in the Drosophila Embryo". *Developmental Biology* 161 (2). Elsevier BV: 563–96. doi:10.1006/dbio.1994.1054.

Tian, D, M Diao, Y Jiang, L Sun, Y Zhang, Z Chen, S Huang, and G Ou. 2015. "Anillin Regulates Neuronal Migration and Neurite Growth by Linking RhoG to the Actin Cytoskeleton". *Curr Biol* 25: 1135–45.

Visa, N, and P Percipalle. 2010. "Nuclear Functions of Actin". *Cold Spring Harb Perspect Biol* 2: a000620.

Wallingford, JB, DW Seufert, VC Virta, and PD Vize. 1997. "p53 Activity Is Essential for Normal Development in Xenopus". *Curr Biol* 7: 747–57.

Wang, D, GK Chadha, A Feygin, and AI Ivanov. 2015. "F-Actin Binding Protein, Anillin, Regulates Integrity of Intercellular Junctions in Human Epithelial Cells". *Cell Mol Life Sci* 72: 3185–3200.

Wang, G, W Shen, L Cui, W Chen, X Hu, and J Fu. 2016. "Overexpression of Anillin (ANLN) Is Correlated with Colorectal Cancer Progression and Poor Prognosis". *Cancer Biomark* 16: 459–65.

Weng, M, and E Wieschaus. 2016. "Myosin-Dependent Remodeling of Adherens Junctions Protects Junctions from Snail-Dependent Disassembly". *J Cell Biol* 212: 219–29.

Yang, MH, MZ Wu, SH Chiou, PM Chen, SY Chang, CJ Liu, SC Teng, and KJ Wu. 2008. "Direct Regulation of TWIST by HIF-1alpha Promotes Metastasis". *Nature Cell Biology* 10 (3). Springer Nature: 295–305. doi:10.1038/ncb1691.

Yang, S, A Lockwood, P Hollett, R Ford, and K Kao. 1998. "Overexpression of a Novel Xenopus Rel MRNA Gene Induces Tumors in Early Embryos". *J Biol Chem* 273: 13746–52.

Yao, M, W Qiu, R Liu, AK Efremov, P Cong, R Seddiki, M Payre, et al. 2014. "Force-Dependent Conformational Switch of α-Catenin Controls Vinculin Binding". *Nat Commun* 5: 4525.

Yonemura, S, Y Wada, T Watanabe, A Nagafuchi, and M Shibata. 2010. "Alpha-Catenin as a Tension Transducer That Induces Adherens Junction Development". *Nat Cell Biol* 12: 533–42.

Young, PE, TC Pesacreta, and DP Kiehart. 1991. "Dynamic Changes in the Distribution of Cytoplasmic Myosin during Drosophila Embryogenesis". *Development* 111: 1–14.

Yu, D, AM Marchiando, CR Weber, DR Raleigh, Y Wang, L Shen, and JR Turner. 2010. "MLCK-Dependent Exchange and Actin Binding Region-Dependent Anchoring of ZO-1 Regulate Tight Junction Barrier Function". *Proceedings of the National Academy of Sciences* 107 (18). Proceedings of the National Academy of Sciences: 8237–41. doi:10.1073/pnas.0908869107.

Zhang, S, LH Nguyen, K Zhou, HC Tu, A Sehgal, I Nassour, L Li, et al. 2018. “Knockdown of Anillin Actin Binding Protein Blocks Cytokinesis in Hepatocytes and Reduces Liver Tumor Development in Mice Without Affecting Regeneration”. *Gastroenterology* 154: 1421–34.

Zhou, J, HY Kim, and LA Davidson. 2009. “Actomyosin Stiffens the Vertebrate Embryo during Crucial Stages of Elongation and Neural Tube Closure”. *Development* 136: 677–88.

Zimmermann, D, Kaitlin E Homa, Glen M. Hocky, Luther W. Pollard, Enrique M. De La Cruz, Gregory A. Voth, Kathleen M. Trybus, and David R. Kovar. 2017. “Mechanoregulated Inhibition of Formin Facilitates Contractile Actomyosin Ring Assembly”. *Nature Communications* 8 (1). Springer Nature. doi:10.1038/s41467-017-00445-3.